INFORMATION TO USERS

This manuscript has been reproduced from the microfilm master. UMI films the text directly from the original or copy submitted. Thus, some thesis and dissertation copies are in typewriter face, while others may be from any type of computer printer.

The quality of this reproduction is dependent upon the quality of the copy submitted. Broken or indistinct print, colored or poor quality illustrations and photographs, print bleedthrough, substandard margins, and improper alignment can adversely affect reproduction.

In the unlikely event that the author did not send UMI a complete manuscript and there are missing pages, these will be noted. Also, if unauthorized copyright material had to be removed, a note will indicate the deletion.

Oversize materials (e.g., maps, drawings, charts) are reproduced by sectioning the original, beginning at the upper left-hand corner and continuing from left to right in equal sections with small overlaps. Each original is also photographed in one exposure and is included in reduced form at the back of the book.

Photographs included in the original manuscript have been reproduced xerographically in this copy. Higher quality 6" x 9" black and white photographic prints are available for any photographs or illustrations appearing in this copy for an additional charge. Contact UMI directly to order.

UMI

A Bell & Howell Information Company
300 North Zeeb Road, Ann Arbor MI 48106-1346 USA
313/761-4700 800/521-0600

Université d'Ottawa · University of Ottawa

PERFORMANCE OF A SMART BASE STATION ANTENNA IN IS-136 CELLULAR SYSTEMS

by
Gopichand V.R. Kongara

A thesis submitted to the
School of Graduate Studies and Research
in partial fulfillment of the requirements for the degree of
Master of Applied Sciences
Ottawa-Carleton Institute for Electrical Engineering

School of Information Technology and Engineering
Faculty of Engineering
University of Ottawa

September, 1998

© 1998, G.Kongara

National Library of Canada
Acquisitions and Bibliographic Services
395 Wellington Street
Ottawa ON K1A 0N4
Canada

Bibliothèque nationale du Canada
Acquisitions et services bibliographiques
395, rue Wellington
Ottawa ON K1A 0N4
Canada

Your file Votre référence

Our file Notre référence

The author has granted a non-exclusive licence allowing the National Library of Canada to reproduce, loan, distribute or sell copies of this thesis in microform, paper or electronic formats.

L'auteur a accordé une licence non exclusive permettant à la Bibliothèque nationale du Canada de reproduire, prêter, distribuer ou vendre des copies de cette thèse sous la forme de microfiche/film, de reproduction sur papier ou sur format électronique.

The author retains ownership of the copyright in this thesis. Neither the thesis nor substantial extracts from it may be printed or otherwise reproduced without the author's permission.

L'auteur conserve la propriété du droit d'auteur qui protège cette thèse. Ni la thèse ni des extraits substantiels de celle-ci ne doivent être imprimés ou autrement reproduits sans son autorisation.

0-612-36710-X

Canada

Abstract

Computer simulations have been used to study the effect of narrow switched-beam transmission and power control at the base station on the interference characteristics and traffic capacity of digital cellular (IS-136) systems. In simulations, four narrow beams in place of a sectored antenna pattern are used, and a power control mode with up to 30 watts maximum transmitted power is applied. Results indicate that with transmission on four narrow beams at the base station, the improvement in carrier to interference ratio (C/I) is more than 4 dB. Furthermore, with narrow beam transmission and the base station power control, the total improvement in C/I is 8 to 10 dB. If this C/I gain is utilized to maximize the amount of served traffic, the system capacity can be enhanced by more than 100%. Therefore, improvements in system performance with increased capacity and improved quality are expected by incorporating narrow beam transmission and base station power control.

Acknowledgements

First and foremost, I would sincerely like to thank my supervisors Dr. Langis Roy and Dr. Sylvain Labonte for their supervision, guidance and encouragement throughout the course of this research.

I am grateful to Ericsson research Canada for funding this project. I also thank Ulf Bernstrom, Richard Brunner, Michel Desgagne, Daniel Dofour, Sara Majur of Ericsson Research Canada for their technical support during this research.

To Mina and Chan, I wish to express my gratitude for their continual support, encouragement and affection. I am grateful to my peers, Mohammed, Bartosz, Jean-Francois, Marco, Joey, Raja, Basavalingam, janardhan, Balu, and all others for the lively discussions that have enlightened the long hours spent on this work.

Finally and most importantly, I am deeply indebted to my parents, wife, sisters and all other family members for their unconditional love, gentle understanding, boundless support and belief in my capabilities.

TABLE OF CONTENTS

Abstract i
Acknowledgements ii
List of Figures vii
List of Tables xii
Glossary xiii

Chapter 1 Introduction

1.1 Objectives 2
1.2 Thesis Organization 2

Chapter 2 Overview of Cellular System Concepts

2.1 Introduction 4
2.2 Frequency Reuse 6
2.3 Call Processing In Wireless Systems 9
2.4 Channel Assignment 10
2.5 Handoff 11
2.6 Propagation Models 12
2.7 Diversity 14
2.8 Interference and System Capacity 14
2.9 Multiple Access Schemes 15
2.10 Mobile Radio Standards in North America 19
2.11 Interference Reduction due to Sector Antennas 21
2.12 Conclusions 24

Chapter 3 Radio Network Simulation Environment

3.1 Introduction 25

3.2 Overview of the Simulator 25

3.3 System Plan and Network Simulation 27

3.3.1 Types of Antenna Supported in the Simulator 28

3.3.2 Propagation 30

3.3.3 Traffic and Call control 31

3.3.4 Beam Selection 32

3.3.5 Power Control 32

3.3.6 System Capacity, Performance and Average System Utilization 33

3.3.7 Simulation Length 34

3.4 Conclusions 34

Chapter 4 Switch-Beam Antenna System for IS-136 Systems

4.1 Concept of the Smart Antenna System 35

4.1.1 Switched Beam Approach 39

4.1.2 Adaptive Beam or Steered Beam Approach 40

4.2 Smart Antenna Realization 41

4.3 Antenna Arrays in Mobile Communications 43

4.3.1 N-Element Linear Array: Uniform Amplitude and Spacing 45

4.3.2 Main Beam Scanning and Phased Arrays 50

4.4 Beamforming 55

4.4.1 Digital Beamforming 56

4.4.2 Analog Beamforming 58

4.4.3 Multiple Beam Antenna Systems 60

4.5 System Model for Simulations & Simulation Results 62

4.5.1 Performance of a Conventional Sectored Antenna System 62

4.5.2 Performance of Switched Beam Antenna System 67

4.6 Discussion 70

4.7 Capacity Estimation 72

4.8 Conclusions 74

Chapter 5 Power Control in Cellular Systems

5.1 Introduction 75

5.2 System Model and Power Control Algorithm 78

5.2.1 Power Control Algorithm 78

5.2.2 Simulation Environment 82

5.3 Simulation Results and Analysis with Power Control 83

5.3.1 Simulation Results with No Power Control for Reference 84

5.3.2 Simulation Results with Downlink Power Control and no limit on Maximum Power 86

5.3.3 Simulation Results with Downlink Power Control and a Limit of 30 watts on Maximum Power Transmitted on the Downlink 93

5.4 Joint Power Control and Switch-Beam Antennas 101

5.4.1 Simulation Results with No Power Limit 102

5.4.2 Simulation Results with a Power Limit of 30 watts 113

5.5 Capacity Estimation 124

5.6 Discussion 128

5.7 Conclusions 130

Chapter 6 Conclusions and Recommendations

6.1 Conclusions 131

6.2 Recommendations for Future Research 132

References 134

LIST OF FIGURES

FIGURE 2.1. A basic cellular system....4

FIGURE 2.2. Frequency reuse concept. Cell with the same letter use the same set of frequencies. 7

FIGURE 2.3. Illustration of the 7/21 reuse concept. Base stations are placed at the corner of the three sectored cell sites and a total of nine clusters are used in the system....9

FIGURE 2.4. (a) Frequency division duplexing and (b) Time division duplexing 16

FIGURE 2.5. Different Access methods: (a). Frequency division multiple access scheme (b) Code division multiple access scheme (c) Time division multiple access scheme....18

FIGURE 2.6. IS-136 Evolution 21

FIGURE 2.7. Omnidirectional interference mode....22

FIGURE 2.8. Sectoring to enhance frequency reuse. Antennas are oriented in the same direction for maximum interference protection. 23

FIGURE 3.1. Simulator Structure 26

FIGURE 3.2. Cellular system model....28

FIGURE 3.3. Sectored antenna pattern [15]....29

FIGURE 3.4. Four narrow beams from a four column antenna array with a 0.5l horizontal element spacing [15]. 29

FIGURE 3.5. C/I versus Cumulative Distribution Function (CDF) 33

FIGURE 4.1. Schematic diagram of a switched beam antenna approach, including duplex filters (Dx), radio receivers (Rx), radio transmitter (Tx) and units for identifying the suitable beam (DOA). 39

FIGURE 4.2. Schematic Diagram of a Adaptive beam approach or steered beam approach. Notation is same as in figure 1. 41

FIGURE 4.3. Far-field geometry of N-element array of isotropic sources positioned along the z-axis 46

FIGURE 4.4. Array factor of an equally spaced (d = 0.5λ), uniformly excited three element linear array. 48

FIGURE 4.5. Array factor of an equally spaced (d = 0.5λ), uniformly excited five element linear array. 49

FIGURE 4.6. Array factor of equally spaced uniformly excited (d = 0.5λ) ten element array 50

FIGURE 4.7. Array factor pattern for 4-element uniformly excited equally spaced (d = 0.5λ) scanning array. 52

FIGURE 4.8. Array factor pattern for 4-element uniformly excited equally spaced (d = 0.4λ) scanning array. 53

FIGURE 4.9. Array factor pattern for 4-element uniformly excited equally spaced (d = 0.6λ) scanning array. 54

FIGURE 4.10. A general Digital Beamforming Antenna System 56

FIGURE 4.11. A Butler Beamforming matrix for a four-element array: (a) 4 x 4 Butler matrix; (b) a hybrid used in the matrix 59

FIGURE 4.12. Four mutually orthogonal overlapped beams produced by the Butler beamforming matrix. 60

FIGURE 4.13. Multiple beam systems: beam crossover 61

FIGURE 4.14. Cumulative Distribution Functions of downlink C/I for a 7/21, 4/12 and 3/9 reuse systems with a conventional sector antenna configuration 63

FIGURE 4.15. Downlink Interference distribution of 3 sectored, 7/21 reuse system. 64

FIGURE 4.16. Downlink Interference distribution of a 3 sectored, 4/12 reuse system. 65

FIGURE 4.17. Downlink Interference Distribution of 3 sectored, 3/9 reuse system 66

FIGURE 4.18. Cumulative Distribution Function of C/I for 4/12 reuse system with narrow beam transmission (4beams/sector) 67

FIGURE 4.19.Downlink Interference Distribution when narrow beam transmission is introduced (4 beams/sector) in a 4/12 reuse system.....68

FIGURE 4.20.Cumulative Distribution Function of C/I for 3/9 reuse with narrow beam transmission(4beams/sector) 69

FIGURE 4.21.Downlink Interference Distribution of 3/9 reuse with narrow beam transmission in the downlink (4beams/sector) 70

FIGURE 4.22.Cumulative Distribution Functions of downlink C/I for a 7/21, 4/12 systems with a conventional sector antenna, and a 4/12 system with four orthogonal downlink beams.....72

FIGURE 4.23.Downlink C/I at 10% CDF level as a function of served traffic for a 7/21 reuse system with a conventional sector antenna(*) and4/12 reuse system with four downlink beams (x). 74

FIGURE 5.1. Two mobiles and two base stations [38] 78

FIGURE 5.2. at ms1 and transmitted power at bs1 [38] 79

FIGURE 5.3. Desired control behaviour in ms2 and in bs1 80

FIGURE 5.4. The control strategy.....81

FIGURE 5.5. Power control Mechanism in Downlink from Simulations.....83

FIGURE 5.6. Downlink C/I distribution when there is no power control scheme added ($\beta = 0$) 84

FIGURE 5.7. The histogram of downlink C/I distribution when $\beta = 0$.....85

FIGURE 5.8. The histogram of downlink interference distribution when $\beta = 0$.....86

FIGURE 5.9. Downlink C/I distribution for $\beta = 0.7$ 88

FIGURE 5.10.Histogram of the downlink C/I distribution when $\beta = 0.7$ 89

FIGURE 5.11.Downlink power distribution for $\beta = 0.7$.....90

FIGURE 5.12.Downlink interference distribution when $\beta = 0.7$ 91

FIGURE 5.13.The C/I distribution for different values of β ranging from 0 to 0.9. 92

FIGURE 5.14.The C/I distribution when $\beta = 0.7$ for different maximum power limits. 95

FIGURE 5.15. Downlink C/I distribution when $\beta = 0.7$ with a maximum power limit of 30 watts. 96
FIGURE 5.16. An histogram of C/I when $\beta = 0.7$ and a maximum power limit of 30 watts 97
FIGURE 5.17. Downlink power distribution when $\beta = 0.7$ and a maximum power limit of 30 watts is applied 98
FIGURE 5.18. Downlink interference distribution when $\beta = 0.7$ with maximum power limited to 30 watts. 99
FIGURE 5.19. C/I distribution comparison with and without power limits for different values of β 100
FIGURE 5.20. Downlink C/I vs Power of the links in the downlink when $\beta = 0.7$ 101
FIGURE 5.21. Downlink C/I distribution when $\beta = 0.65$ 104
FIGURE 5.22. Histogram of downlink C/I distribution when $\beta = 0.65$ 105
FIGURE 5.23. Downlink interference distribution when $\beta = 0.65$ 106
FIGURE 5.24. Downlink power distribution when $\beta = 0.65$ 107
FIGURE 5.25. Downlink C/I distribution when $\beta = 0.9$ 108
FIGURE 5.26. Histogram of the downlink C/I distribution when $\beta = 0.9$ 109
FIGURE 5.27. Downlink Interference distribution when $\beta = 0.9$ 110
FIGURE 5.28. Downlink power distribution when $\beta = 0.9$ 111
FIGURE 5.29. Downlink C/I distribution for different values of β ranging from 0 to 0.99 112
FIGURE 5.30. Downlink C/I distribution when $\beta = 0.65$ 115
FIGURE 5.31. Histogram of the downlink C/I distribution when $\beta = 0.65$ 116
FIGURE 5.32. Downlink interference distribution when $\beta = 0.65$ 117
FIGURE 5.33. Downlink power distribution when $\beta = 0.65$ 118
FIGURE 5.34. Downlink C/I distribution when $\beta = 0.9$ 119
FIGURE 5.35. Histogram of the Downlink C/I distribution when $\beta = 0.9$ 120
FIGURE 5.36. Downlink Interference distribution when $\beta = 0.9$ 121
FIGURE 5.37. Downlink power distribution when $\beta = 0.9$ 122

FIGURE 5.38. Downlink C/I distribution plots for different values of β ranging from 0 to 0.99 123

FIGURE 5.39. Cumulative distribution functions of downlink C/I for (a) for a 4/12 reuse system with a conventional 3 sector antenna system, (b) 4/12 reuse system and 3 sector with downlink power control (β = 0.7), (c) 4/12 reuse, 3 sector, downlink power control (β = 0.7) and a restriction on the maximum power transmitted in the downlink (30 watts), (d) 4/12 reuse, 3 sector, 4 beams/ sector, switch-beam antenna system, (e) 4/12 reuse, 3 sector, 4 beams/sector and downlink power control is applied(β = 0.65), (f) 4/12 reuse, 3 sector, 4 beams/sector, switch-beam antenna system, downlink power control (β = 0.9), and a restriction on the maximum power transmitted in the downlink (30 watts) 125

FIGURE 5.40. Cumulative Distribution Functions of downlink C/I for 4/12 reuse with switch-beam antennas and downlink power control, and 3/9 reuse with switch-beam antennas and downlink power control 127

LIST OF TABLES

TABLE 2.1. Major Mobile Radio Standards in North America 19

TABLE 2.2. IS-136 Evolution 20

TABLE 4.1. Array Aperture Phase Distribution 59

TABLE 4.2. Served traffic and downlink C/I at 10% CDF level fro 7/21, 4/12 and 3/9 systems at full load 64

TABLE 4.3. Parameters characterizing the C/I distributions in Figure 4.22 73

TABLE 5.1. C/I distribution at 10% CDF and at 3% CDF for β ranging from 0 to 0.9 93

TABLE 5.2. C/I values at different values of β 113

TABLE 5.3. C/I values for different values of β 124

TABLE 5.4. Summary of C/I values at 10% CDF and at 3% CDF presented in Figure 5.39. 126

GLOSSARY

AMPS Advanced mobile phone system, an analog cellular system in the 800 MHz band.

Adaptive antenna/ smart antenna/ intelligent antenna refers to a group of core RF technologies that control directional antenna arrays by means of sophisticated digital signal processing algorithms.

Adjacent channel interference The interference on a voice channel (VC) or a control channel (CC) frequency is caused by a distant voice channel or control channel on the adjacent (next higher or lower) frequency. Adjacent channel interference is common in cellular networks due to frequency reuse.

Antenna Gain The gain of an antenna compared to a dipole or a quarter wave antenna. Sometimes the gain is compared to an isotropic antenna, and this is referred to as dBi. dBi = dBd + 2.1

Analog Control Channel A special transceiver in the base station which communicates with analog and IS-54B (dual-mode) mobiles to carry out the access, paging, call setup/ release, and handoff protocols.

Analog Voice Channel May refer to either an analog transceiver (hardware) or to the radio frequency to which the transceiver is set (i.e the frequency channel on which an analog conversation is being carried)

Base Station A site that contains the cellular radio equipment. It can have one or more cells.

Bit Error Rate The number of errors, expressed as a fraction of the total number of bits sent, of a digital signal.

Cell Boundary The defined limits of a particular cell. Usually defined to be 39 dBuV/m for AMPS system. However some coverage is usually available well outside the boundary.

CDMA Code Division Multiple Access. A wideband spread spectrum system whereby many users can share the same spectrum simultaneously, discriminating the code that is sent.

Cell A group of co-located channels that cover the same area. A base can have one or more cells by using directional antennas.

Cell Site The location of the cell

Cellular Operator The owner and/or operator of a cellular network.

Channel A pair of frequencies used by the mobile i.e. one frequency for transmitting and the other for receiving.

Co-channel Interference The interference on a voice-channel or control channel frequency which is caused by a distant voice channel or control channel on the same frequency. Co-channel interference is inherent in cellular networks due to frequency reuse in non-adjacent cells.

Collinear Antenna A gain antenna with dipoles stacked vertically.

Combiner A device for combining several transmit channels.

Coupler A device for connecting two or more sources of RF energy to a single cable or port.

Coverage The area over which the service is of an acceptable standard

D-AMPS A full-compatible ("dual mode") digital extension to the AMPS standard, in 800 MHZ band based on IS-136 standard.

D-AMPS 1900 An "upbanded" implementation of the D-AMPS standard in the 1900 MHz band.

dB Decibels. A unit for expressing the relative strength of two signals.

dBm An absolute unit of signal strength corresponding to one milliwatt of power.

dBW = dBm + 30

dBd Gain relative to a dipole antenna.

dBi Gain relative to a hyphothetical isotropic antenna. (It is 2.1 times higher than dBd for the same antenna)

Digital Control Channel (DCCH) A special transceiver in the base station which communicates only with IS-136 digital mobiles to carry out the access, paging, call setup and hand-off protocols.

Digital Traffic Channel (DTC) May refer to either a digital transceiver (hardware) or to the radio frequency to which the transceiver is set (i.e. the frequency channel on which digital traffic is being carried). Note that a single frequency can support up to three or six simultaneous digital conversations, hence the term "traffic" instead of "digital voice channel".

Downlink Refers to base station to mobile communication path, sometimes referred to as the "forward" path. Uplink and downlink characteristics are often significantly different; for example, the downlink signal to noise (S/N) ratio at a particular location can be fairly good, while the uplink S/N is poor.

ERP Effective radiated power. the power expressed in watts, that is radiated in the direction of maximum antenna gain calculated by multiplying the power at the antenna terminals by that gain.

FDMA (Frequency Division Multiple Access) In these systems, the users are assigned a particular pair of frequencies (channels) on request for the duration of a particular call.

GOS (Grade of Service) The probability that a call will fail due to the unavailability of links or circuits.

Handoff The ability of a cellular mobile to be able to move through the coverage area, handing off from cell to cell in order to maintain a good signal quality. The hand is ideally not perceptible to the user.

Interference The reception of unwanted signals that are impressed on the desired signal. In cellular systems most interference comes from other parts of the same network.

IS-136 It is a digital cellular standard used in North America and is based on Time Division Multiple Access (TDMA) scheme

MAHO (Mobile Assisted Handoff) Refers to the digital handoff process, where the mobiles scans the control channel frequencies in adjacent cells and report their downlink signal strengths to the mobile switching centre. The prior analog approach was based on uplink signal strengths, which sometimes resulted in the mobile being ordered to switch to a cell where the downlink signal was too weak.

Multipath The interference patterns created by the addition of signals from more than one path. Virtually all mobile systems including cellular, operate in a multipath environment.

Omnidirectional Antenna An antenna radiating energy equally in all directions (horizontally) around it.

Portable A hand-held cellular telephone.

Roaming Using a cellular phone through a system other than the usual "home" switch.

Sector Antenna A directional antenna that produces coverage of one or more sectors of the total base station coverage.

Signal to Interference ratio The power ratio between the received signal source and the interference source.

Signal to Noise ratio S/N The power ratio between the received signal source and the noise source.

Mobile Switching Centre (MSC) In cellular radio, the connecting switch between the telephone network and the radio base station, also called the mobile exchange.

TDMA (Time Division Multiple Access) A digital (usually radio) system that allows a number of users to use the same system by being assigned a particular time slot.

Traffic Calls in progress. Measured in Erlangs as one call for one hour equals one Erlang.

Transceiver A transmitter and receiver in one unit such as mobile telephone.

Uplink Refers to the mobile to base station communication path. Some times referred to as reverse path. Due to asymmetry of cellular systems (low power mobiles versus high-power base stations), the uplink path characteristics are often significantly different than the downlink characteristics.

CHAPTER 1

INTRODUCTION

The goal of wireless communication is to allow users to communicate reliably in any form at any time, and without regard to location and mobility. In our highly mobile society, the demand for wireless communications is experiencing unprecedented growth, with annual worldwide revenue projections that exceed $100 billion by the turn of the century. Further to this, market research indicates that if networks and products provide portable communications service at a quality and cost similar to that of wireline service, a high percentage of the population will subscribe to wireless service.

The challenge is to offer reliable communications through cellular phones in the same manner as with wireline services, whether in a busy downtown or a peaceful country area. This will most certainly involve a sophisticated radio communication system whose engineering requires knowledge of the spatial and temporal statistics of the signal attenuation, the multipath delay spread, and the statistical characteristics of interference. These properties of a radio channel can have a strong impact on the performance of cellular communication systems.

Unfortunately, radio channel behaviour is statistical in nature, changing from one situation to another. Its properties vary depending on the operating frequency and geographical position where the services are provided. For example, in a downtown area the radio signal undergoes all sorts of attenuation, interference and fading etc., whereas in a suburban area we may have line of sight communication. Therefore, the architecture of wireless communication systems must be flexible and easily adaptable to different scenarios.

Cellular systems offer both indoor and outdoor usage. Current day cellular communications equipment with greater functionality is made possible through the application of digital techniques and technologies. Lately, there has been significant demand for high capacity

digital cellular systems. The demand for higher capacity has placed a great deal of strain on the limited frequency spectrum that is allocated for cellular communications. Consequently, cellular operators are forced to find ways of enhancing the capacity of their networks. One basic approach is to build additional small cell sites to increase capacity. Building new cellular sites means finding suitable base station locations and extending required infrastructure and so this method may not be cost effective. Cell sectorization is another method to increase capacity, but is already exploited to its practical limit in many deployed systems. In this context smart antennas, where narrow beams are selectively used for transmission and reception so as to avoid spreading radio signals unnecessarily over a wide area, have been recognized as one potentially economical approach to enhance capacity. This thesis work is in pursuit of the possible capacity enhancements using smart antennas in lieu of conventional antennas for existing digital cellular communication systems in the 800 MHz band.

1.1 Objectives

The main objective of this thesis is to investigate the performance of multibeam antennas in IS-136 cellular system by means of the statistical distributions of carrier to interference ratio (C/I) in the downlink. The questions of how much C/I gain improvement a switch-beam antenna gives over the conventional 3 sectored antenna system and whether it is feasible to employ 4/12 reuse instead of the current 7/21 reuse plan, will be addressed. Based on computer simulations, the capacity gains of a multibeam antenna transmitting four narrow beams per 120^{o} sector in the downlink will be determined.

While the use of switched narrow beam antennas transmitting at constant power level constitutes a worthwhile investigation of smart antennas, it would be interesting to assess what additional benefits can be derived from transmitting variable amounts of power in each beam according to a mobile's location. Therefore, the second objective of this thesis is to estimate the capacity gain by implementing power control of the narrow beam in conjunction with the multibeam capability in the downlink, also through computer simulations.

1.2 Thesis Organization

The remaining chapters of this thesis are organized as follows. In chapter 2, the basic concept of cellular systems, frequency reuse, interference and system capacity are introduced. Air interface schemes such as FDMA, CDMA, and TDMA used in mobile communications are presented. Furthermore, mobile radio standards used in North America are summarized. After the overview, the simulation environment used for estimating radio network performance is presented in chapter 3. In chapter 4, a brief description of phased antennas, array factor, and beamforming techniques such as digital beamforming and analog beamforming techniques is given. The capacity and performance potential of switch-beam antenna solutions are investigated by using computer simulations. In chapter 5 the downlink power control algorithm used in the simulations is described. Computer simulation results for the 4/12 reuse cell plan with downlink power control are presented with and without power constraint on the maximum power transmitted. Simulation results follow for joint power control and switch-beam antennas. The chapter concludes with capacity estimations for the joint power control and the switch-beam antenna. Finally, chapter 6 presents the thesis conclusions and discusses the scope for further research.

CHAPTER 2

OVERVIEW OF CELLULAR SYSTEM CONCEPTS

A basic understanding of the operation of a cellular system, as well as its numerous performance parameters, is necessary before undertaking the study of switch-beam antenna enhancements. This chapter, therefore, provides an overview of the relevant cellular system concepts.

2.1 Introduction

The concept of cellular radio involves containing a group of frequencies within a "cell," reusing the frequencies in the same vicinity, but separating them in space to allow reuse without any serious interference.

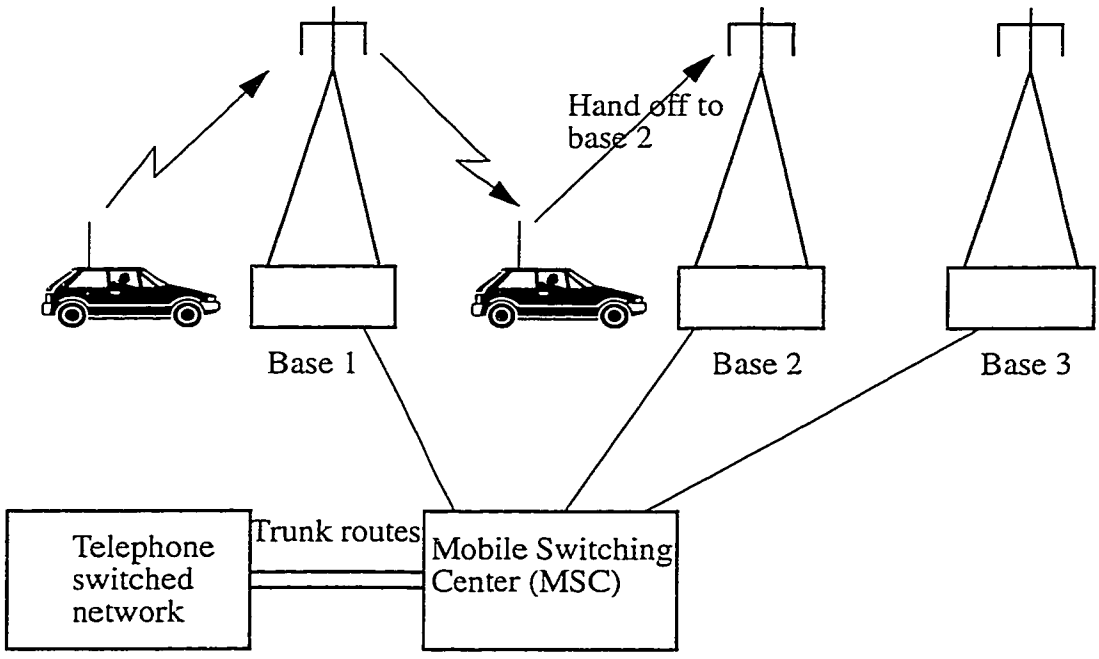

FIGURE 2.1. A basic cellular system.

Cellular radio systems provide high quality service that is often comparable to that of land-line telephone systems. High capacity is achieved by limiting the coverage of each base station transmitter to a small geographic area called a cell so that the same radio channels may be reused by another base station located some distance away. A basic cellular system is illustrated in Figure 2.1. In normal applications, the cells are arranged in such a way that continuous coverage is provided within the service area.

The heart of a cellular system is the cellular switch, or Mobile Switching Center (MSC). The cellular switch connects the base stations to the Public Switched Telephone Network (PSTN) and to each other as required. A feature of the cellular architecture is the continuous monitoring of the call progress and the ability to reconfigure the system quickly so that switching occurs without disturbing the user.

All cellular systems have the following features [25]

- Frequency reuse,
- Ability to hand-off a mobile from cell to cell according to signal field strength and/or noise requirements,
- Multi-cell and multi-base configurations,
- Ability to work in a controlled interference environment,
- Access to a fixed telephone network with mobiles receiving and sending calls through the PSTN.

The mobile station communicates via radio with one of the base stations and may be handed-off to any number of base stations throughout the duration of a call. The mobile station contains a transceiver, an antenna and control circuitry and may be mounted on a vehicle or used as a hand-held unit. The base stations consist of several transmitters and receivers which simultaneously handle full duplex communications. The base station serves as a bridge between all mobile users in the cell and connects the simultaneous mobile calls via

telephone lines or microwave links to the cellular switch. The cellular switch coordinates the activities of all of the base stations and connects the entire cellular system to the PSTN.

Communication between the base station and mobile stations is defined by a standard common air interface that specifies four different channels. The channels used for voice transmission from the base stations to mobiles are called forward voice channels (FVC) and the channels used for voice transmission from mobiles to the base station are called reverse voice channels (RVC). The two channels responsible for initiating the mobiles are called forward control channels (FCC) and reverse control channels (RCC). Control channels transmit and receive data messages that carry call initiation and service requests, and are monitored by mobiles when they do not have a call in progress. Forward control channels also serve as beacons which continually broadcast all of the traffic requests for all the mobiles in the system. Supervisory and data messages are sent in a number of ways to facilitate automatic channel changes and handoff instructions for the mobiles before and during a call.

2.2 Frequency Reuse

The cellular concept is based on replacing a single, high power transmitter (large cell) with many low power transmitters (small cells), each providing coverage to only a small portion of the service area. Each base station is allocated a portion of the total number of channels available to the entire system, and nearby base stations are assigned different groups of channels so that all the available channels are assigned to a relatively small number of neighbouring base stations. Neighbouring base stations are assigned different groups of channels so that the interference between base stations (and the mobile users served by these base stations) is minimized. By systematically spacing base stations and their channel groups throughout the coverage area, the available channels are distributed throughout the geographic region and may be reused as many times as necessary, so long as the interference between co-channel stations is kept below acceptable levels. The design process of selecting and allocating channel groups for all of the cellular base stations within a system is called *frequency reuse* or *frequency planning*. Figure 2.2, illustrates the concept of cellular fre-

quency reuse, where cells labelled with the same letter use the same group of channels. The frequency reuse plan is overlaid upon a map to indicate where different frequency channels are used. The hexagonal cell shape is conceptual and a simplistic model of the radio coverage of each base station. The actual radio coverage of a cell is known as the footprint and is determined from field measurements or propagation prediction models.

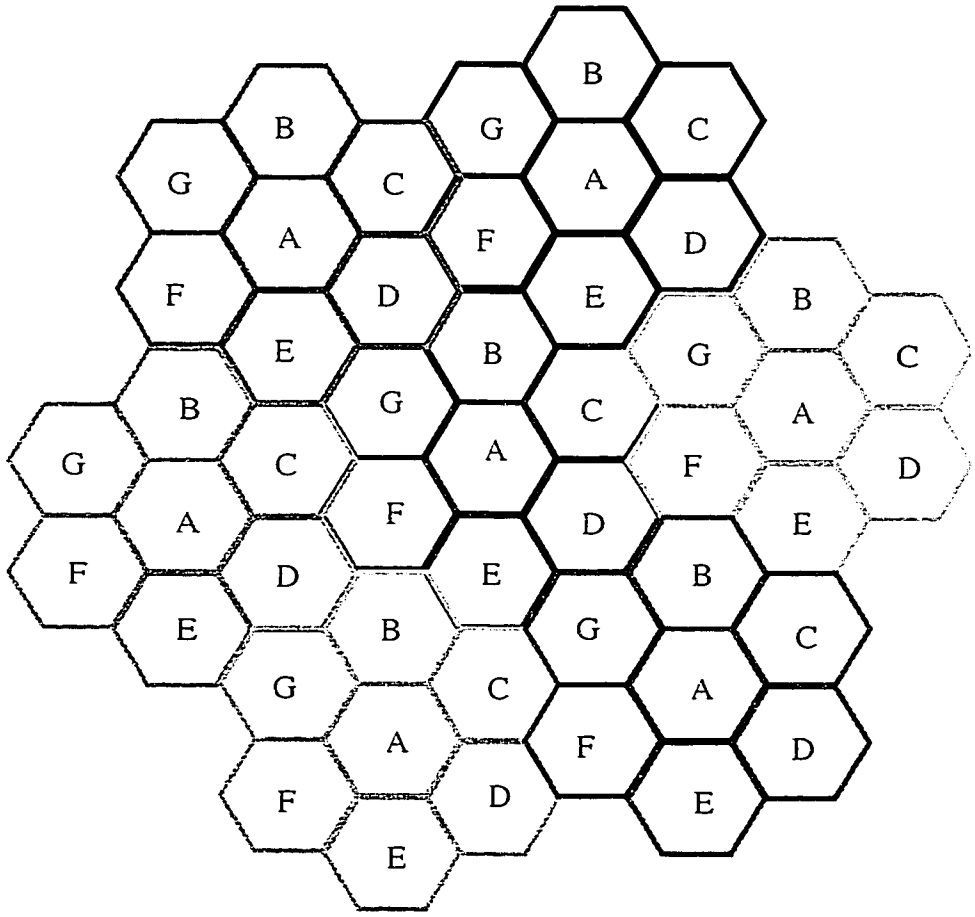

FIGURE 2.2. Frequency reuse concept. Cell with the same letter use the same set of frequencies.

When using hexagons to model coverage areas, base station transmitters are at the centre of the cell (centre-excited cells) or on three of the six vertices (edge-excited cells). Usually, omni directional antennas are used in center-excited cells and sectored directional antennas are used corner excited cells. However in practice, the base station may be positioned up to

one-fourth of the cell radius away from the ideal location due to terrain and other constraints.

To understand the concept of reuse consider a cellular system which has a total of S duplex channels available for use. If each cell is allocated a group of k channels ($k < S$), and if the S channels are divided among N cells into unique and disjoint channel groups which each have the same number of channels, the total number of available radio channels can be expressed as

$$S = k\,N \qquad (1)$$

The N cells which collectively use the complete set of available frequencies is called a cluster. If a cluster is replicated M times within the system, the total number of duplex channels, C, can be used as a measure of capacity and is given

$$C = M\,k\,N = M\,S \qquad (2)$$

From equation 2, the capacity of a cellular system is directly proportional to the number of times a cluster is replicated in a fixed service area. The factor N is called the cluster size and is typically equal to 4, 7, or 12. If the cluster size N is reduced while the cell size is kept constant, more clusters are required to cover a given area and hence more capacity is achieved. A larger cluster size indicates that the ratio between the cell radius and the distance between co-channel cells is large. Conversely, a small cluster size indicates that co-channel cells are located much closer together. The value for N is a function of how much interference a mobile or base station can tolerate while maintaining a sufficient quality of communication. The frequency reuse factor of a cellular system is given by 1/N, since each cell within a cluster is only assigned 1/N of the total available channels in the system.

In Figure 2.3, the 7/21 frequency reuse plan for a M = 9 cluster cellular system is demonstrated. Here 7/21 means 7 cells per cluster and each cell in the cluster is subdivided into 3 sectors. Base station antennas are placed at the corner of the three sectors of the cell site each covering 120^{o} of the cell site. For example, if there are 21 channels available in the sys-

tem, then each sector will be allotted with one channel in 3 sectored case (in the omni case each cell is allotted with 3 channels). Since there are 9 clusters in the system, the total available channels in the system are 21 x 9 which is equal to 189 channels. The 21 channels (or channel groups if there are several channels per sector) are allocated to cells in such a way that the same channel groups are not used in the neighbouring cells thereby reducing the interference from the co-channels used in the system.

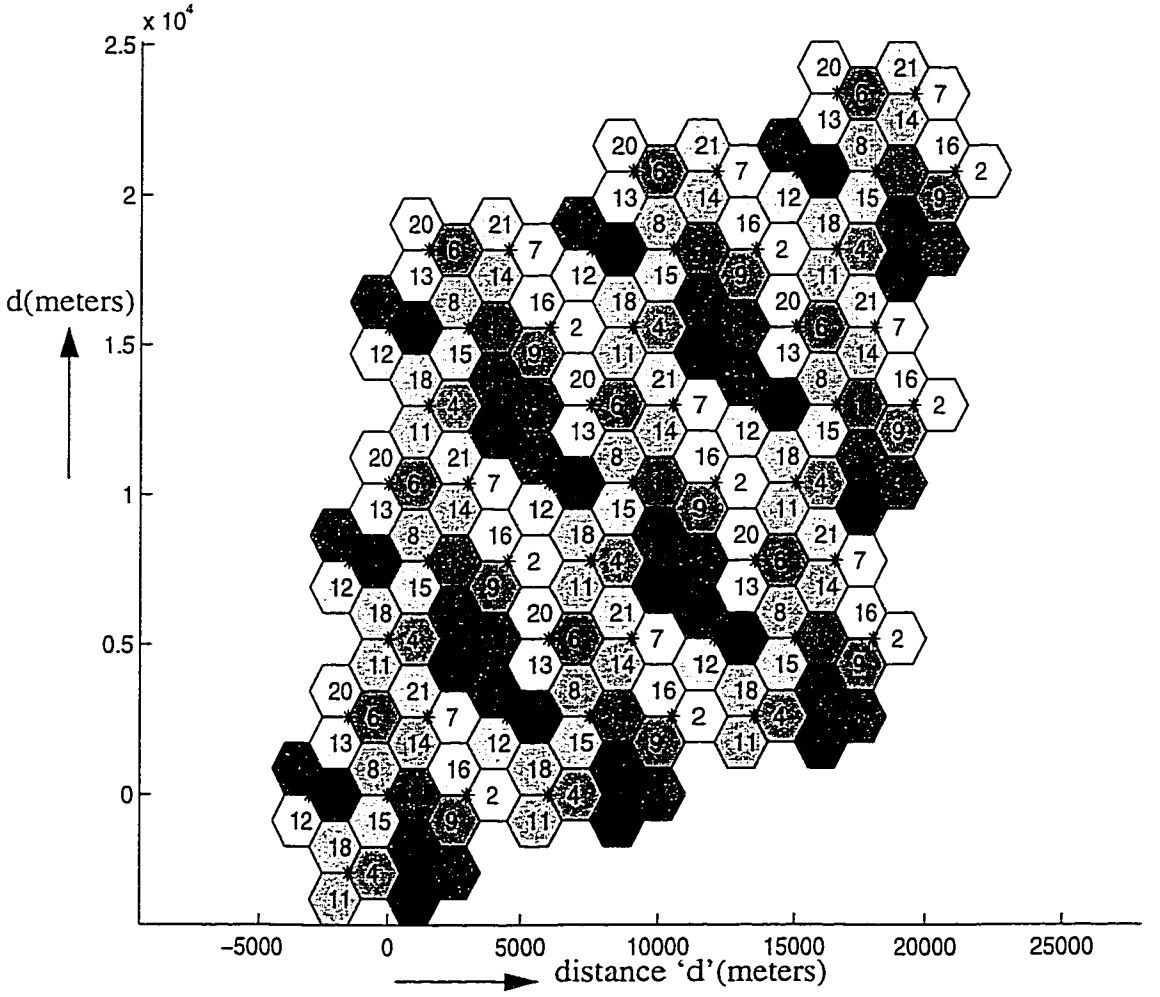

FIGURE 2.3. Illustration of the 7/21 reuse concept. Base stations are placed at the corner of the three sectored cell sites and a total of nine clusters are used in the system.

2.3 Call Processing In Wireless Systems

Call processing involves a number of coordinated procedures performed by the portable, base station, and the mobile switching center. These procedures are invoked during call setup, call handover, and call termination. The call setup and call handover procedures are particularly important because they affect the system performance directly. For example, it is desirable to set up or handover a call to a base station and use a channel that will not cause any ongoing calls to be prematurely terminated. At call setup it is acceptable to block a call which will potentially cause a number of dropped calls after it is set up. The following paragraph describes simplified examples of call processing operations.

When a portable enters the wireless service area, it registers with the base station it can most clearly detect. this is generally the closest base station to that particular portable. Should the portable ever detect a base station with a stronger received signal than the one to which it is registered, it will attempt to register with the new base station. This ensures that each portable can move anywhere within the range of the system, and still originate and receive the calls.

An outgoing call attempt originating at a portable is routed through the base station to which the portable is registered. If an outgoing call attempt finds the base station busy, an attempt will be made to set up the call to another base station in the area. If a base station is available, the channel with the least amount of interference received by the portable will be used to set up the call. If no acceptable base station or channel is found, then the call is blocked. Incoming calls to the portables are routed through the base stations in the other directions. If at any time the signal to interference ratio of the call becomes unacceptable at either the portable or at the base station, a call handover attempt is made. If a call handover cannot be achieved within a fixed amount of time the call will be dropped.

2.4 Channel Assignment

Each base station is equipped with resources to service a certain number of traffic channels. The channels that a base station is allowed to use may either be pre-set in the base station

when it is installed, or be allowed to dynamically change so that the base station can operate on any free channel in the available band.

The first scheme is called fixed channel assignment (FCA). In a fixed channel assignment strategy, each cell is allocated a predetermined set of voice channels. Any call attempt within the cell can only be served by the unused channels in that particular cell. If all the channels are in that cell are occupied, the call is blocked and the subsriber does not receive the service.

The second scheme is called dynamic channel assignment (DCA). In a dynamic channel assignment strategy, voice channels are not allocated to different cells permanently. Instead, each time a call request is made, the serving base station requests a channel from the MSC. The switch then allocates a channel to the requested cell following an algorithm that takes into account the likelihood of future blocking within the cell, the frequency of the candidate channel, the reuse distance of the channel, and other cost functions. Dynamic channel allocation offers improved capacity and efficient spectrum utilization compared to fixed channel assignment. Dynamic channel assignment reduces the likelihood of blocking, which increases the trunking capacity of the system, since all the available channels in a given region are accessible to all of the cells.

2.5 Handoff

When a mobile moves into a different cell while a conversation is in progress, the MSC automatically transfers the call to a new channel belonging to the new base station. The handoff operation not only involves identifying a new base station, but also requires that the voice and control signals be allocated to channels associated with the new base station. In IS-136 systems, handoff decisions are mobile assisted. In mobile assisted hand off (MAHO), every mobile station measures the received power from surrounding base stations and continually reports the results of these measurements to the serving base station. A handoff is initiated when the power received from the base station of a neighbouring cell begins to exceed the power received from the current base station by a certain level or for a certain

period of time. During the course of a call, if a mobile moves from one cellular system to a different cellular system controlled by a different MSC, an intersystem handoff will be initiated. An MSC initiates an intersystem handoff when a mobile signal becomes weak in a given cell and the MSC cannot find another cell within its system to which it can transfer the call in progress.

2.6 Propagation Models

Propagation models are focused on predicting the average received signal strength at a given distance from the transmitter, as well as the variability of the signal strength in close spatial proximity to a particular location. Propagation models that characterize the signal strength over large transmit - receive (T-R) separation distances are called large scale propagation models. On the other hand propagation models that characterize the signal strength over very short travel distances (a few wavelengths) or short time durations (on the order of seconds) are called small scale or fading models. There are a number of models that can be used to describe the radio environment. Propagation parameters are observed to vary significantly depending upon urban or rural areas [26]. Most models consider the path attenuation (or negative path gain), shadowing and signal fading effects. Theoretical and measurement-based propagation models indicate that, averaged received signal power decreases logarithmically with distance for both indoor or outdoor radio channels.

The average large scale path loss for an arbitrary T-R separation is expressed as a function of distance by using a path loss exponent, n [26].

$$\overline{PL}(d) \propto \left(\frac{d}{d_0}\right)^n \qquad (1)$$

or

$$\overline{PL}(d) = \overline{PL}(d_0) + 10n\log\left(\frac{d}{d_0}\right) \qquad (2)$$

where n is the path loss exponent which indicates the rate at which the path loss increases with distance, d_0 is the close-in reference distance which is determined from measurements close to the transmitter, and d is the T-R separation distance. The bars in equations (1) and (2) denote the ensemble average of all possible path loss values for a given value of d. The value of n depends on the specific propagation environment. For example in free space, n is equal to 2, in urban area for cellular radio n varies from 2.7 to 3.5 and in shadowed urban cellular radio environment n is between 3 and 5.

The model in equation (2) does not consider the fact that the surrounding environmental clutter may be vastly different at two different locations having the same T-R separation. Measurements have shown that at any value of d, the path loss $PL(d)$ at a particular location is random and distributed log-normally (in dB) about the mean distance dependent value. That is,

$$\overline{PL}(d) = \overline{PL}(d_0) + 10n\log\left(\frac{d}{d_0}\right) + X_\sigma \qquad (3)$$

and

$$P_r(d) = P_t(d) - PL(d) \quad \text{(antenna gains included in } PL(d)\text{)} \qquad (4)$$

where P_r is the received power at a distance d, P_t is the transmitted power, $PL(d)$ is the path loss at a distance d, and X_σ is a zero-mean gaussian distributed random variable (in dB) with standard deviation σ (also in dB). The lognormal distribution describes the random shadowing effects which occur over a large number of measurement locations which have the same T-R separation, but have different levels of clutter on the propagation path. This phenomenon is referred to as log-normal shadowing. The close-in reference distance d_0, the path loss exponent n and the standard deviation σ, statistically describe the path loss model for an arbitrary location having a specific T-R separation.

Although large scale fading caused by shadowing due to variations in both the terrain profile and the nature of the surroundings can be described by equation (3), there is also small scale

fading to be considered. Small scale fades are characterized by deep amplitude fluctuations which occur as the mobile moves over distances of just a few wavelengths. These fades are caused by multiple reflections from the surroundings in the vicinity of the mobile. Small scale fading typically results in a Rayleigh fading distribution of signal strength over small distances [26].

2.7 Diversity

The Rayleigh fading channel poses a demanding problem to wireless system designers. Diversity is a commonly used technique to overcome this short term fading. A diversity scheme is a method that is used to recover information from several signals transmitted over independently fading paths. The objective is to combine the multiple signals and reduce the effect of excessively deep fades. Since the chance of having two deep fades from two uncorrelated signals at any instant is rare, the effect of the fades can be reduced by combining them. Common methods of combining techniques include selective combining, maximum ratio combining, and equal-gain combining. Different diversity techniques include: space diversity, frequency diversity, polarization diversity, time diversity, and angle diversity. The most commonly used diversity is space diversity. Space diversity is based on the fact that when two antennas are spatially separated by a considerable amount, the signals received by these two antennas are un correlated. So the possibility of a deep fade occurring on the signals received by the two antennas is rare. The multibeam antenna concept studied in this thesis is a form of angle diversity (explained in chapter 4).

2.8 Interference and System Capacity

Interference is a major limiting factor in the performance of cellular radio systems. Major types of system generated cellular interference are co-channel interference and adjacent channel interference. In a cellular system, for a given coverage area there are several cells that use the same set of frequencies. These cells are called co-channel cells and the interference between signals from these cells is called co-channel interference. To reduce co-chan-

nel interference, co-channel cells must be physically separated by a certain minimum distance to provide sufficient isolation due to propagation.

Given a modulation technique and channel plan for a system, a small but significant portion of the transmitted power may spill into adjacent frequency channels. This interference is called adjacent channel interference. Some of the signal also spills into the second, third, fourth, etc. adjacent frequency channels. The level of this interference is generally quite low, but it may still have an effect on the use of these adjacent channels. This interference is termed as alternate channel interference.

There is another type of interference encountered in TDMA systems due to synchronization problems. Synchronization is a time domain issue referring to the frame level or slot level timing of a system. Two systems are synchronized if they start and stop sending the radio bursts at the same time. In typical wireless systems, portables extract their timing information for synchronization from the base station to which they are communicating. However, if all of the base stations in the environment are not synchronized to each other, some additional interference arises as the transmissions of one radio system overlap others. This type of interference can be avoided by employing synchronization between the base stations.

From a design point of view the smaller the reuse, the maximum is the capacity in the system. But at the same time reducing the reuse factor means the co-channel frequency has to be reused at a closer distance. This might cause the interference and the quality of the channel in use to be deteriorated.

2.9 Multiple Access Schemes

It is often desirable to allow the subscriber to send simultaneously information to the base station while receiving information from the base station. This effect is called duplexing. Duplexing may be done using frequency or time domain techniques. Frequency division duplexing (FDD) provides two distinct bands of frequencies for every user. The forward

band provides traffic from base station to the mobile, and the reverse band provides traffic from mobile to the base.

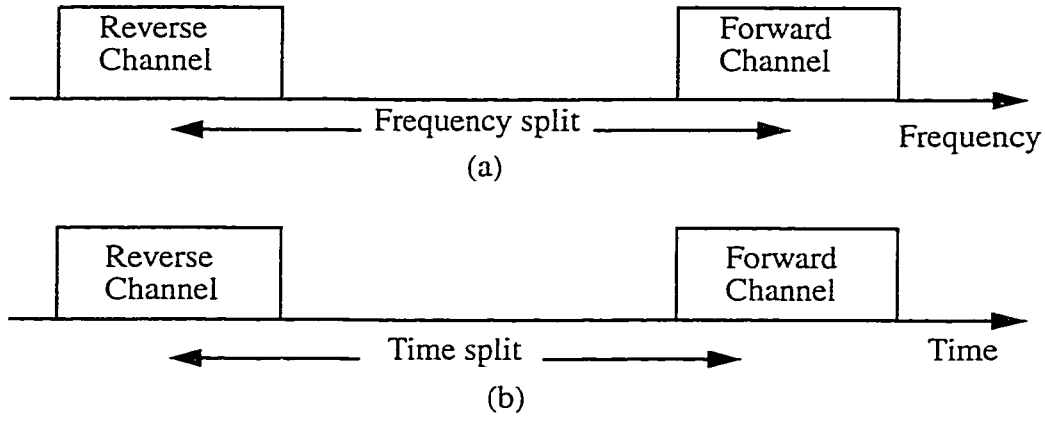

FIGURE 2.4. (a) Frequency division duplexing and (b) Time division duplexing

Figure 2.4 illustrates the frequency division duplexing and time division duplexing. Time division duplexing (TDD) uses time instead of frequency to provide both forward and reverse links. If the time split between the forward and reverse time slot is small, then the transmission and reception of data appears simultaneous to the user. TDD allows communication on a single channel and does not require a duplexer.

Multiple access schemes are used to allow many mobile users to share simultaneously a finite amount of radio spectrum. Frequency Division Multiple Access (FDMA), Time Division Multiple Access (TDMA), and Code Division Multiple Access (CDMA) are the three major access techniques used to share the available bandwidth in a wireless communication system [25].

In Figure 2.5 different multiple access schemes, FDMA, CDMA, TDMA are demonstrated. In conventional analog systems, FDMA is used so multiple communications can occur at the same time without interference. Every channel is assigned to a specific frequency band. To

listen to another channel, the receiver must be tuned to another band. Two frequencies are actually utilized since duplex communication is used.

In CDMA it uses one frequency or one channel to carry more than one subscriber at the same time. Each message is encoded with an unique code and at the receiving end the encoded message is decoded and reassembled. Since each call is identified by a unique code, this allows the call to be distinguished from the other calls broadcast on the same channel.

TDMA systems divide each channel into different time slots and in each time slot only one user is allowed either to transmit or to receive. TDMA is used in digital systems to overcome the limitation of only one call per channel, like in FDMA. TDMA systems transmit data in bursts and it can take bursts of up to eight different users (eight users in GSM and six users in IS-136 systems) on to the same carrier frequency. TDMA when combined with time division duplexing, one carrier frequency can be used for both transmit and receive unlike in FDMA where we require two different frequency carriers for transmit and receive.

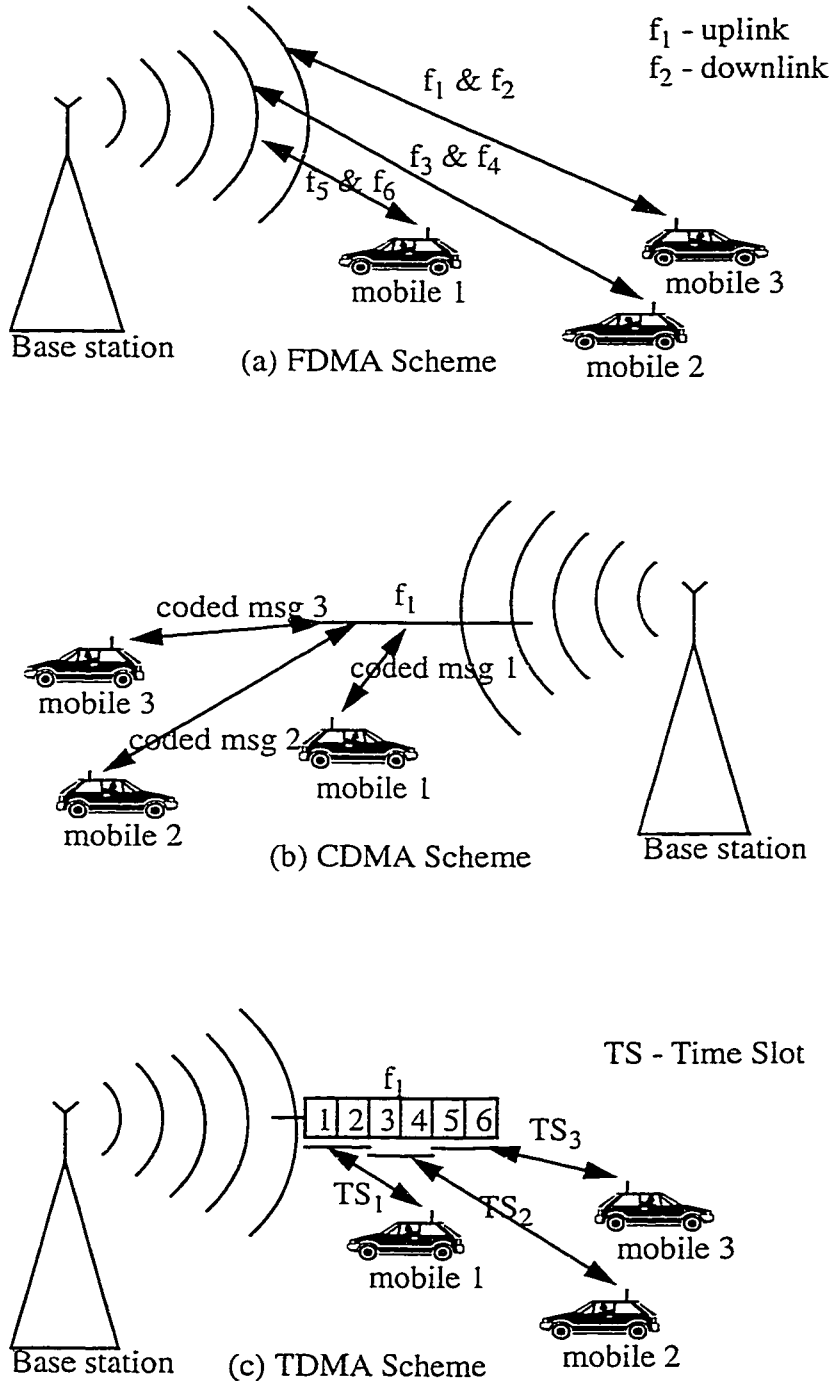

FIGURE 2.5. Different Access methods: (a). Frequency division multiple access scheme (b) Code division multiple access scheme (c) Time division multiple access scheme

2.10 Mobile Radio Standards in North America

Many mobile radio standards have been developed for wireless systems throughout the world. Table 2.1 lists the most common paging, cordless, cellular, and personal communications standards used in North America [27].

TABLE 2.1. Major Mobile Radio Standards in North America

Standard	Type	Year of Introduction	Multiple Access	Frequency Band	Modulation	Channel Bandwidth
AMPS	Cellular	1983	FDMA	824-894 MHz	FM	30 KHz
NAMPS	Cellular	1992	FDMA	824-894 MHz	FM	10 KHz
USDC	Cellular	1991	TDMA	824-894 MHz	$\pi/4$-QPSK	30KHz
CDPD	Cellular	1993	FH/ Packet	824-894 MHz	GMSK	30KHz
IS-95	Cellular/ PCS	1993	CDMA	824-894 MHz 1.8-2.0 GHz	QPSK/ BPSK	1.25MHz
GSC	Paging	1970's	Simplex	Several	FSK	12.5 KHz
POC-SAG	Paging	1970's	Simplex	Several	FSK	12.5KHz
FLEX	Paging	1993	Simplex	Several	4-FSK	15 KHz
DCS-1900 (GSM)	PCS	1994	TDMA	1.85 - 1.99 GHz	GMSK	200 KHz

TABLE 2.1. Major Mobile Radio Standards in North America

Stand-ard	Type	Year of Intro-duction	Multi-ple Access	Fre-quency Band	Modula-tion	Chan-nel Band-width
PACS	Cordless/ PCS	1994	TDMA/ FDMA	1.85 - 1.99 GHz	π/4-DQPSK	300 KHz
MIRS	SMR/ PCS	1994	TDMA	Several	16 - QAM	25 KHz

TABLE 2.2. IS-136 Evolution

Standard	Description
EIA 553 (origi-nally IS-3)	The original AMPS 800 MHz (analog only) standard. Cov-ers air protocols for analog control channels and analog voice channels (AVCs)
IS-54 (Rev.B)	The Digital-AMPS 800 MHz dual mode (analog and digital) standard. Covers analog control channel (ACC), analog voice channels (AVS) and digital traffic channels (DTCs). Addresses dual-mode compatibility issues for both base and mobile stations, and includes features such as message wait-ing indicator (MWI) and calling Number Identification (CNI). Note that IS-54-B-compliant mobile must support both analog and digital modes
IS-136 Rev.0	Adds the Digital Control Channel (DCCH) standard at 800 MHz (in addition to ACC, AVC, DTC). Adds digital only features such as Sleep mode (to extend the mobile's battery life), and Short message service (SMS).
IS-136 Rev.A	The Digital-AMPS Dual-Band standard. Specifies DCCH and DTC operation in the 1900 MHz band (the so-called North -American "PCS band"). Also specifies 800 MHz analog and digital operation as per IS-136 Rev.0 and IS-54 Rev.B. Note that (unlike the previous standards), IS-136 Rev.A does not require mobile terminals to support both bands; 1900-MHz-only mobiles are permitted.

The evolution of the IS-136 (Digital AMPS) standard in North America is described in Table 2.2.

Figure 2.6 shows the applicable air interface standards to mobile communications in North America, the functions they support and their relationships to each other. Note how IS-136 Rev.0 contains the entire IS-54 Rev.B standard, which in turn contains the entire EIA-553 specification. This reflects the effort required to make new standards backward compatible with existing ones.

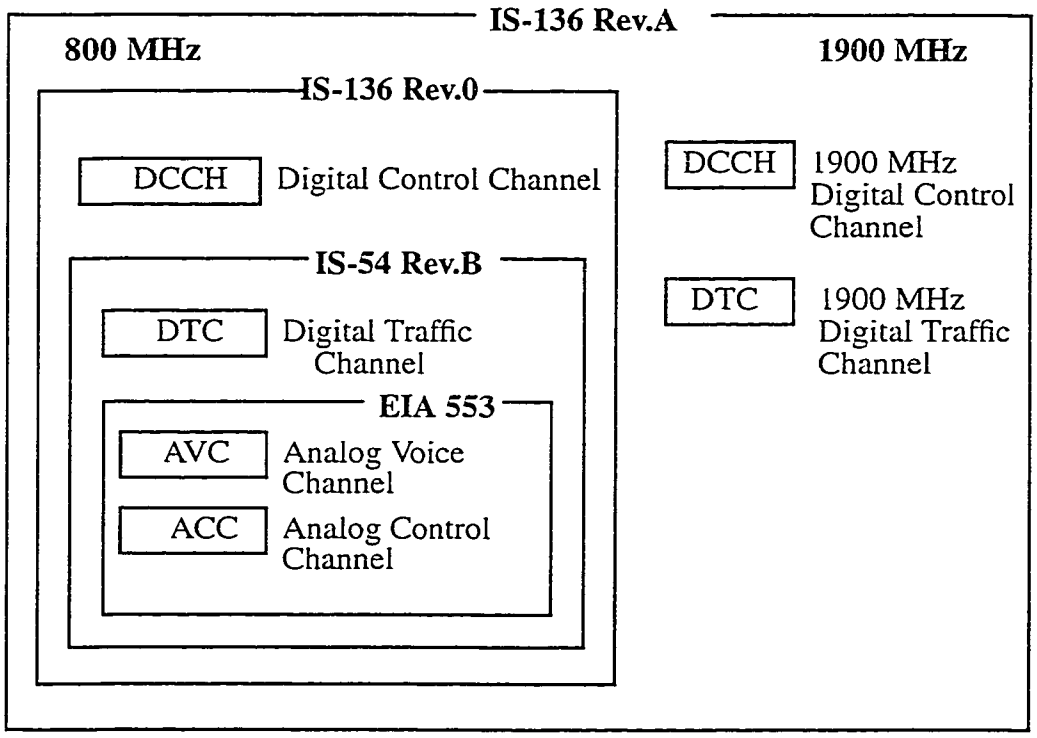

FIGURE 2.6. IS-136 Evolution

2.11 Interference Reduction due to Sector Antennas

The co-channel interference in a cellular system may be decreased by replacing a single omni-directional antenna at the base station by several directional antennas, each radiating within a specified sector. By using directional antennas, a given cell will receive interference and transmit with only a fraction of the available co-channel cells. The technique for decreasing co-channel interference and thus increasing system capacity by using directional

antennas is called sectoring. Sector antennas are important tools in minimizing interference in the system. The factor by which the co-channel interference is reduced depends on the amount of sectoring used. Figure 2.7 and Figure 2.8 illustrates the basic principle of sector antennas.

In this Figure 2.7, consider a mobile roaming from cell E_1 to E_2, both of which use the same frequencies. If the cell sites are omnidirectional and E_1 is relatively high, the mobile might rome well into cell D before a handoff occurs. All the time it is getting closer and closer to E_2 and the probability of interference is increasing.

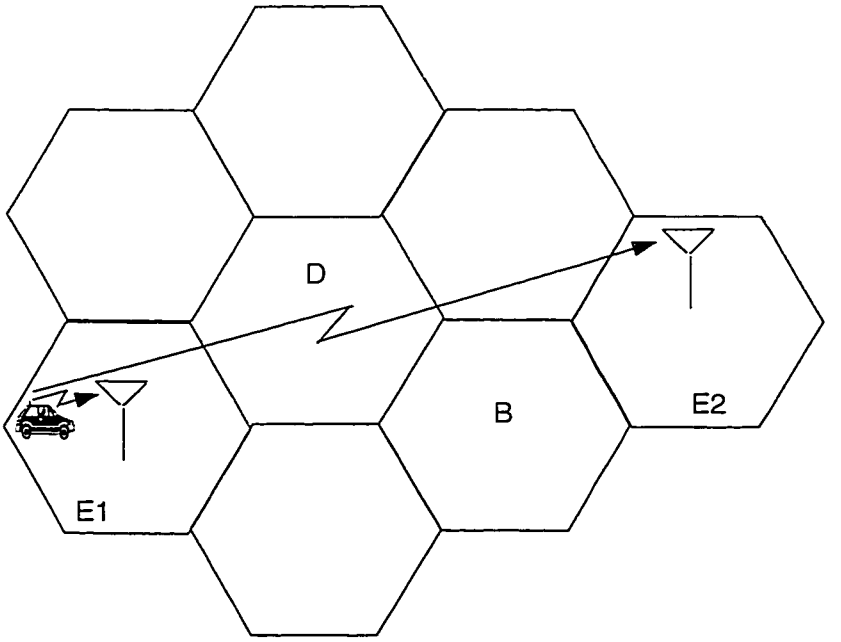

FIGURE 2.7. Omnidirectional interference mode.

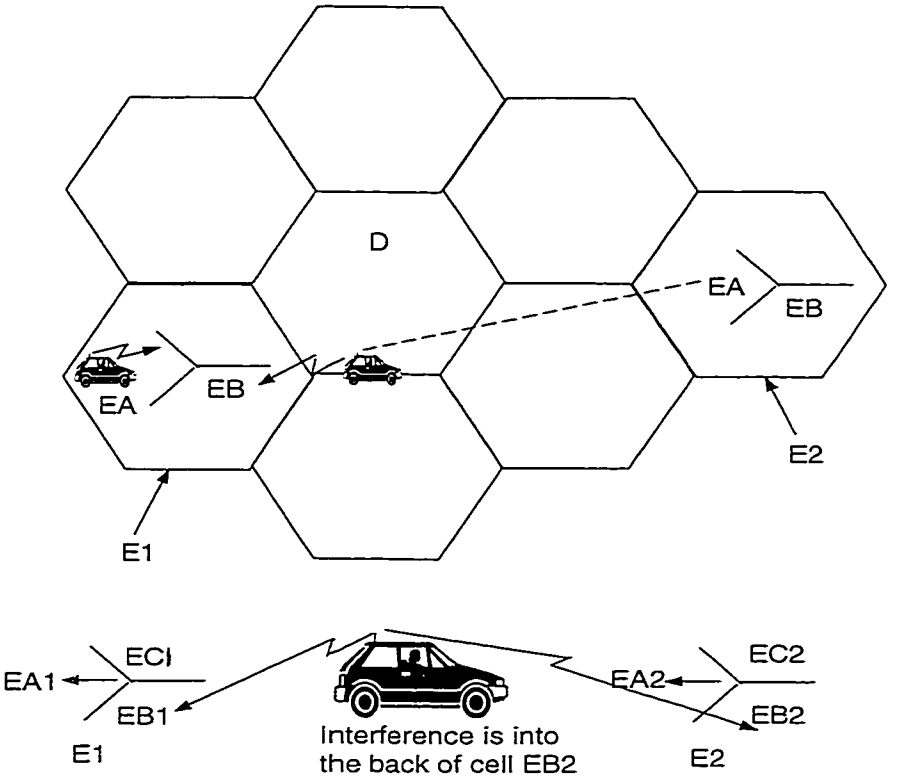

FIGURE 2.8. Sectoring to enhance frequency reuse. Antennas are oriented in the same direction for maximum interference protection.

As shown in Figure 2.8, sectoring E_1 and E_2 can improve things considerably. When the car begins its journey (at maximum distance from E_2), the situation is the same as for the unsectored site. However, when the mobile passes the base station on the way to E_2, a handoff is initiated to cell E_B. The mobile is using cell E_B at E_1 but is behind the antenna for cell E_B at site E_2. This gives the added protection of the effective front-to-back ratio of the antenna against interference. When, finally the mobile hand off to cell E_2, it uses cell E_A and again interferes with cell E_1 only via the back of the antenna. Interference protection can thus be increased by use of sectored antennas and antenna sectors as narrow as 60^o can be used effectively.

In practice, the reduction in interference offered by sectoring can be used to reduce the cluster size and this in turn improves the capacity of the system. The improvement in interference with 120^{o} sectoring allows us to use 7-cell reuse as compared to 12-cell reuse for the worst possible situation in the unsectored case [25]. Thus the sectoring reduces interference which amounts to an increase in capacity by a factor of 12/7, or 1.714. The penalty for improved S/I and the resulting capacity improvement is an increased number of antennas at each base station, and a decrease in trunking efficiency. (As the number of sectors increases, the total number of channels available in the system has to be divided equally among all the sectors and hence fewer number of channels are available for the mobiles to choose from in a given sector. This is called trunking efficiency). Since sectoring reduces the coverage area of a particular group of channels, the number of hand-offs increases, as well.

2.12 Conclusions

In this chapter, the basic concept of cellular systems, frequency reuse, interference and system capacity were introduced. Air interface schemes such as FDMA, CDMA, and TDMA used in mobile communications were described and mobile radio standards used in North America were summarized. It was seen that techniques such as cell sectoring can enhance system capacity. This general knowledge will be useful in the following chapters where interference reduction due to narrow beam and multibeam transmission in the downlink is investigated.

CHAPTER 3

RADIO NETWORK SIMULATION ENVIRONMENT

3.1 Introduction

Simulation is the process of designing a mathematical or logical model of a real system and then conducting computer-based experiments with the model to describe, explain, and predict the behaviour of the real system. A simulator is a computer program which simulates the operation of a system as closely as possible. Therefore, it is essential to understand the important aspects of the chosen simulator with respect to the operation of wireless systems, and then apply appropriate mathematical and probablistic behaviour models in the simulation. This chapter describes the major issues in the simulation of wireless systems.

3.2 Overview of the Simulator

The network simulator is designed to be an easy-to-use simulation tool and is widely used for radio network simulations in Ericsson. It is well suited to system-independent studies of radio network algorithms. The simulator is implemented in Matlab and consists of a set of Matlab functions. A simulation program is formed by combining and modifying these functions.

The environment and activity of the wireless system are simulated using mathematical models. The simulator takes into account: the physical arrangement of the cell structure, map attributes (physical surroundings); different models of radio propagation; various algorithms to establish calls, reassign calls, perform power control; different antenna models (omni, sector, multibeams) for transmission and reception, modelling of the dynamic mobile environment (including hand-offs); and different population models and traffic densities.

Several options exist that specify the output of the simulator. The statistics that determine the grade of service of the system are saved. These include call event activities, signal to interference ratio in uplink and downlink, power transmitted in the uplink and downlink, interference and signal strengths in the uplink and downlink. The call event activities include call setup, call handover, call blocked, call dropped and call ended. The simulator can analyse these result files to display statistics on channel and radio usage, call distribution profiles, signal to interference distribution, interference distribution and power distribution. The probability of a dominant interferer can be obtained by analysing the result files.

The basic operational structure of the simulator is shown in Figure 3.1. The network simulator simulates signals propagating between the base stations (BSs) and mobile stations (MSs). All links established between the base station and mobile stations are assumed to be duplex links with a constant duplex distance.

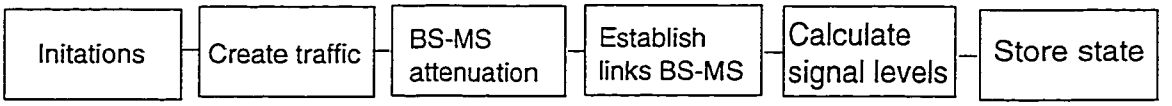

FIGURE 3.1. Simulator Structure

The sequence of actions in the simulator is outlined below.

- Initiations: the tasks include creation of the cell plan, creation of the lognormal map, placing base stations in the cells, assignment of channel plan.
- Create traffic: creation of mobiles uniformly distributed in the cellular network.
- BS-MS attenuation: calculation of negative path gain (path loss) between each BS-MS combination.
- Establish links BS-MS: based on the path gain values between each mobile and base station, each mobile is assigned to a certain base station. The power levels and channel to be used on that link are taken from the channel plan. Blocked calls are logged and removed.

- Calculate signal levels: calculation of transmit/receive signals in the uplink and downlink, calculation of received signal strength, interference, C/I.
- Store state: store the state of the system

Figure 3.1 applies only to the static traffic. In the case of dynamic traffic, additional blocks are introduced to account for the movement of the mobiles. In this work, it is assumed that all the mobiles are static and the system is not followed continuously. Instead, each iteration corresponds to a traffic situation uncorrelated to the previous one, i.e "snapshots" are taken of the situation in the network. This makes it possible to follow the network over a longer time period than what would otherwise be possible. The time between the iterations is not specified, but since the iterations correspond to entirely different traffic situations the time between them is considerably longer than the call hold time.

3.3 System Plan and Network Simulation

The system model used in the simulator is shown in Figure 3.2. The model choosen basically because, it represents the typical urban cellular environment of a 7/21 reuse system. The model shown in the Figure 3.2 consists of 9 clusters with seven cells in each cluster. The radius of each cell is fixed at 1000 meters. Each of the 7 cells in the cluster is divided into 3 sectors. Within a cluster each channel is used once. Hence the number of channels in the system equals number of cells multiplied by the number of channels per base station in one cluster. For example number of cells in a cluster is equal to 21 (3 sectors/cell), and number of frequencies available in each sector is equal to 1. There are 9 cluster in the system. Thus the total number of channels in the system is equal to 9x21x1 = 189 frequencies, with each frequency being repeated 9 times in the system i.e. once in each cluster. Here the frequency reuse is 7. Similarly for a reuse of 4 and 3, the number of cells in each cluster are equal to 4 and 3 respectively. In the simulations all three reuse factors are used for comparing the results and for the capacity estimations.

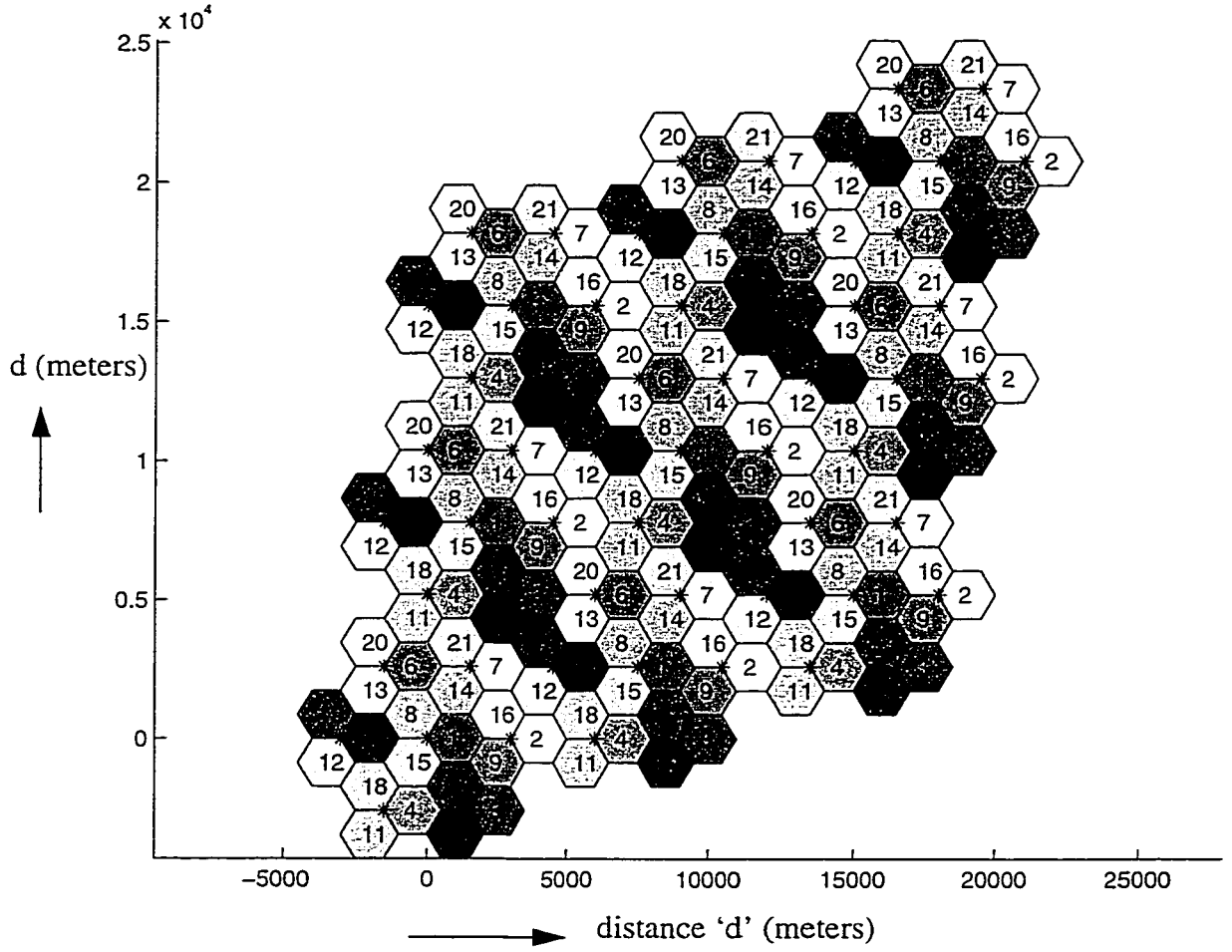

FIGURE 3.2. Cellular system model

3.3.1 Types of Antenna Supported in the Simulator

The simulator supports three antenna types: omni, sectored and multibeams in each cell. By definition, the omni antenna has 0 dBi gain. In the simulations an omni cell is replaced by 3 directional antennas. In the multibeam case, each sector antenna is replaced by a four column antenna array with a 0.5λ horizontal element spacing which produces four directional narrow beams in each 120° sector. Figure 3.3 and Figure 3.4 show the sectored antenna pattern and multibeam antenna patterns used in the simulator. The synthesis of the multibeams is explained in chapter 4. The beamwidth of these beams is approximately 26°.

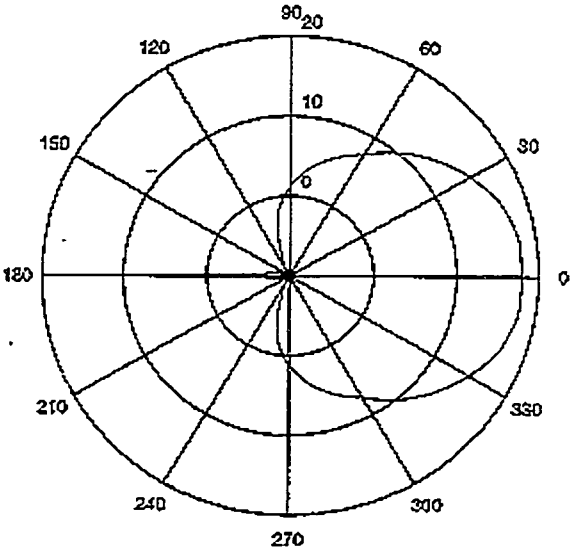

FIGURE 3.3. Sectored antenna pattern [15].

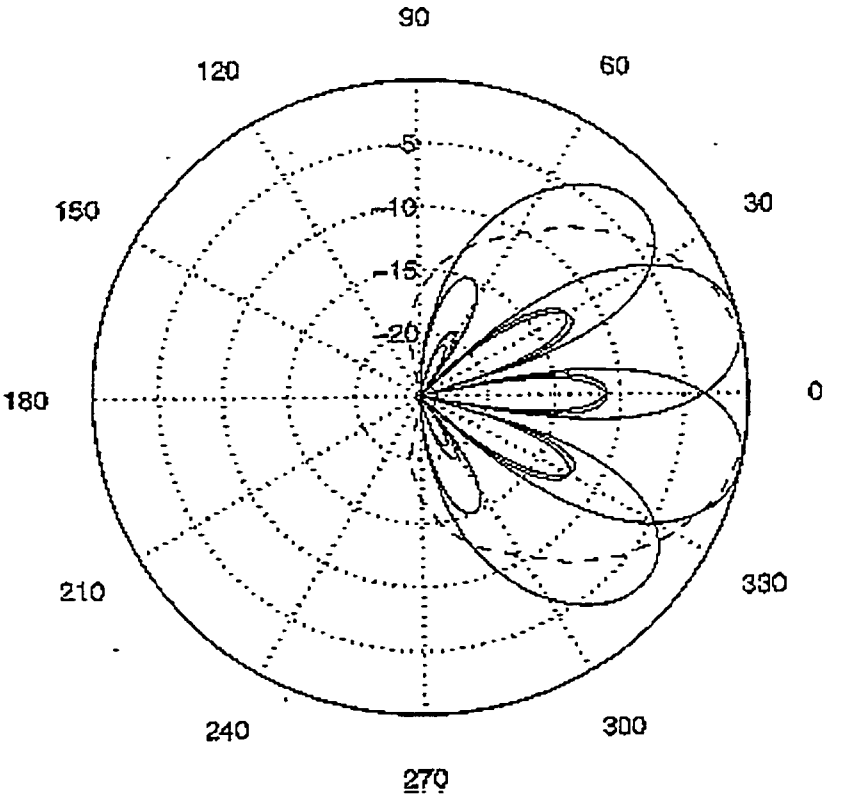

FIGURE 3.4. Four narrow beams from a four column antenna array with a 0.5λ horizontal element spacing [15].

3.3.2 Propagation

The received signal strength in BS/MS depends on the distance between transmitter and receiver, output power, fading, noise and interference.

Output powers are set constant in the first part of simulations for both the uplink and downlink. In the latter part of the simulations power control is employed whereby power in the downlink is varied as per the algorithm described in Chapter 5. In all the simulations the uplink power is kept constant i.e no uplink power control is employed. It is assumed that the capacity in the system is limited by interference than the noise. All the simulation results presented are for the interference limited system.

The interference on a voice channel or control channel frequency caused by a distant voice channel or control channel on the same frequency is called cochannel interference. Adjacent channel interference is defined as the interference caused by voice channel or control channel on an adjacent (next higher or lower) frequency. Adjacent channel interference is inherent in all cellular communications. In all the simulations, adjacent channel power is set 20 dB below the desired channel power.

For each BS-MS combination, a gain matrix G is calculated according to

$$G = G_D + G_A + G_F$$

where G_D is the distance gain (negative path gain), G_A is the antenna gain and G_F is the log-normal fading gain.

The attenuation of a signal due to the distance between transmitter and receiver is here referred to as distance gain and is given by the Okumura-Hata formula [26], and This expression is same as the equation 2.1 and equation 2.2 in Chapter 2.

$$G_D = -\{k + 10n \log(d)\} \text{ [dB]}$$

where 'k' is attenuation constant and 'n' is Propagation exponent

where 'd' is distance between MS - BS in meters and Attenuation constant is distant independent term in the Hata formula. The propagation exponent is set at 3.5 corresponding to an urban environment.

G_A is the antenna gain and depends upon the type of antenna used in the simulator: if an omni is used then G_A is equal to 0 dBi; if it is 3 sectored then G_A is around 18 dBi; in the 4 beam case, the effective gain is 18 dBi as is in the case of 3 sectored case due to power reduction in the transmitted power at the base station. Side lobe levels are kept 20 dB below the main lobe level.

G_F is the shadow fading or log-normal fading gain (in fact negative gain) due to, for example, houses or hills. These are modelled as map attributes in the simulator. Fast multipath fading is not simulated. To the log-normal fading value obtained from the above equation, a lognormal fading standard deviation of 6 dB is added.

To avoid border effects, a wrap around technique that "folds" a rhombic area is used. If no wrap around is used, MSs close to the borders of the cell area would have a more advantageous interference situation than MSs in the interior of the area, as the outer MSs are not disturbed from all directions. To solve this problem, the cell area is folded so that MSs on the south border are disturbed by the BSs on the north border and MSs on the east border are disturbed by the BSs on the west border etc.

After the folding is done, the linear gain values for each MS-BS combination are calculated and the shadow fading is added, forming the G matrix.

3.3.3 Traffic and Call control

In all the simulations the mobiles are assumed to be static. The traffic is modelled according to a uniform distribution. Offered traffic is defined as the number of mobiles served per base station. If number of base stations in the system are b and offered traffic is 'm' mobiles per base station, then the offered traffic in the system is equal to b x m. The traffic is generated randomly and spread out uniformly with a total of b x m mobiles served in the network.

Once the mobiles are generated, then the closest base stations to each mobile is indexed. At call connect, the static MSs randomly chose a base station among the BSs that have a G (defined in the previous section) less than the handover margin from the maximum G for that mobile. Handover margin is set at 3 dB for these simulations. For example, a mobile trying to connect to a base station and if the gain between the mobile and three closest base stations falls within the range of 3 dB then the mobile chooses the base station randomly among these three base stations.

A fixed frequency plan is used. To avoid interference from adjacent channels in neighbouring cells, the channel allocation to the cells is optimized for maximum separation. The MS is assigned a channel randomly out of the set of free channels at the desired BS. If no channel is available, the call is blocked. An MS/BS cannot be connected to several BSs/MSs on the same channel, i.e. no macro diversity is implemented. No calls are dropped owing to the bad link quality, i.e. mobiles continue to transmit and receive on the channel allocated to it despite poor quality on that particular link.

3.3.4 Beam Selection

When four narrow beams per sector are transmitted a two step procedure is followed. First the base station selection for the mobile is performed as outlined above for the sectored antenna pattern. Once the mobile is allocated to the base station, it is then required to transmit on one of its four beams. The G matrix calculation is done again taking into consideration the four narrow-beam antenna patterns. The mobile chooses the strongest of the four beams based on the new values. The beam identified for the mobile is used for both transmission and reception.

3.3.5 Power Control

Power control simulations employ the algorithm outlined in Chapter 5. In this algorithm, power transmitted and the C/I information in a first iteration is used to adjust the power on the downlink in the second iteration. Chapter 5 discusses the power control algorithm and

constraint on the maximum power transmitted. In the simulations only downlink power control is employed. No uplink power control is employed and power is constant on all uplinks.

3.3.6 System Capacity, Performance and Average System Utilization

Served traffic in the system is defined as the average number of users per cell divided by the number of channels in the system. Hence a system with a 7/21 frequency reuse pattern can serve a traffic of 1/21 user/cell/channel at full load. System capacity is defined as the maximum amount of traffic it is possible to serve in compliance with the quality criterion.

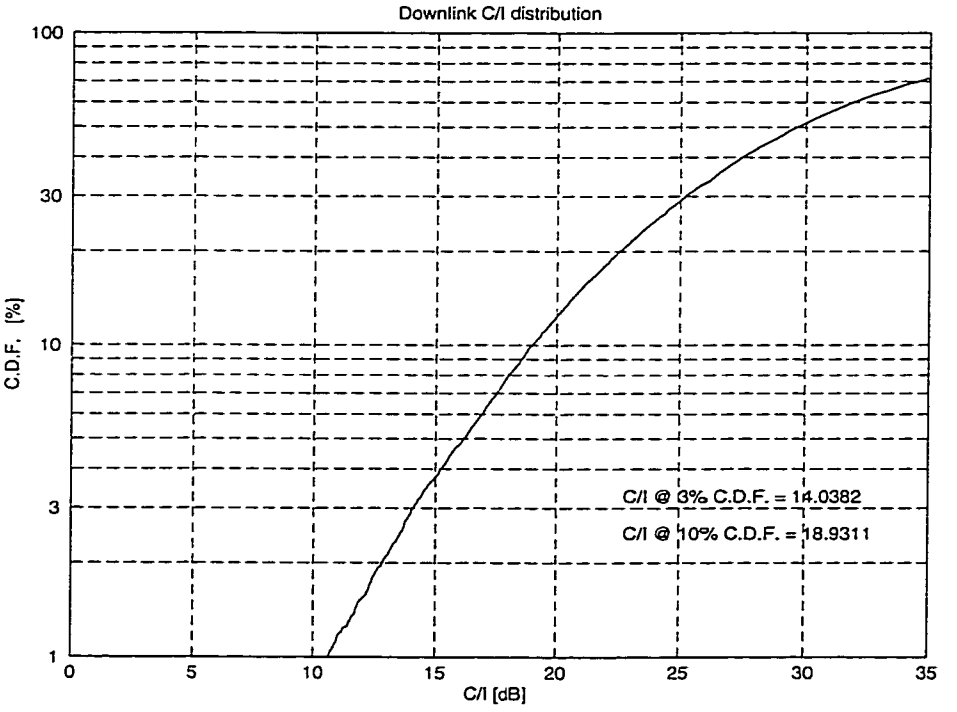

FIGURE 3.5. C/I versus Cumulative Distribution Function (CDF)

Downlink performance is measured as the C/I value at the level of 10% of the downlink cumulative distribution function (CDF) and this is equivalent to 90% of the mobiles in the system having a C/I higher than the value of absicssa. In Digital AMPS, acceptable quality is usually defined by C/I at the 10% CDF level higher than 17 dB i.e. 90% of the mobiles in the system should have a C/I higher than 17 dB. For example, the plot shown in Figure 3.5 is the

C/I vs CDF of the 4/12 reuse system when the narrow-beam transmission is introduced in the system. In this Figure, at 10% CDF the C/I value is 18.93 dB which means, 90% of the connections have a C/I gain of 18.93 dB and above and the rest 10% have less quality than 18.93 dB. This meets the quality criteria of 17 dB as 90% of the links have the quality above 17 dB specified above.

The average system utilization is the ratio of the average number of active communication connections to the total number of communication connections available in the system. All the simulations are carried out at 100% traffic load i.e. number of frequencies per cell is equal to number of mobiles in the cell, in order to assess worst case interference scenario.

3.3.7 Simulation Length

There is a trade-off between speed and precision in the context of computer simulations. In general, simulations require a long period of time to execute. However longer simulations yield more precise results. The simulation results are based on 19440 mobiles in each case. When the downlink power control and narrowbeam transmission are simulated in a 4/12 reuse system with 9 clusters at 100% traffic load, the simulation time is about 18 hours on an Ultra Sparc machine.

3.4 Conclusions

In this chapter, a description of the simulator is given. Different parameters and their values used in the simulator are mentioned. Different antenna patterns used in the simulator are presented. System capacity, system performance and average system utilization are defined, and finally simulation length is specified for the simulations carried out in this thesis work.

CHAPTER 4

SWITCH-BEAM ANTENNA SYSTEM FOR IS-136 SYSTEMS

As was mentioned in section 2.11, cell sectoring is an effective way to reduce cochannel interference and hence increase in system capacity. However, sectorization has been already utilized to its practical limit in many deployed cellular systems. As the demand for wireless service continues to increase, there is a need to explore other techniques to improve capacity in the current spectrum limited cellular systems. In this context smart antennas may potentially improve the system capacity while at the same time extending radio coverage and meeting the quality requirements

In this chapter, state-of-the art realizations of smart antennas for cellular systems will be critically reviewed, leading to the selection of a switched-beam configuration for further study. Then the design and operation of a 4 element switched beam array will be presented in detail. Finally, the impact of the switched beam antenna on system performance in terms of interference and capacity measures will be determined.

4.1 Concept of the Smart Antenna System

A smart antenna is viewed as a mean to obtain significantly improved spectral efficiency, better quality of service, higher capacities while at the same time achieving considerable savings in base station costs. The increase in capacity is achieved by reducing interference more effectively than with conventional base station antennas, which effectively improves the Signal to Interference ratio (C/I). Base station antennas can be classified according to the method by which they process the incoming signals.

A conventional omni-directional antenna exhibits no particular directional properties. Such an antenna cannot distinguish between the desired signals and interfering signals and is inca-

pable of spatial filtering. Spatial filtering is the process which emphasizes the signal received from certain desirable directions and de-emphasizes signal received from other directions. There are several ways to implement spatial filtering. One way is sectorization and another is the use of angular diversity.

In angular diversity, each sector in a cell is subdivided into smaller angular regions, each of which is covered by a narrow beam width antenna. In a simple scheme the antenna which provides the best signal for a particular mobile is selected, and the other antennas that provide inferior signals are disregarded.

A third method to introduce spatial filtering into the system involves the use of adaptive antenna arrays or phased arrays. In this case, a steerable array is used at the base station. This array consists of M antenna elements that are typically spaced one-half wave length apart at the signal frequency. The adaptive array steers a directional beam to maximize the signal from a desired user while nullifying the signals from all other directions, hence reducing cochannel interference. It is possible to use the same physical antenna elements for all channels to adapt an independent beam pattern for each channel in the system. [39]

Adaptive phased arrays are controlled by sophisticated digital signal processing (DSP) algorithms. A smart antenna evaluates signal conditions continuously for each signal that is transmitted or received. The smart antenna then uses this information to determine how to manipulate the incoming signal to maximize performance. The smart antenna constructs a composite signal from multiple antenna feeds by optimizing signal characteristics. [16]

With phased array technology, many of the system parameters that are considered constraints in a single antenna system now become parameters at the disposal of the system designer to further optimize system performance. The advantages of using smart antennas are outlined below.

- Coverage

Adaptive beamforming can increase the cell coverage range substantially through antenna gain and interference rejection. With adaptive antennas employed at base stations there

could be fewer sites required. A larger coverage area is normally achieved with base station antennas placed at a greater height above the average terrain. However, this system trade-off between antenna height and coverage area can be eased by using the number of antenna elements as a design parameter. This leads to substantially eased siting requirements in many situations.

- Capacity

The beamforming at the basestation improves the C/I in the system. The gain achieved through the beamforming may be sufficient to use tighter frequency reuse, thereby increasing the capacity of the system. So, frequency reuse patterns can be substantially improved or reduced through intelligent use of adaptive antennas.

- Signal Quality

In interference limited environments, the additional improvement in tolerable C/I at a single element results from interference rejection afforded against directional interferers. The level of improvement depends on the distribution of cochannel users in neighbouring cells.

- Power Control

Power control requirements of the various modulation methods are somewhat eased through the introduction of adaptive antenna technology. The dynamic link budget control is normally a difficult process, but it can be made substantially easier through the use of angular information about the user signals provided by the adaptive antennas. Power control can be used to ensure maximum use of dynamic range.

- Access Technology

Adaptive beamforming provides an added dimension to the radio interface in addition to any modulation techniques such as FDMA, TDMA, and CDMA. The benefits are multiplicative i.e. temporal gains are multiplied by spatial gains. Equalization is inherent in uplink processing where paths from different angles of arrival are separated by using a particular adaptive beamforming technique. On the downlink, the energy can be focused at the mobile so that long delay multipath components can be reduced substantially. This enables the system to

combat Inter Symbol Interference (ISI) through spatial discrimination of interfering signals. The system can handle a rapidly varying delay spread profile on both links as well as through appropriate signal processing at the basestation on both transmit and receive.

- Hand-Over

In many cases, adaptive antenna technology provides mobile unit location information that can be used by the system to substantially improve hand-offs. With sufficiently accurate position estimates, prediction of velocities is possible which allows further improvements in hand-off strategies. Deciding which cell to handover a mobile is an easier task when we know where the mobile is and how fast it is moving.

- Base station Transmit Power

Using adaptive beamforming, the maximum peak EIRP required per user on a particular channel is less than without adaptive beamforming. The average EIRP is similarly reduced. Though power transmitted is less by using adaptive beamforming, while the antenna array is still able to maintain the same power level at the mobile unit as in the case with out the use of an adaptive antenna.

- Portable Terminal Transmit Power

By introducing adaptive antenna in a system without changing other parameters (e.g. cell size), the transmission power levels required for portable terminals can be reduced as well. The reduction in transmission power levels, which results from the increase in antenna gain at the base station, relaxes the requirements on batteries. Other relevant issues include increased fade margin for improved signal quality (e.g., higher data rates, increased coverage area per cell to decrease deployment costs). With appropriate link management in the system, the power budgets for each of the radio links can be optimized for each particular link dynamically, a process made substantially easier through the use of mobile position estimates provided by adaptive antennas. With the adaptive antennas at the base stations, the transmit power levels from and to the mobile can be kept minimum to provide the requested service.

4.1.1 Switched Beam Approach

There are two basic approaches of smart antennas: switched beam approach and adaptive beam approach. These two types differ according to the method by which they process the incoming signal information. The switched beam approach shown in Figure 4.1 is the basic approach requiring minimum level of complexity.

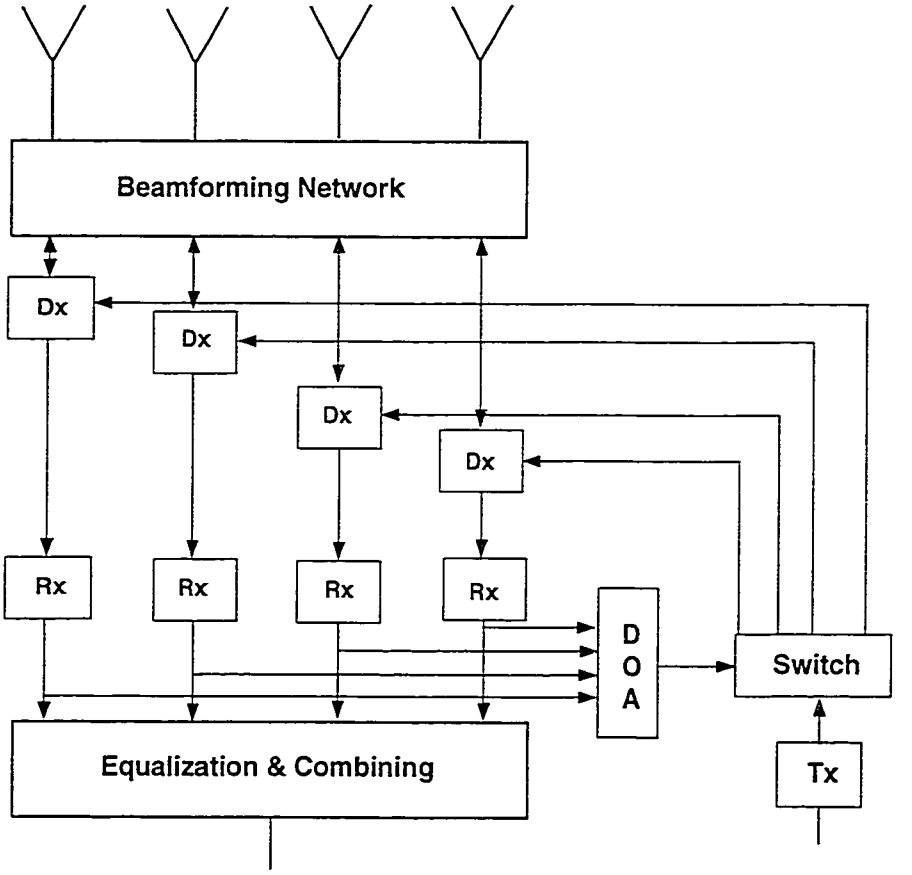

FIGURE 4.1. Schematic diagram of a switched beam antenna approach, including duplex filters (Dx), radio receivers (Rx), radio transmitter (Tx) and units for identifying the suitable beam (DOA) [15].

Here, the same fixed beamforming is adopted in both uplink and downlink. The best beam for downlink transmission is selected from a set of fixed beams derived from the uplink information through the Direction of Arrival (DOA) information.

The DOA can be an estimate of the direction to the mobile station or simply an identification of the best uplink beam. The DOA estimation may be based on signal strength or signal quality so this approach may not require phase coherence between different receiver or transmitter branches. In this approach the number of downlink beams is however limited to the number of receiver branches.

4.1.2 Adaptive Beam or Steered Beam Approach

An adaptive beam approach utilizes fully steerable beams as shown in Figure 4.2. In this approach, the uplink DOA information is used to perform digital beamforming at the base-band. This approach requires one individual transmitter for each antenna element and phase coherency of the branches on both the receiving and transmitting side. Hence this approach probably requires continuous phase calibration since any phase deviation will be detrimental to the beam forming. The advantage is that downlink beamforming is not limited to a fixed set of beams or beamforms. If the positions to the mobiles and interferers are known with sufficient accuracy, downlink interference nulling may be employed.

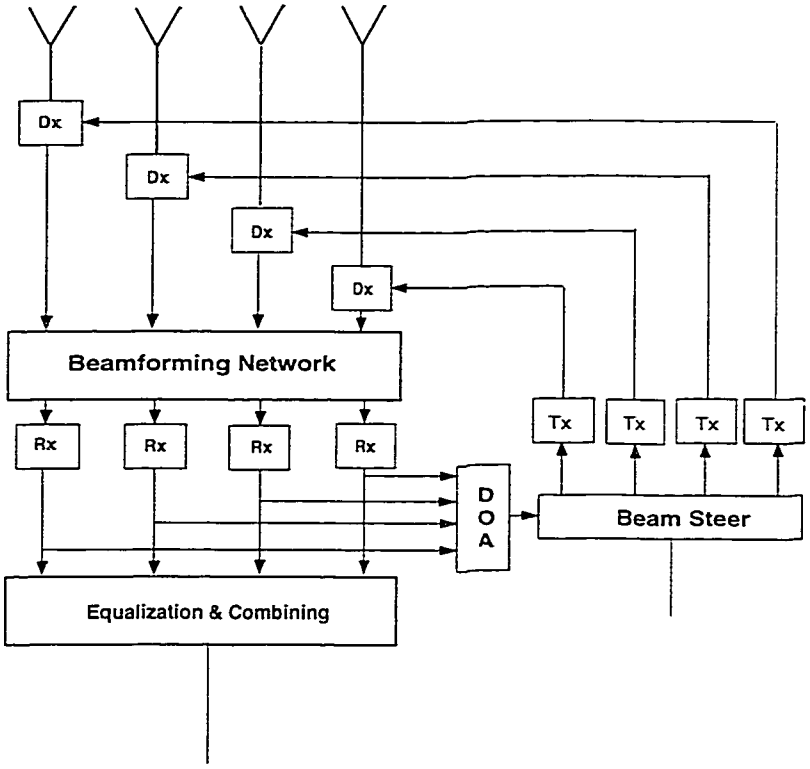

FIGURE 4.2. Schematic Diagram of a Adaptive beam approach or steered beam approach. Notation is same as in Figure 4.1.

4.2 Smart Antenna Realization

In this section, some of the previous contributions mentioned in the literature on smart antennas are outlined. In [1], the performance enhancement of a multibeam adaptive base station antenna was analysed. A comparison between an adaptive antenna capable of forming eight beams and an omni directional antenna showed that the former could provide a three fold increase in spectral efficiency. In [2], the application of adaptive antenna techniques to additionally increase the channel capacity is discussed. Directional sensitivity obtained by employing an antenna array at the base station is proposed. The algorithm given in this paper is based on a high-resolution direction finding step, followed by a linear combination of the sensor outputs to extract the individual signal components.

In [3], the performance of a TDMA system employing smart antennas at the base station is considered. Two adaptation schemes are analysed, the switched-beam approach and an adaptive array based on an adaptation algorithm to maximize the signal to interference and noise ratio. In [4], the performance of adaptive arrays for high data rate indoor environments is examined. The influence of the geometric parameters of the array has been emphasized and showed that at high data rate the radius of the array is a crucial parameter.

In [5], the multibeam antenna proposed in this paper uses selection combining to switch the signals from the two strongest directional beams to the base station's main and diversity receivers. Experimental results showed that in heavy and light urban areas the gain improvements are approximately 2.9 dB and 5.2 dB from 12 and 24 beam antennas respectively.

How an operator can improve the capacity in the network or decrease the number of sites in the network by the use of switch- beam antenna is demonstrated with the simulation results in [6]. Assessment of the impact of the number of beams is also discussed.

The performance and feasibility of switched-beam smart antennas for cellular radio systems is investigated in [7]. Practical considerations such as power control and the limited deployment of smart antenna cells are also addressed. In [8], capacities of different systems like omni, 3 sector, 6 sector and switched beam antenna were compared. The trunking efficiencies of these systems are also compared. The smart antenna system has the best C/I performance at low path loss exponent. However 6 sector cells out-perform smart system in high path loss environments.

Preliminary measurement results for an 8 element adaptive antenna array in an urban environment are presented in [9]. Capacity enhancement while taking into account parameters such as power control, number of hand over channels, radiation pattern and different reuse patterns is studied in [10].

Implementation of a prototype four-element adaptive antenna array for IS-136 base stations is described in [11]. Experimental results showed a 5 dB higher gain at 10^{-2} BER in a

Rayleigh fading environment than a two element array using post detection diversity combining. This corresponds to 40% increase in capacity in a typical mobile radio environment.

A simple method of estimating the spatial signature at lower computational cost than with singular value decomposition (SVD) [12] is proposed in [13]. It is found that the adaptive smart antenna system, which employs the proposed estimation scheme in [13] for a single user scenario, can obtain as high an antenna gain as that of using the method in [12] when SNR is reasonably high.

In [14], an overview of how antenna array technology can be used to improve digital cellular systems is given. In [15], the use of adaptive antennas to receive and transmit in narrow beams improves both uplink and downlink C/I. A much tighter frequency reuse can be employed in the system with the gain achieved due to this beamforming, thereby increasing the capacity of the system.

4.3 Antenna Arrays in Mobile Communications

Usually the radiation pattern of a single element antenna is relatively wide, and each element provides low values of directivity (gain). In the proposed antenna system, the objective is to design antennas with very directive characteristics (very high gains) to reduce the co-channel interference in the system. This can only be accomplished by increasing the electrical size of the antenna. Enlarging the dimensions of the single elements often lead to more directive characteristics. Another way to enlarge the dimensions of the antenna, without necessarily increasing the size of the individual elements, is to form an assembly of radiating elements in an electrical and geometrical configuration. This structure formed by multi-elements, is referred to as an array. In most cases the elements of an array are identical. This is often convenient and more practical.

Neglecting coupling between the elements, the total field of the array is determined by the vector addition of the fields radiated by the individual elements. To provide very directive patterns it is necessary that the fields from the elements of the array interfere constructively

(add) in the desired direction and interfere destructively (cancel each other) in the remaining directions. In an array of identical elements, there are five controls that can be used to shape the overall pattern of the antenna [17]. These are:

1. the geometrical configuration of the overall array (linear, circular, rectangular, spherical, etc.)

2. the relative distance between the elements

3. the excitation amplitude of the individual elements

4. the excitation phase of the individual elements

5. the relative pattern of the individual elements

Arrays offer the unique capability of electronic scanning of the main beam. By changing the phase of the exciting currents in each element antenna of the array, the radiation pattern can be scanned through the space. The array is then called a *phased array* [18]. Arrays are found in many geometrical configurations. The most elementary is that of a *linear array* in which the array element centres lie along a straight line. The elements may equally or unequally be spaced. When the array element centres are located in a plane it is said to be a *planar array.* In mobile applications we mostly use linear arrays. From standard antenna theory, the total field of a two element linear array is equal to the field of a single element positioned at the origin multiplied by a factor called the array factor. For a two element array of constant amplitude, the array factor is given by [17]

in normalized form

$$(AF)_n = \cos[1/2(kd\cos\theta + \beta)] \qquad (1)$$

where k is the phase constant i.e.$2\pi/\lambda$, d is the distance between the elements, θ is the usual spherical coordinate, and β is the phase between the antenna elements.

The array factor is a function of the geometry of the array and the excitation phase. By varying the separation d and / or the phase β between the elements, the characteristics of the array factor and of the total field of the array can be controlled.

The far-zone field of a uniform two-element array of identical elements is equal to the product of the field of a single element, at a selected reference point (usually the origin), and the array factor of that array. That is

$$\mathbf{E}(\text{total}) = [\mathbf{E}(\text{single element at reference point})] \times [\text{array factor}] \qquad (2)$$

This is referred to as pattern multiplication for arrays of identical elements. It is also valid for arrays with any number of identical elements which do not necessarily have identical magnitudes, phases and or spacing between them.

The array factor, in general, is a function of the number of elements, their geometrical arrangement, their relative magnitudes, their relative phases, and their spacings.

4.3.1 N-Element Linear Array: Uniform Amplitude and Spacing

The array factor shown in equation (1) is for a 2 element array and then generalized to include N elements in the array. Referring to the geometry in Figure 4.3, let us assume that all the elements have identical amplitudes but each succeeding element has a β progressive phase lead current excitation relative to the preceding one (β represents the phase by which the current in each element leads the current of the preceding element). An array of identical elements all of identical magnitude and each with a progressive phase is referred to as a uniform array.

The array factor can be obtained by considering the elements to be point sources. If the actual elements are not isotropic sources, the total field can be formed by multiplying the array factor of the isotropic sources by the field of a single element.

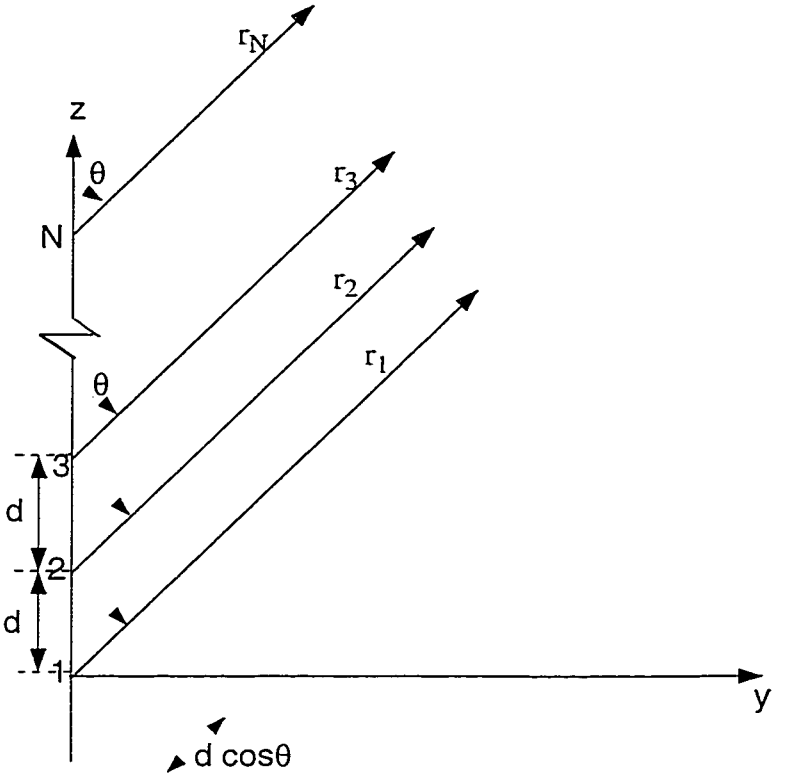

FIGURE 4.3. Far-field geometry of N-element array of isotropic sources positioned along the z-axis [17]

The array factor is given by,

$$AF = 1 + e^{j(kd\cos\theta + \beta)} + e^{j2(kd\cos\theta + \beta)} + \ldots\ldots + e^{j(N-1)(kd\cos\theta + \beta)} \quad (3)$$

which can be written as,

$$AF = \sum_{n=1}^{N} e^{j(n-1)(kd\cos\theta + \beta)} \quad (4)$$

or more simply,

$$AF = \sum_{n=1}^{N} e^{j(n-1)(\psi)} \qquad (5)$$

$$\text{where } \psi = kd\cos\theta + \beta \qquad (6)$$

Multiplying both sides of equation (6) by $e^{j\psi}$ and after mathematical simplification equation (5) reduces to,

$$(AF)_n = \left(\frac{1}{N}\right)\left[\frac{\sin\left(\frac{N}{2}\psi\right)}{\sin\left(\frac{1}{2}\psi\right)}\right] \qquad (7)$$

For small values of ψ, the above expression can be written as

$$(AF)_n = \left[\frac{\sin\left(\frac{N}{2}\psi\right)}{\left(\frac{N}{2}\psi\right)}\right] \qquad (8)$$

This is the normalized array factor for an N element, uniformly excited, equally spaced array which is entered about the coordinate origin. From Figure 4.4 to Figure 4.6, the array factors for three values of N are presented for an array having $d = 0.5\lambda$.

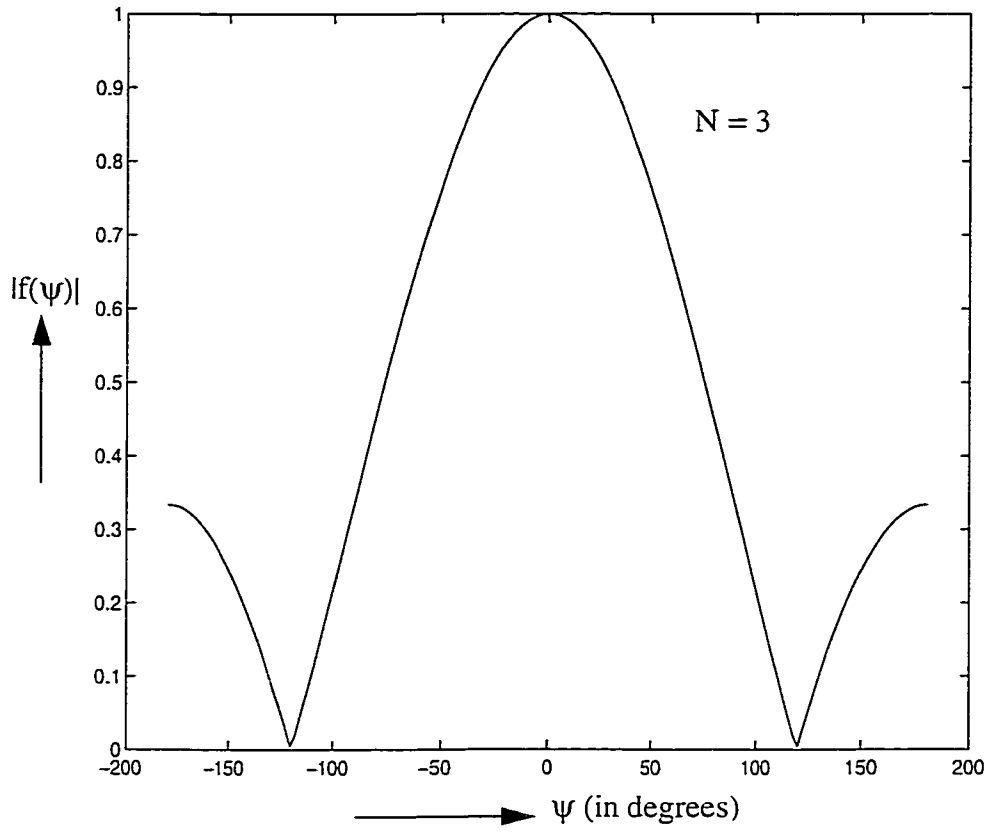

FIGURE 4.4. Array factor of an equally spaced (d = 0.5λ), uniformly excited three element linear array.

By examining Figure 4.4, Figure 4.5 and Figure 4.6 a number of trends can be seen.

1. As N increases the main lobe narrows.

2. As N increases there are more side lobes in one period of f(ψ), the normalized array factor. In fact, the number of full lobes (one main lobe and the side lobes) in one period of f(ψ) equals N-1. Thus there will be N-2 side lobes and one main lobe in each period.

3. The minor lobes are of width $2\pi/N$ in the variable ψ and the major lobes are twice this width.

4. The side lobe peaks decrease with increasing N. A measure of the side lobe peaks is the side lobe level, which is defined as

SLL = |maximum value of largest side lobe| / |maximum value of main lobe|

and is often expressed in decibels.

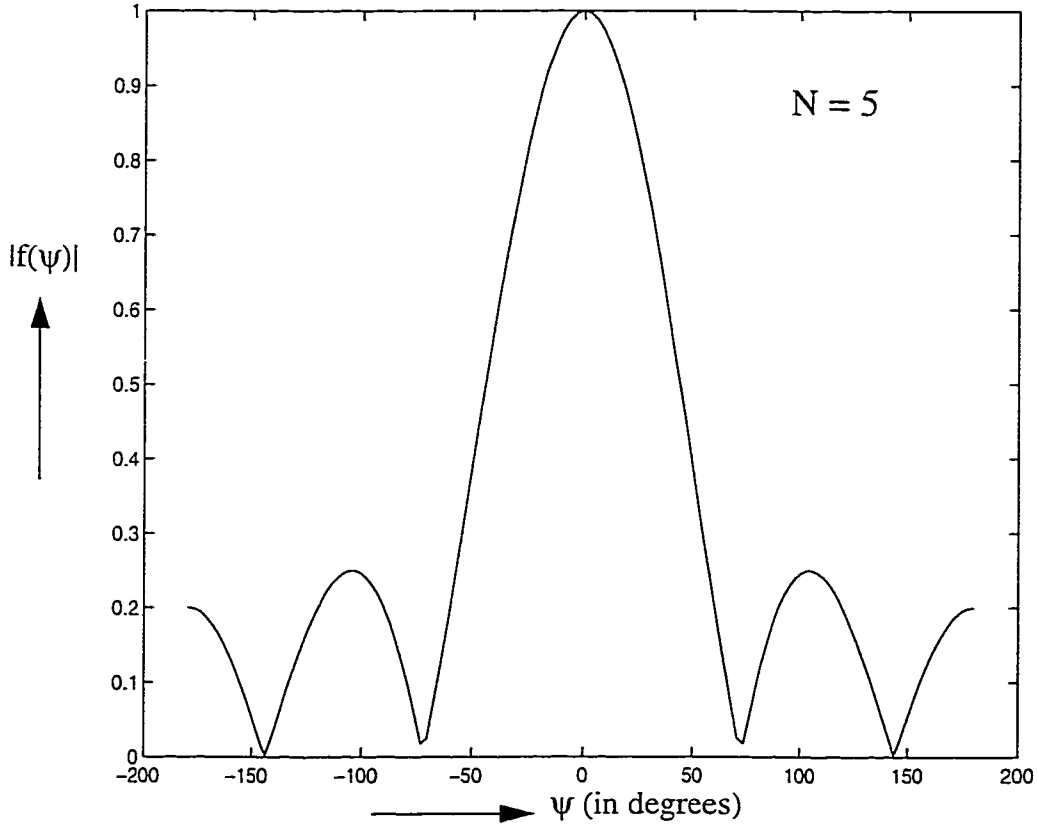

FIGURE 4.5. Array factor of an equally spaced (d = 0.5λ), uniformly excited five element linear array.

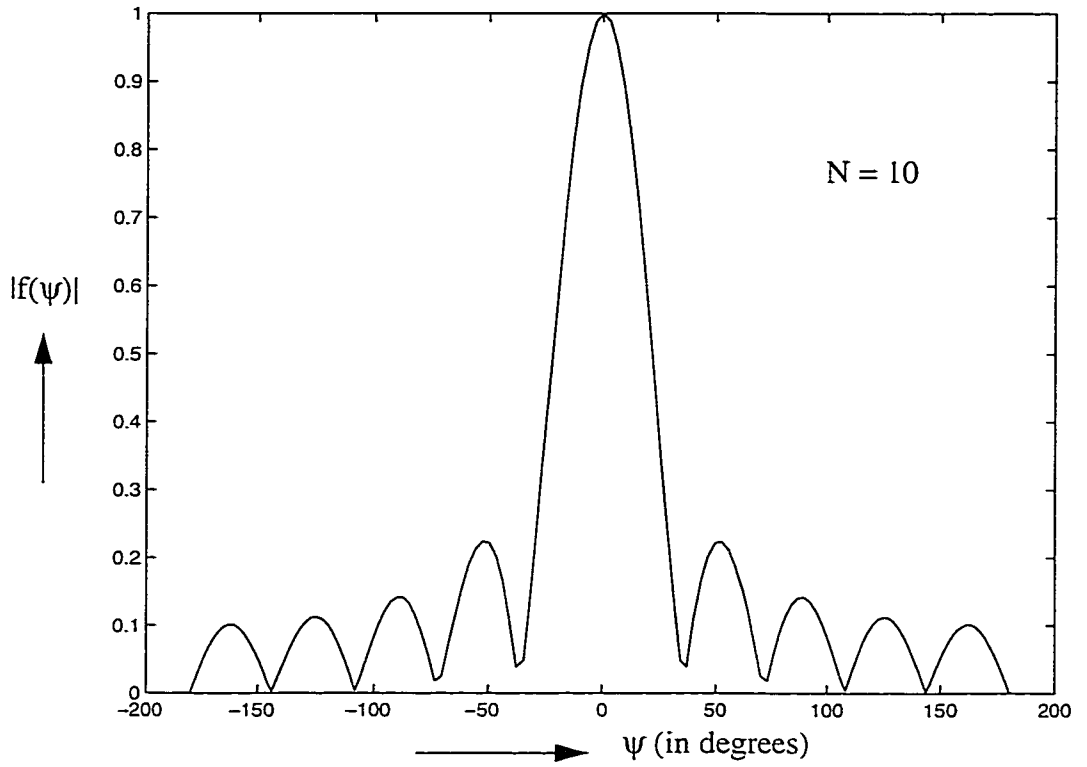

FIGURE 4.6. Array factor of equally spaced uniformly excited (d = 0.5λ) ten element array

4.3.2 Main Beam Scanning and Phased Arrays

A maximum of an array factor occurs for $\psi = 0$. Let θ_0 be the corresponding value of θ for which the array factor is maximum. Then from equation 6, we have, $0 = kd\cos\theta_0 + \beta$, or

$$\beta = -kd\cos\theta_0 \qquad (9)$$

This is the element-to-element phase shift in the excitation currents required to produce an array factor main beam maximum in a direction θ_0 relative to the line along which the array elements are disposed.

For the broadside case ($\theta_0 = 90^o$), $\beta = 0$. For the end fire case ($\theta_0 = 0^o$ or 180^o), $\beta = -kd$ or kd. This main beam scanning by phase control feature can be explicitly incorporated into ψ by substituting (9) into (6),

$$\psi = kd\ (\cos\theta - \cos\theta_0) \qquad (10)$$

An array antenna whose main beam maximum direction or pattern shape is controlled primarily by the relative phase of the element excitation currents is referred to as a ***phased array.*** By controlling the progressive phase difference between the elements the maximum radiation can be squinted in any desired direction to form a scanning array. This is the basic principle of electronic scanning phased array operation. Figure 4.7 shows the patterns of a linear array with different linear phase shifts. Note that as the beam is scanned from broadside ($\theta_0 = 90^o$) the main beam broadens. If the phase of each element is changed with time according to Equation (9) the pattern is scanned and thus the main beam pointing direction θ_0 changes with time.

This is called beam broadening. Remember that the entire pattern is formed by rotating the pattern shown around the z-axis. It turns out that as the main beam is scanned away from broadside the main beam broadening is just about compensated by the reduced volume contained in the total pattern (formed by rotation about the array axis).

Figure 4.8 shows the array factor pattern when the spacing between the array elements is reduced to $\mathbf{0.4\lambda}$ of a uniformly spaced and uniformly excited four element scanning array. For equally spaced arrays with spacings less than half-wave length, as the beam approaches endfire it is not broadening as rapidly as is the pattern volume decreasing. Therefore, the directivity remains nearly constant for wide scan angles about broadside but increases near endfire.

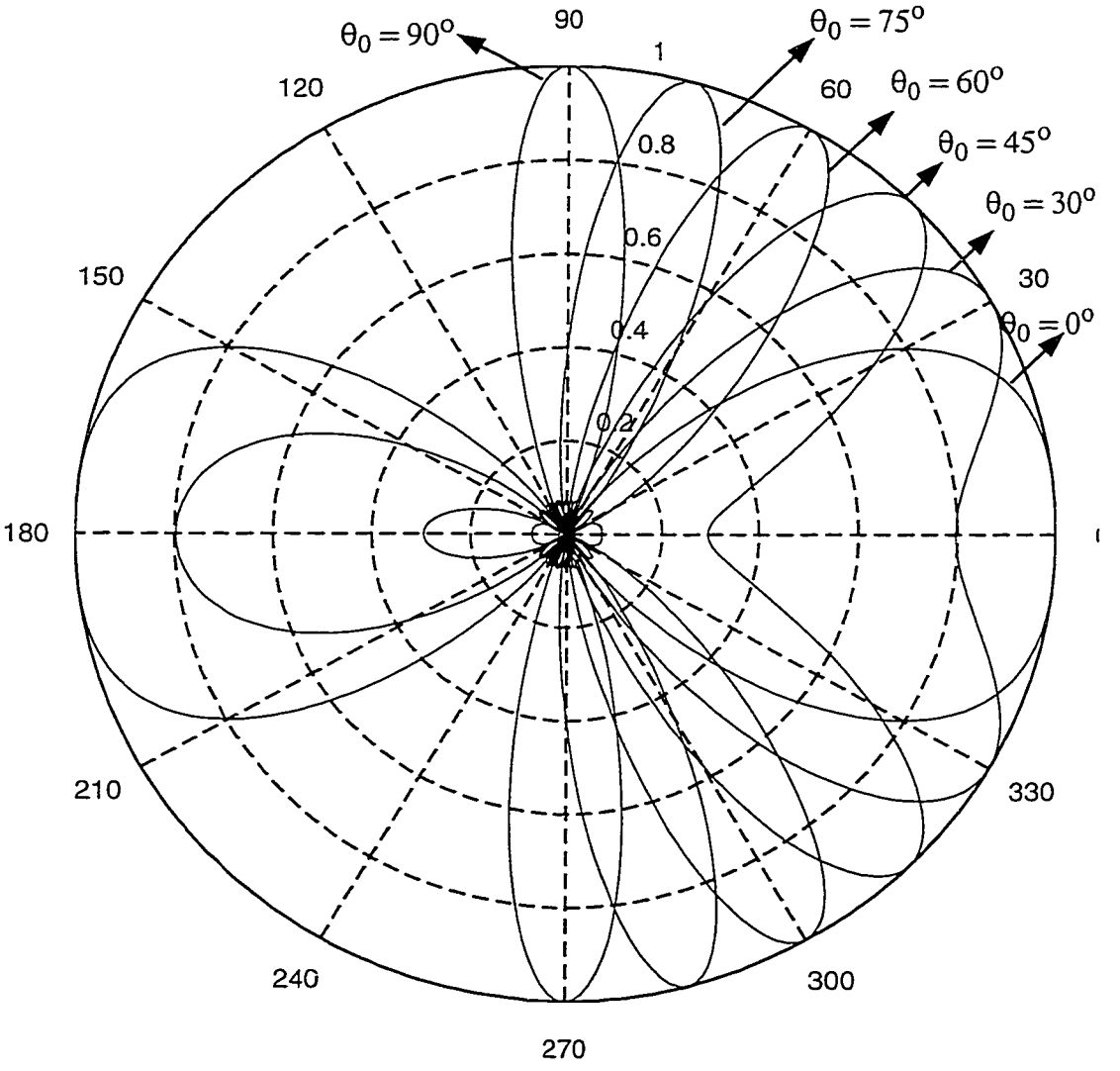

FIGURE 4.7. Array factor pattern for 4-element uniformly excited equally spaced (d = 0.5λ) scanning array.

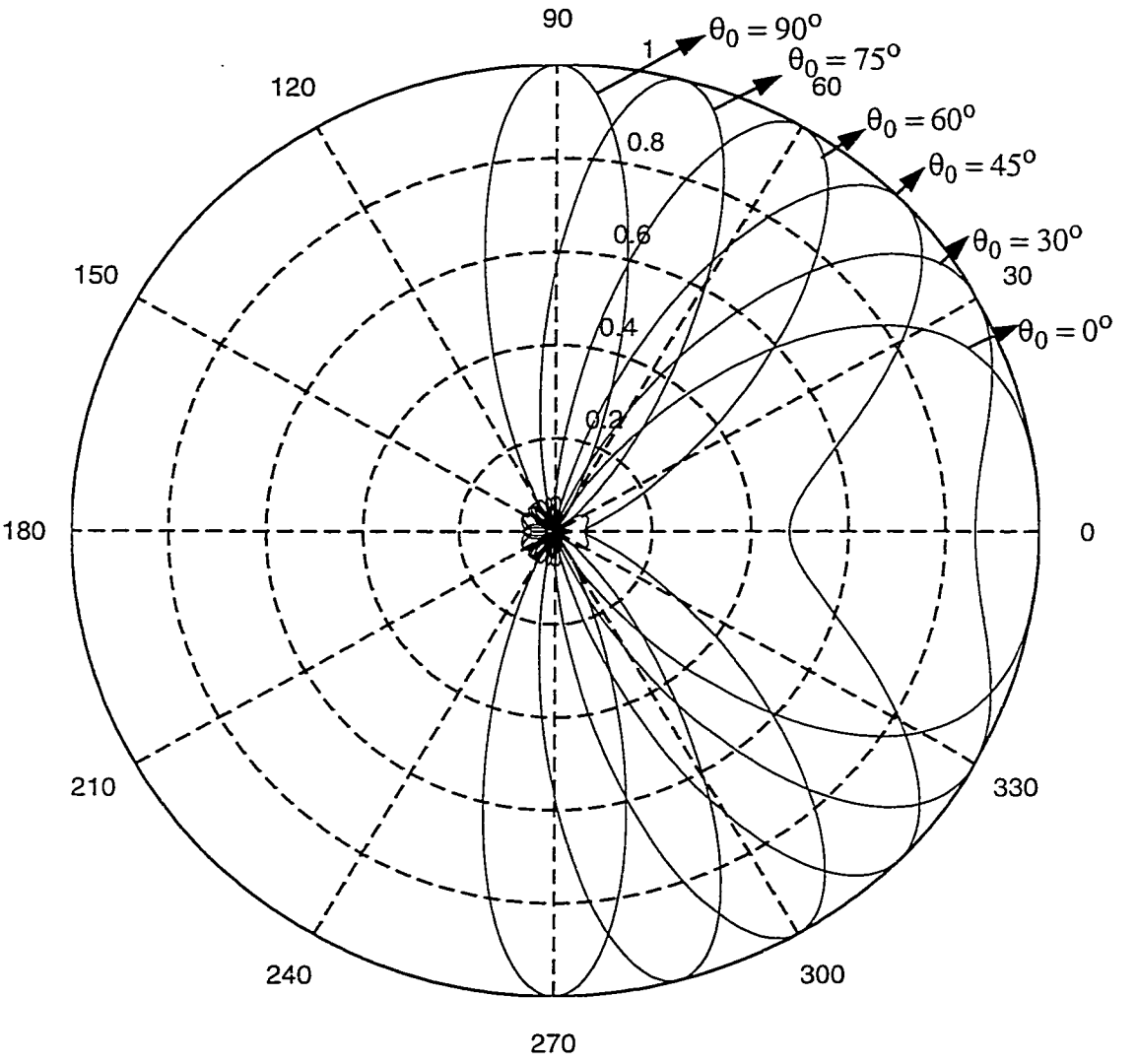

FIGURE 4.8. Array factor pattern for 4-element uniformly excited equally spaced ($d = 0.4\lambda$) scanning array.

Figure 4.9 shows the array factor pattern when the spacing between the array elements is increased to $\mathbf{0.6\lambda}$ of a uniformly spaced and uniformly excited four element scanning array. For slightly greater than half-wavelength spacings, a grating lobe begins to appear for scan angles near endfire and the directivity decreases. For spacings greater than a half-wavelength, part or all of a grating lobe will become visible before endfire is reached.

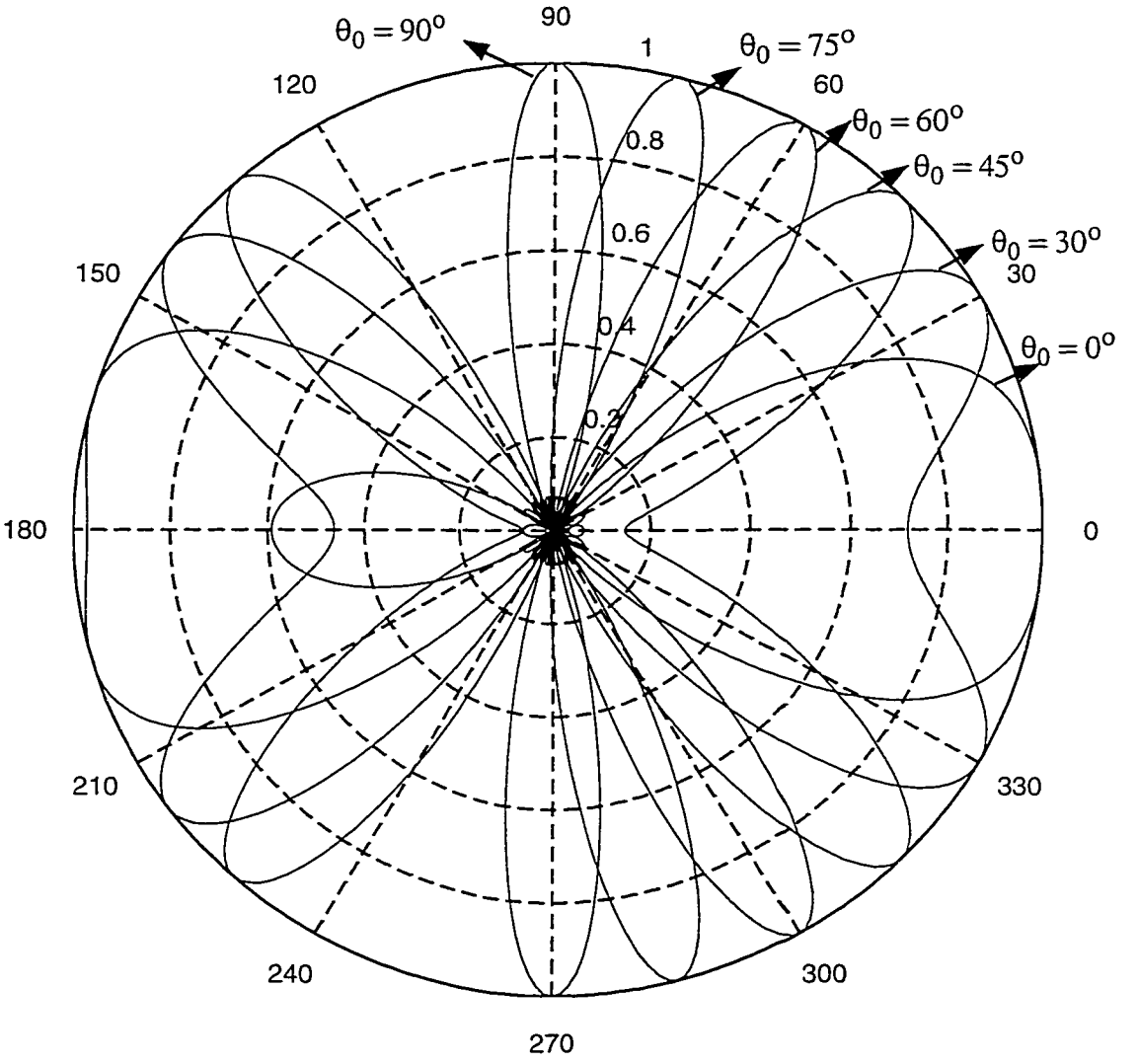

FIGURE 4.9. Array factor pattern for 4-element uniformly excited equally spaced (d = 0.6λ) scanning array.

When large inter-element spacings are used and many grating lobes appear in the visible region the array is called an interferometer. However, if large element antennas are used, the element pattern will also have a relatively narrow beam which will decrease the size of the grating lobes.

Apart from grating lobes (undesired radiation), the performance of an element operating in the array environment is different from its performance when it is isolated. Each element of the array is effected by the presence of the other elements. This is due to mutual coupling between the elements. Since this mutual coupling depends on the array geometry, the performance of the elements will vary with the location in the array as well as scan angle. During the design of a phased array the problem of mutual coupling has to be given serious consideration to avoid any mutilation of beam patterns. Another important design issue is feed mechanism to the array and proper power distribution to the array elements.

Since the phased arrays are being discussed in the context of switch-beam antennas, the idea here is to produce four narrow beams in a 120^{o} sector of a cell in a cellular system. The phase variation between the array elements is established by using either a digital beamformer or analog beamformer to produce four narrow beams in a 120^{o} sector. In the next section the beamforming networks to produce the desired beam pattern are discussed.

4.4 Beamforming

The term beamforming relates to a function performed by a device in which energy radiated by an antenna is focused along a specific direction in space. The objective is to either preferentially receive a signal from that direction or to preferentially transmit in that direction. Beamforming is often referred to as spatial filtering. Several approaches can be used to direct the radiated power from an antenna array in narrow beam. The phase front on the antenna elements corresponding to a beam can be generated at base-band using digital beamforming or at RF using analog beamforming. Base band beamforming techniques always require phase coherence all the way to the antenna elements. One main advantage of using analog beamforming at the RF stage is that, it avoids maintaining phase coherence between the radio transmitter and the beamformer.

4.4.1 Digital Beamforming

Digital beamforming (DBF) is a combination of antenna technology and digital technology. A general DBF antenna system shown in Figure 4.10 consists of three major components: the antenna array, the digital transceivers, and the digital signal processor.

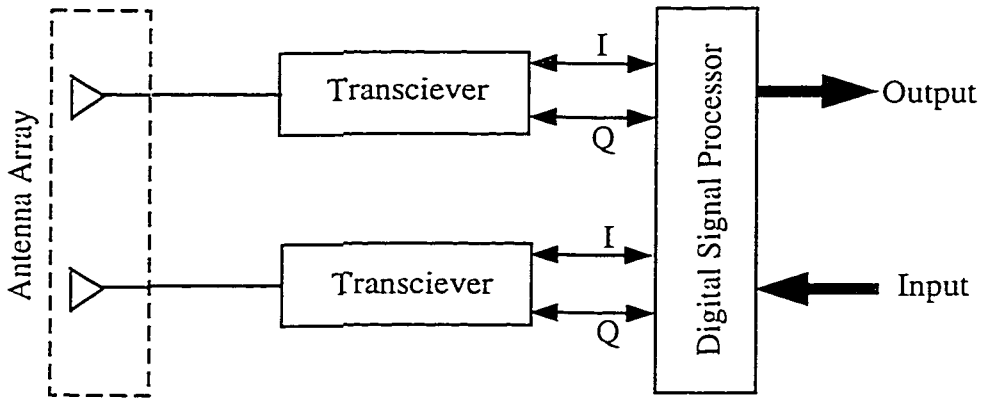

FIGURE 4.10. A general Digital Beamforming Antenna System

In digital beamforming antenna system, the received signals are detected and digitized at the element level. By capturing the RF information in the form of digital stream, a large domain of signal processing techniques and algorithms can then be used to extract information from the spatial domain data. Digital beamforming is based on capturing the radio frequency (RF) signals at each of the antenna elements and converting them into two streams of binary base-board signals (i.e. in-phase (I) and quadrature-phase (Q) channels). Within the digital base-band signals, the amplitudes and phases of the signal received are included. The beamforming is carried out by weighting these digital signals, thereby adjusting their amplitudes and phases such that when added together they form the desired beam. This process can be carried out using a special purpose digital signal processor. That is, the function, which is usually carried out using an analog beamforming network, is now carried out using a digital processor. This approach preserves the total information available at the radiating element. The important part in this DBF is the accurate translation of analog signals to digital signals. By using digital beamforming, a wide range of types of beams can be produced

including scanned beams, multiple beams, shaped beams, and beams with steered nulls. The following are some of the attractive features of using digital beamforming over conventional phased arrays [40].

1. A large number of independently steered high-gain beams can be formed without any resulting degradation in signal to noise ratio.

2. All of the information arriving at the antenna array is accessible to the signal processors so that system can be optimized.

3. Beams can be assigned to individual users, thereby assuring that all links operate with maximum gain.

4. Adaptive beamforming can be easily implemented to improve the system capacity by suppressing cochannel interference. Adaptive beamforming can be used to enhance the system immunity to multipath fading.

5. DBF systems are capable of carrying out antenna system real time calibration in the digital domain. Therefore, the requirements for a close match amplitude and phase between transceivers can be relaxed, because variation in these parameters can be corrected in real time.

Adaptive beamforming technology is also referred to as smart antenna technology in some literature. The use of "smart" reflects the antenna's ability to adapt to the environment in which it operates. So "smart antennas" and "adaptive antennas" are interchangeable and in this work these two names are used interchangeably.

Though current day technology supports the implementation of digital beamforming in mobile communications, practical aspects such as implementation costs and the complexity of the circuitry are some of the major obstacles in implementing these systems. In this context analog beamforming gives a more promising result with lower costs. Although analog beamforming techniques do not yield as much gain as the digital beamforming, the implementation costs and complexity of the circuitry are less and hence are an attractive solution

as far as an operator's point of view is concerned. In this work an analog beam former will be used to generate four narrow beams per sector.

4.4.2 Analog Beamforming

When an antenna array is illuminated by a source, samples of the source's wavefront are recorded at the location of the antenna elements. The outputs from elements can then be subjected to various forms of signal processing, wherein phase or amplitude adjustments are made to produce outputs that can provide concurrent angular information for signals arriving in several different directions in space [40]. When the outputs of the elements of an array are combined via some passive phasing network, the phasing will usually arrange for the output of all the elements to add coherently for a given direction. The network that controls the phases and amplitude of the excitation current is usually called the beamforming network. If beamforming is carried out at RF, the analog beamforming network usually consists of devices that change the phase and power of the signals. In mobile communications it is desirable to form multiple beams that are offset by finite angles from each other. The design of a multiple beam beamforming network is much more complicated than that of a single beam beamforming network and involves the use of a beamforming matrix. The best known passive beamforming network is Butler Matrix [19]. In such a matrix, an array of hybrid junctions and fixed phase shifters is used to achieve the desired beam pattern. A Butler matrix is the analog implementation of the fast Fourrier transform, and as such requires N log N signal combinations (sums, differences) to excite N beams of an N-element array from N input ports. An example of a four beam, four element Butler beamforming matrix is shown in Figure 4.11. This matrix uses four 90^{o} phase lag hybrid junctions with the transmission properties shown in Figure 4.11(b) and two 45^{o} fixed phase shifters. By tracing the signal from the four ports to the array elements, one should be able to verify the aperture relative phase distribution corresponding to the individual ports of a four-port Butler matrix, shown in Table 4.1. The basic Butler matrix produces symmetrical orthogonal beams. If the elemental spacing is $\lambda/2$, the system produces four beams as shown in Figure 4.12 (although with significant side lobes).

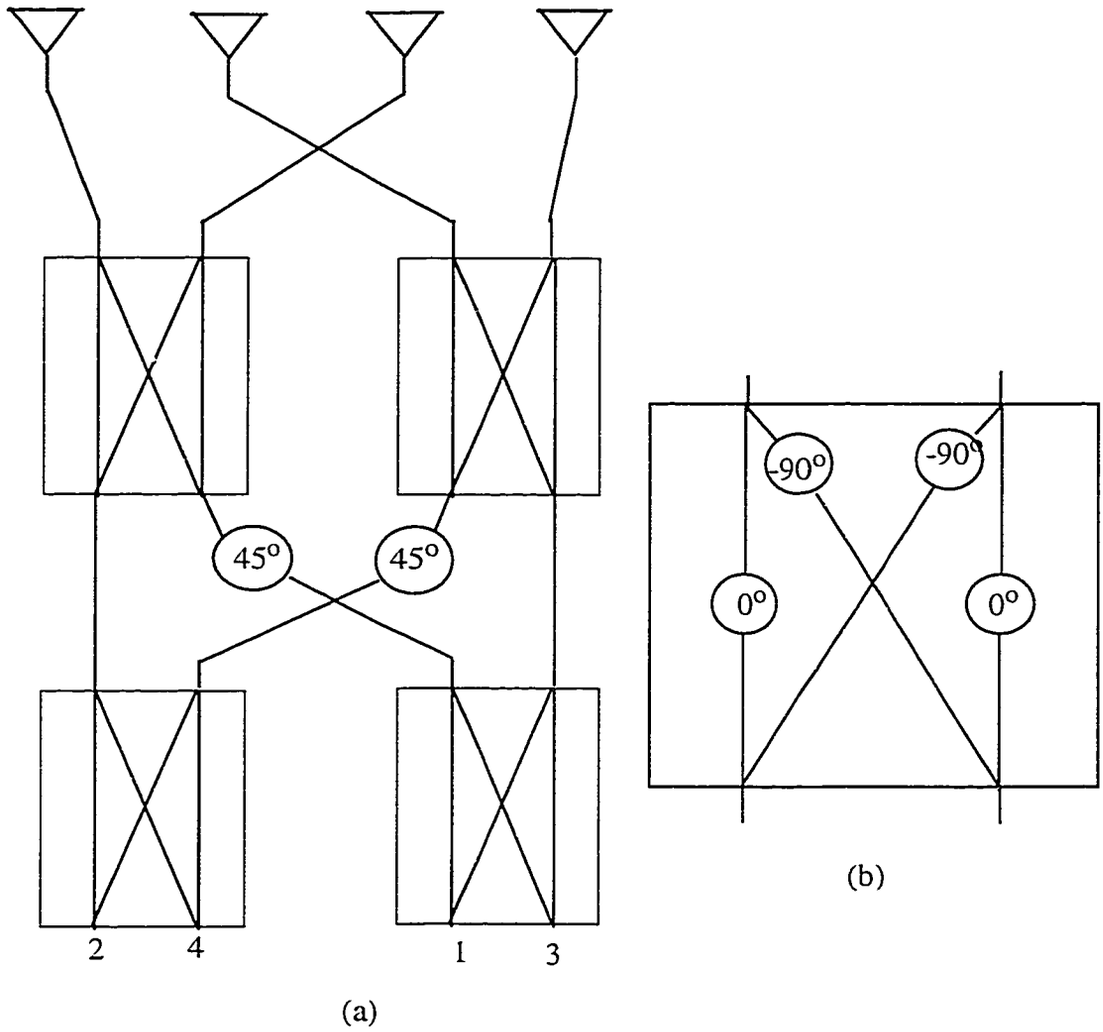

FIGURE 4.11. A Butler Beamforming matrix for a four-element array: (a) 4 x 4 Butler matrix; (b) a hybrid used in the matrix

TABLE 4.1. Array Aperture Phase Distribution

	Phase Distribution			
Port 1	0°	-135°	-270°	-405°
Port 2	0°	-45°	-90°	-135°
Port 3	0°	45°	90°	135°
Port 4	0°	135°	270°	405°

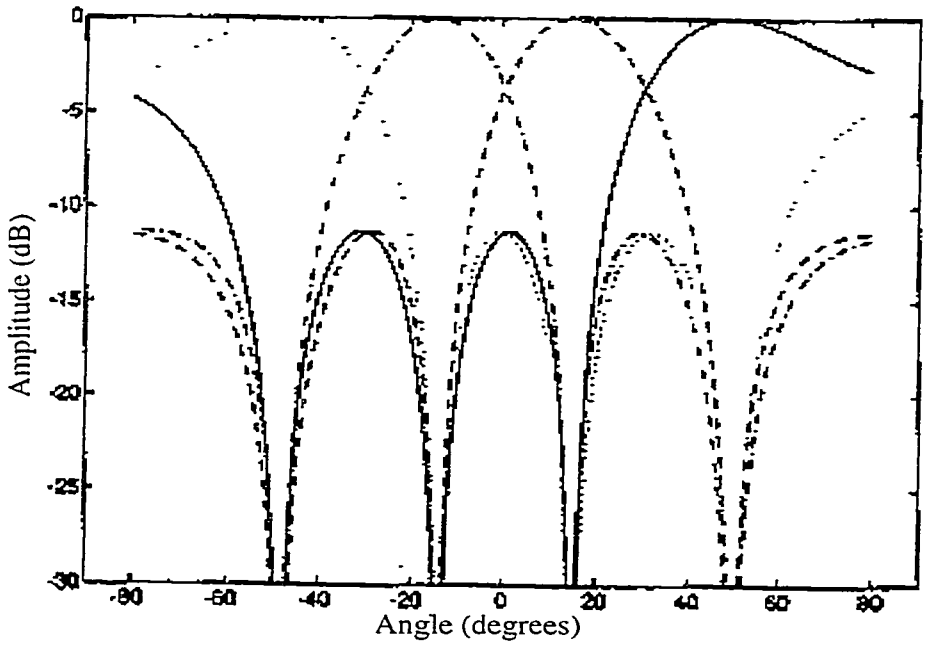

FIGURE 4.12. Four mutually orthogonal overlapped beams produced by the Butler beamforming matrix [40].

4.4.3 Multiple Beam Antenna Systems

While phased arrays have a single output port, multiple beam systems have a multiplicity of output ports, each corresponding to a beam with its peak at a different angle in space. Many antenna requirements emphasize high gain with low side lobes. In addition, it is often important that the system have a high beam cross over level so that nearly the system gain is available within any point in the antenna field of view. The beam crossover level is shown in Figure 4.13 as the relative gain of either of two adjacent beams at the point of their intersection.

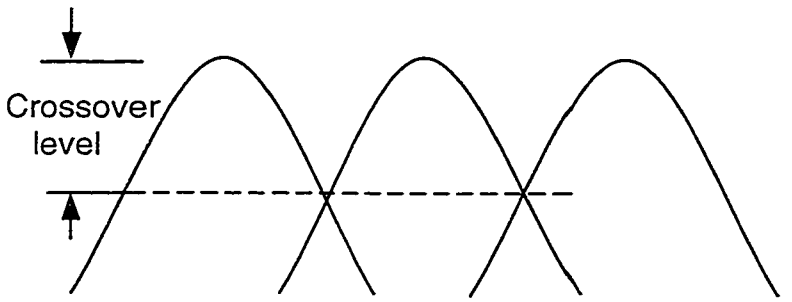

FIGURE 4.13. Multiple beam systems: beam crossover

Beam crossover loss is an important factor in the design of multiple-beam systems. Ideally, one would like to produce low-sidelobe beams and stack them close together so that the crossover levels are only a decibel or two below the beam peaks. When implemented with a passive, lossless beamformer, this condition leads to excessive network loss because of the non orthogonality of the closely packed beams. Considerable work has been done with regard to side lobe level suppression and can be found in [20] to [24]. Another critically important feature of multiple-beam forming networks is that they should be lossless, or have minimal loss, in order that the reduced gain not render the system impractical. Other disadvantages of multiple-beam beamformers include the difficulty of reconfiguring beamformer (i.e., to expand or modify its characteristics). As the number of beams increases, the SNR of channels being carried by the individual beams decreases. This comes from the fact that noise is introduced due to the additional RF and IF components that needed to increase the beamformer's capacity. Another disadvantage is that the separation between the multiple beams cannot be any less than that for orthogonal beams without considerable decrease in system SNR. In the next section system level simulations are carried out using a network simulator by employing switch beam antennas in place of sector antenna pattern.

In section 4.3 and section 4.4 a brief description was given on antenna arrays and beamforming techniques. The basic antenna used for simulations is a four column antenna array with a horizontal element spacing of 0.5 λ [15]. Such an antenna array with an antenna gain around 18 dBi will have an area slightly below 1 m^2 at cellular (850 MHz) and 0.25 m^2 at

PCS bands (1900 MHz). The antenna patterns of a sectored pattern and 4 narrow beams per 120^{o} sector are shown in Figure 3.3 and Figure 3.4 (Chapter 3). These antenna patterns are used in the simulator.

4.5 System Model for Simulations & Simulation Results

A homogeneous system comprising nine clusters of the same size is studied. Traffic is generated with equal probability over the simulated area and all mobile stations are static. Channel utilization is 100%. The system level simulations are carried out in an interference limited system consisting of 3 sector cells. No adjacent channel interference is included in the model. In the simulations the mobile transmitter was considered as a point source and the angle between the base station and mobile station was assumed to be known, that is the estimation of the direction of arrival was assumed to be perfect.

The propagation environment is assumed to follow the 35log(d) Okumura-Hata path loss model with an additional lognormal fading having a standard deviation of 6 dB, as discussed in Chapter 3. The cell radii are set to 1000 meters. Downlink performance is measured as the C/I value at the 10% level of the downlink cumulative distribution function (CDF). In IS-136 systems, the acceptable quality level is usually defined by C/I at the 10% CDF level higher than 17 dB. Served traffic is defined as the average number of users per cell divided by the number of channels in the system. No downlink or uplink power control is employed in the system i.e. all the links transmit at the same power level.

4.5.1 Performance of a Conventional Sectored Antenna System

Initially, systems with conventional 3 sector antennas were simulated at full load. These results are used as a reference for the performance of switched-beam antenna. Figure 4.14 presents cumulative distribution functions of downlink C/I for a 7/21 reuse, 4/12 reuse and 3/9 reuse systems with a conventional sector antenna. Figure 4.15 to Figure 4.17 present the interference distribution of 7/21, 4/12, 3/9 reuse systems with this antenna configuration.

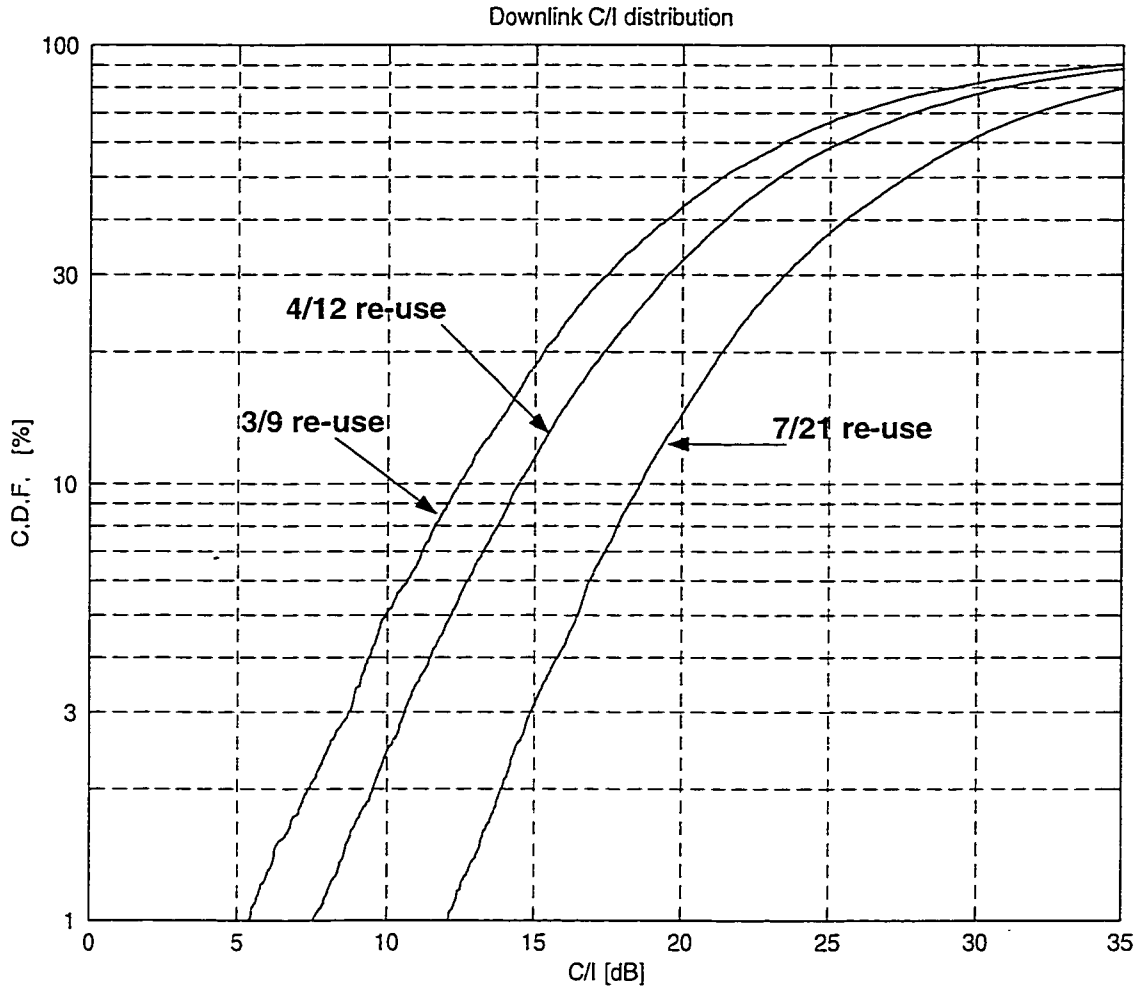

FIGURE 4.14. Cumulative Distribution Functions of downlink C/I for a 7/21, 4/12 and 3/9 reuse systems with a conventional sector antenna configuration

In Table 4.2 the served traffic and the downlink C/I values at the 10% CDF level are presented for different frequency reuse patterns.

TABLE 4.2. Served traffic and downlink C/I at 10% CDF level fro 7/21, 4/12 and 3/9 systems at full load

Frequency reuse pattern	Served traffic (user/ cell/channel	Downlink C/I at 10% CDF level (dB)	Downlink C/I at 3% CDF level (dB)
7/21	0.048	18.57	14.87
4/12	0.083	14.45	10.58
3/9	0.111	12.40	8.70

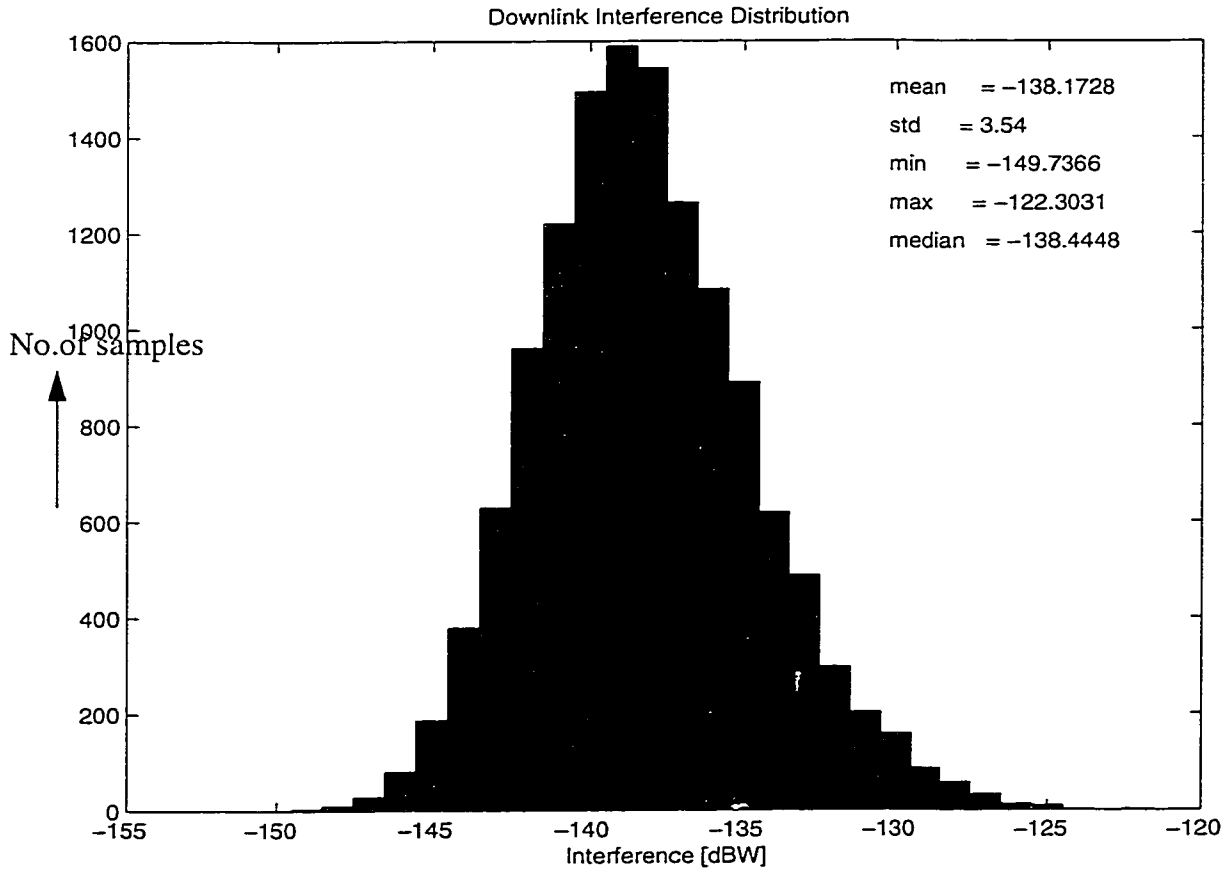

FIGURE 4.15. Downlink Interference distribution of 3 sectored, 7/21 reuse system.

Figure 4.15 presents the downlink interference for a 3 sectored 7/21 reuse in the system. The mean of the interference distribution is -138.17 dBW. In general, the mean is the average of the distribution. If the mean of the interference distribution is minimum i.e. large negative number, then the interference in the system is less and C/I is high. The median represents the maximum number of links having a particular interference level while standard deviation gives the distribution spread. The min. and max. values are the minimum and maximum values of the distribution.

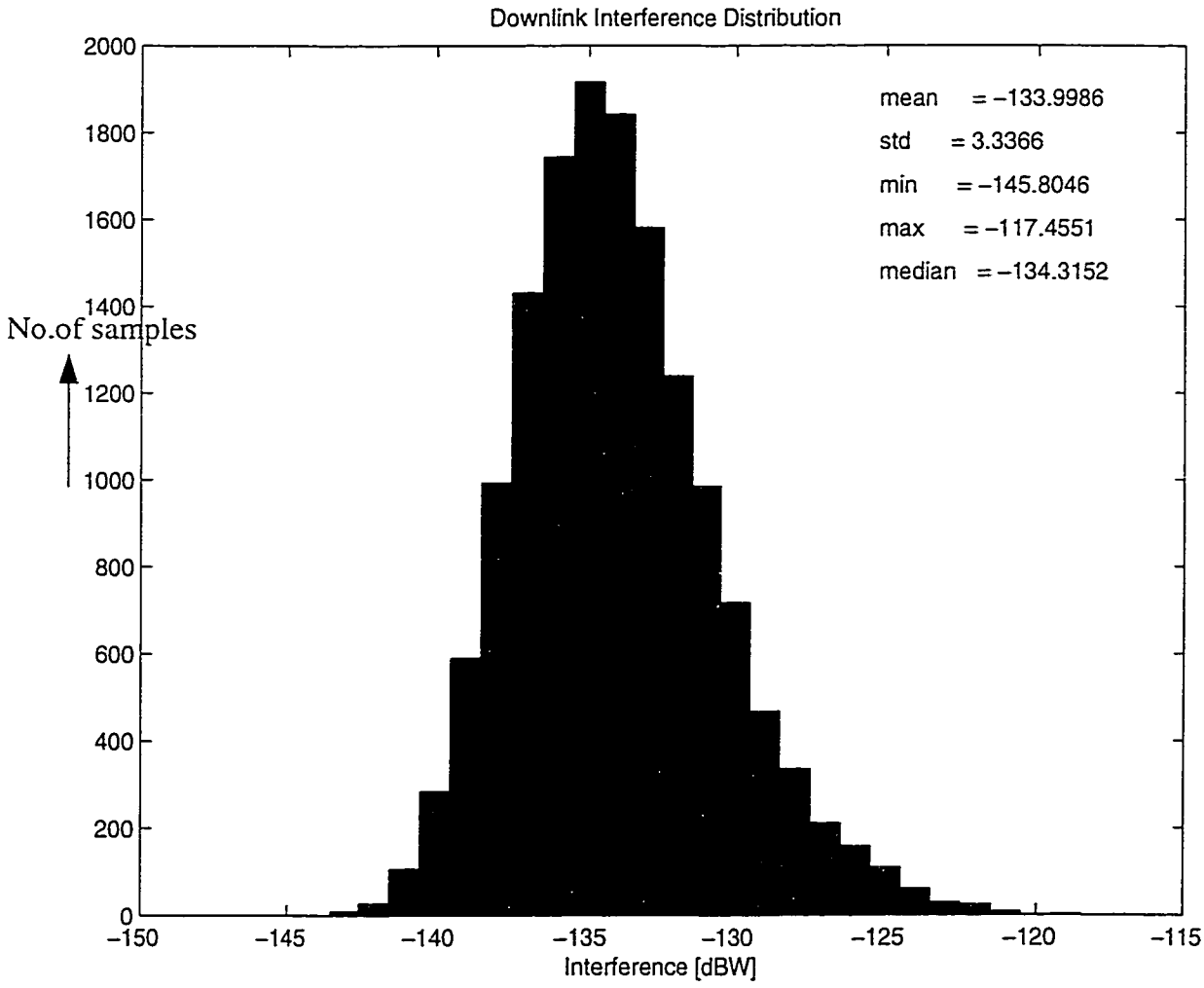

FIGURE 4.16. Downlink Interference distribution of a 3 sectored, 4/12 reuse system.

In Figure 4.16 the downlink distribution of a 3 sectored, 4/12 reuse system is presented. The mean of the interference distribution is -133.99 dBW. The minimum and maximum values are -145.8 and -117.45 dBW respectively.

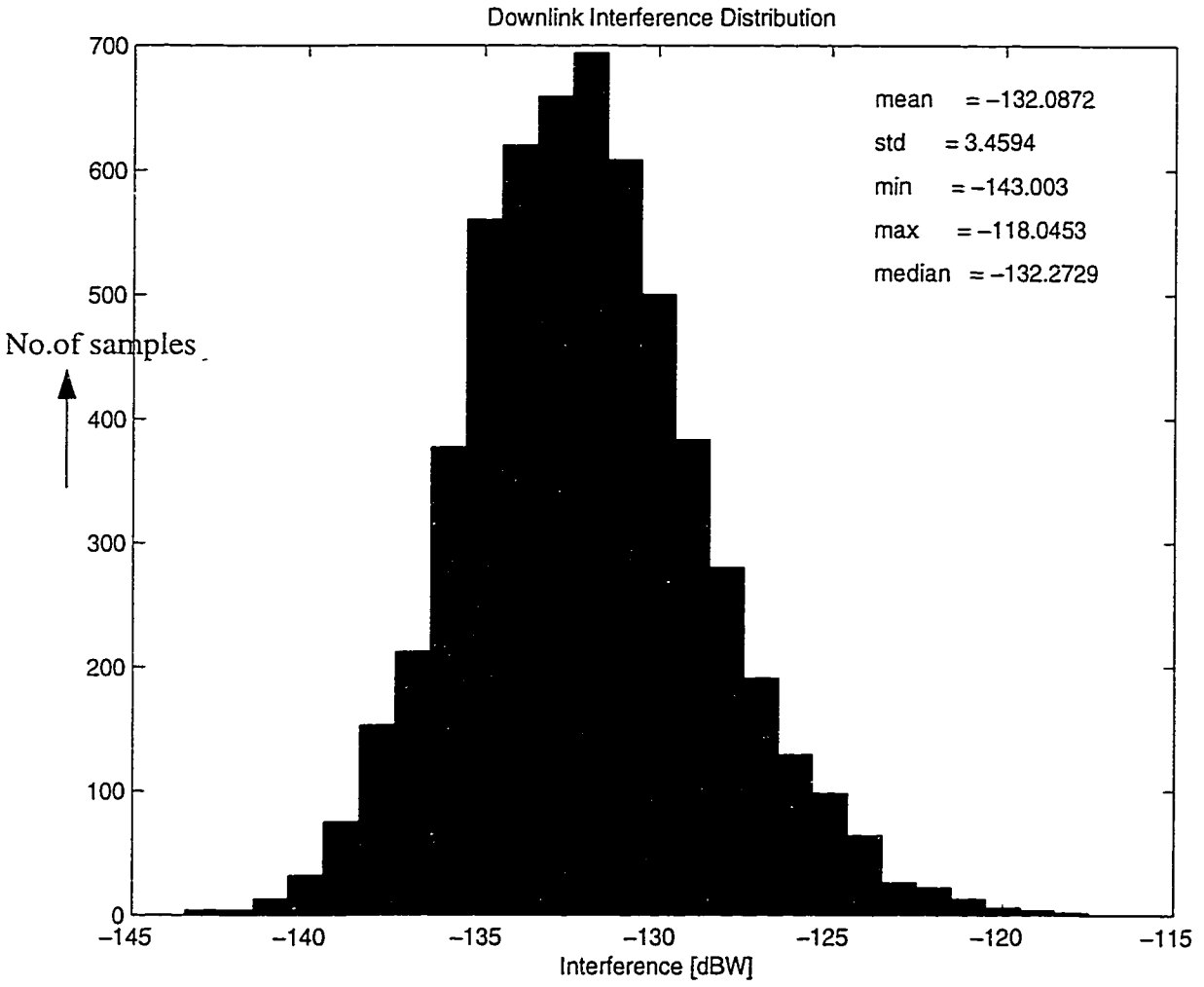

FIGURE 4.17. Downlink Interference Distribution of 3 sectored, 3/9 reuse system

In Figure 4.17 downlink interference distribution for 3 sectored, 3/9 reuse system is presented. The mean of the interference in the downlink for 3/9 reuse is -132.08 dBW. The minimum and maximum values of the distribution are -143 and -118 dBW respectively.

4.5.2 Performance of Switched Beam Antenna System

In this section results with downlink beamforming are presented. The transmission in the downlink is through a narrow beam based on the position of the mobile. The downlink Cumulative Distribution Function of C/I using narrow beam transmission for the 4/12 reuse system is presented in Figure 4.18. The downlink C/I distribution has a different shape when the narrow beam transmission is introduced. The C/I at 10% CDF is 18.93 dB with narrow-beam transmission in the downlink compared to 14.45 dB of C/I at the same value with three sectored antenna pattern in the system (Figure 4.14). This gives a 4.48 dB gain of C/I with the introduction of narrowbeams in the system.

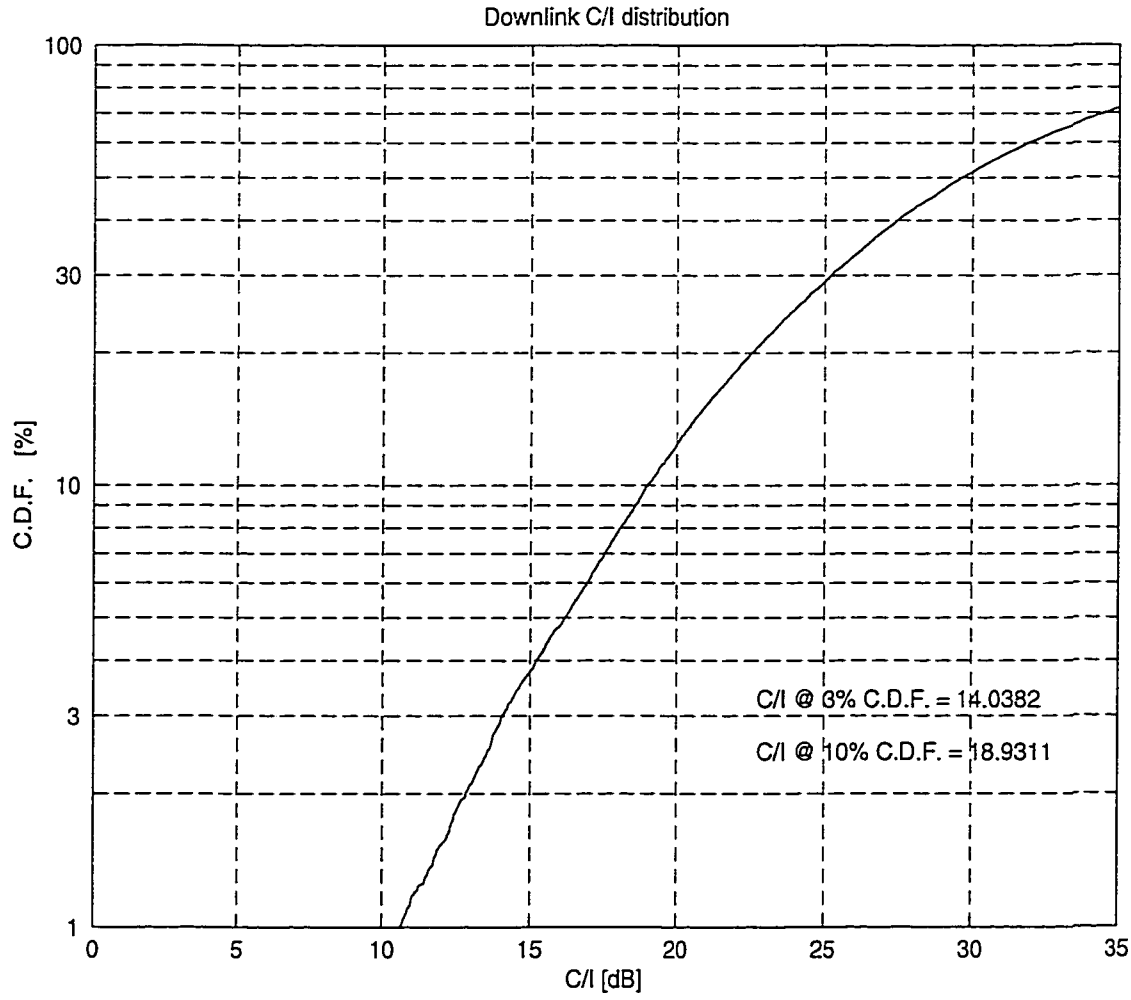

FIGURE 4.18. Cumulative Distribution Function of C/I for 4/12 reuse system with narrow beam transmission (4beams/sector)

The interference in the system is considerably reduced when the narrow beam transmission is introduced. From Figure 4.16, the mean of the distribution is -133.99 dBW, while in Figure 4.19 the interference distribution has a mean value of -139.57 dBW. The minimum value of the interference is also reduced from -145 dBW to -156 dBW with the introduction of narrowbeam transmission in the downlink whereas the maximum value of the distribution remains same at -117 dBW for both sectored and narrowbeams.

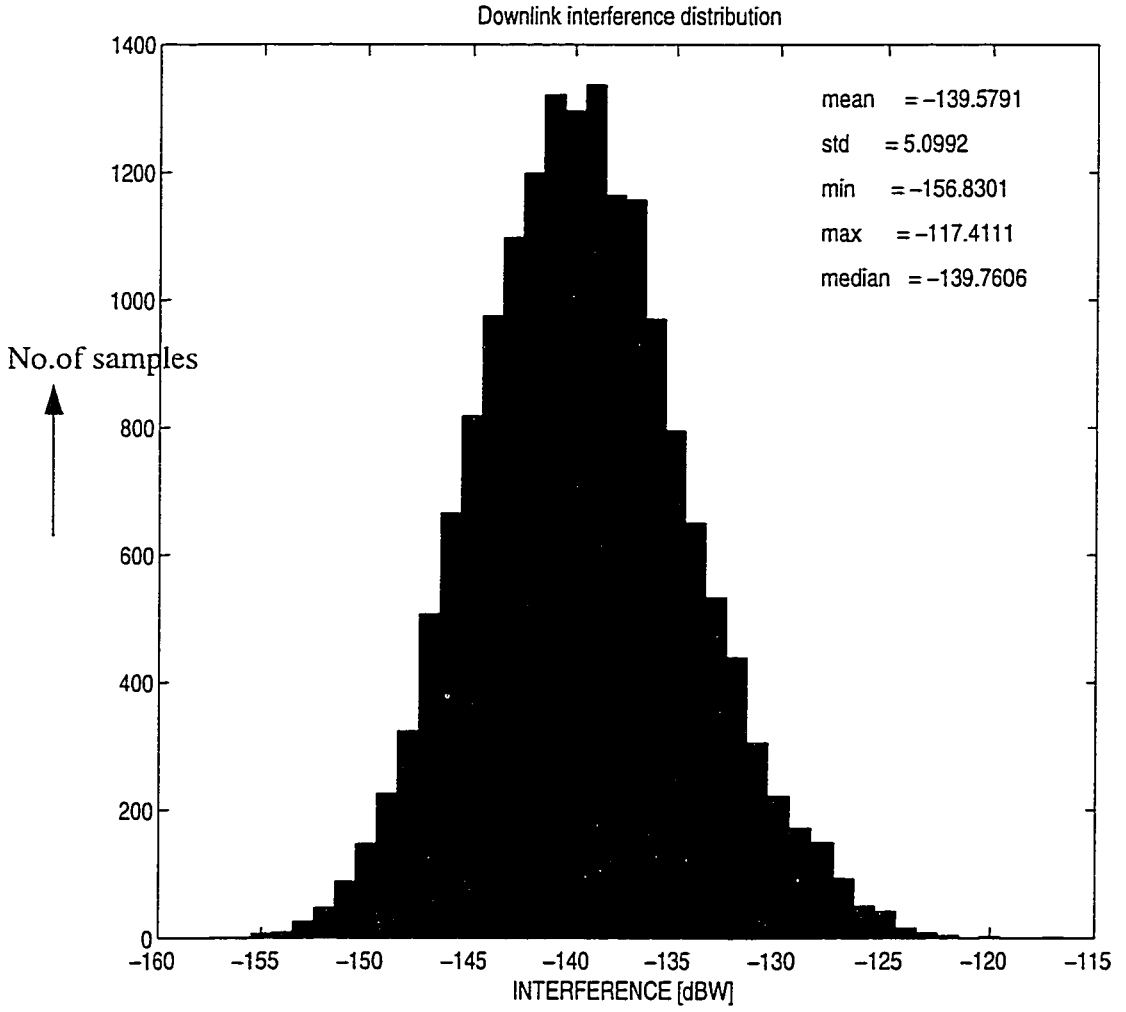

FIGURE 4.19. Downlink Interference Distribution when narrow beam transmission is introduced (4 beams/sector) in a 4/12 reuse system.

The simulation results of 3/9 reuse system with narrowbeam transmission are presented in Figure 4.20 and Figure 4.21. In 3/9 reuse system with narrowbeam transmission the C/I at

10% CDF is 16.71 dB at 100% traffic load. The interference distribution of 3/9 reuse system is presented in Figure 4.21 and the mean of the interference distribution in the system is at -137.3 dBW. This represents a C/I gain of 4.3 dB with respect to the conventional sectored antenna case. The fact that the interference is greater than with 4/12 reuse is obvious because, as we use tighter reuse the chances of interference from the mobiles using the same channels is high even with narrowbeam transmission since clusters are closely spaced now and reuse distance is less with 3/9 reuse. In order to use 3/9 reuse system with a maintained quality, schemes like downlink/uplink power control can be added to increase the C/I gain in the system as will be discussed in Chapter 5.

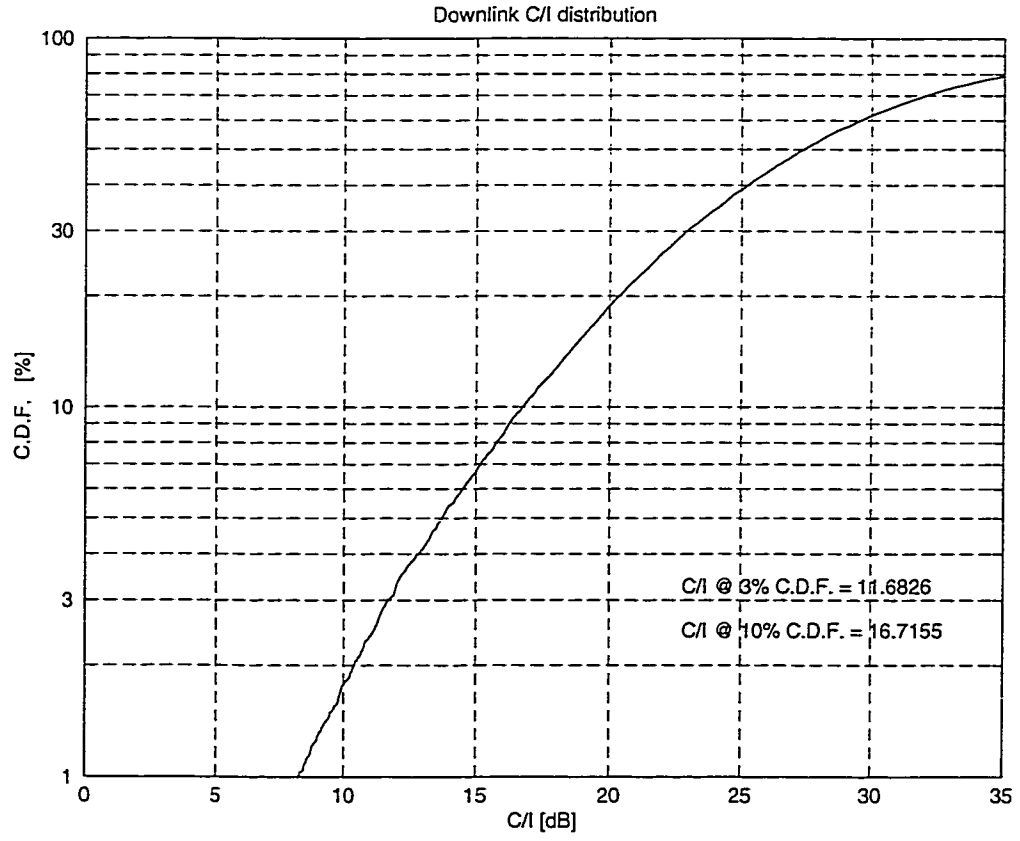

FIGURE 4.20. Cumulative Distribution Function of C/I for 3/9 reuse with narrow beam transmission(4beams/sector)

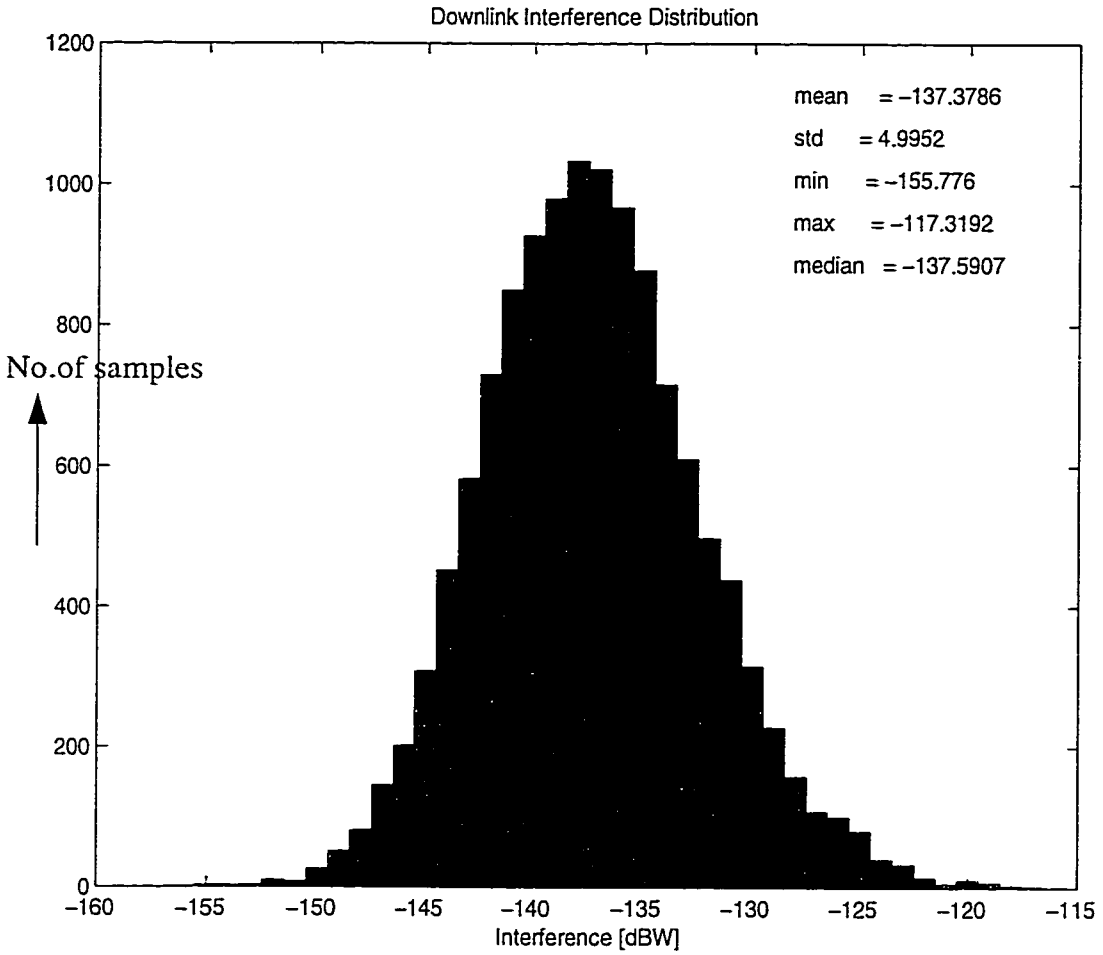

FIGURE 4.21. Downlink Interference Distribution of 3/9 reuse with narrow beam transmission in the downlink (4beams/sector)

4.6 Discussion

With the switched beam antenna configuration, the mobile is allocated a narrow beam for base-to-mobile transmission. The directive nature of the beams ensures that, in a given system, the mean interference power experienced by a single user due to other active mobiles on the same channel is much less than what would be experienced if a conventional sector antenna were used. When a 4/12 reuse pattern is employed at full load with a conventional 3 sector antenna, downlink C/I is reduced by almost 4 dB compared to 7/21 reuse system.This is illustrated in Figure 4.14 and Table 4.2. When a 4/12 reuse pattern is employed at full load

with a conventional 3 sector antenna, downlink C/I is reduced over 4 dB compared to 7/21 reuse system rendering the 4/12 reuse scheme impractical due to the 17 dB C/I requirement for IS-136 systems (Figure 4.14 and Table 4.2). By introducing beamforming in the downlink and transmitting through one of the 4 narrow beams based on the mobile's location, the C/I reduction is completely recovered (Figure 4.18). This improvement therefore allows the use of 4/12 reuse rather than the conventional 7/21 plan at 100% traffic load and at maintained quality level, resulting in enhanced capacity. Further improvement in the downlink C/I with the implementation of power control will be discussed in Chapter 5.

In terms of implementation issues, the beam selection for the downlink transmission is the one that is strongest in the direction of the mobile. The base station determines this from the direction of the path on which the strongest component of the desired signal arrives at the basestation. Thus, the beam to be transmitted in the downlink is determined from the Direction of arrival of the signal (DOA) from the mobile. It follows that the errors in DOA estimation have to be minimized in order to avoid the wrong beam selection for downlink transmission.

On the downlink, the base station points a beam in the mobile's direction. Since a narrow-beam is pointed at the mobile the probability that the mobile is in deep fade is extremely small. This is due to reduced multipath from narrow beam and increased radiated power due to antenna array gain at the mobile. Furthermore, at the base station, power is not a critical resource and a relatively high-power beam can be used to boost the C/I level if necessary. This is in contrast to the uplink case in which a mobile transmits using an omnidirectional antenna with very limited power.

A difficulty arising from the use of multi-element linear array to produce narrow beams is that of spacing between the array elements. If the spacing between the elements is greater than $\lambda/2$, then grating lobes begin to appear. For an antenna array oriented along the x-axis, every array lobe in the forward half-space for $0 \leq \phi < \pi$, may be accompanied by a grating lobe in $\pi \leq \phi < 2\pi$ reverse half-space as mentioned in section 4.3.2. This effect is generally undesirable, so element spacings are typically kept less than $\lambda/2$. It should be noted that the

elements of the array may not be very closely spaced, since two closely spaced antenna elements will exhibit mutual coupling effects, resulting in deteriorated impedance matching and distorted beam pattern. The mutual coupling between the elements tends to increase as the spacing between the elements decreases. Thus spacing between antenna elements must be large enough to avoid significant mutual coupling, but at the same time be small enough to avoid grating lobes. As a compromise, it is generally advisable to maintain a half wavelength separation between the array elements.

4.7 Capacity Estimation

In Figure 4.22 cumulative distribution functions of downlink C/I are shown for the 7/21, and 4/12 reuse system with a conventional sector antenna along with that of the 4/12 reuse system using four narrow switched beams. All systems are operated at 100% traffic load.

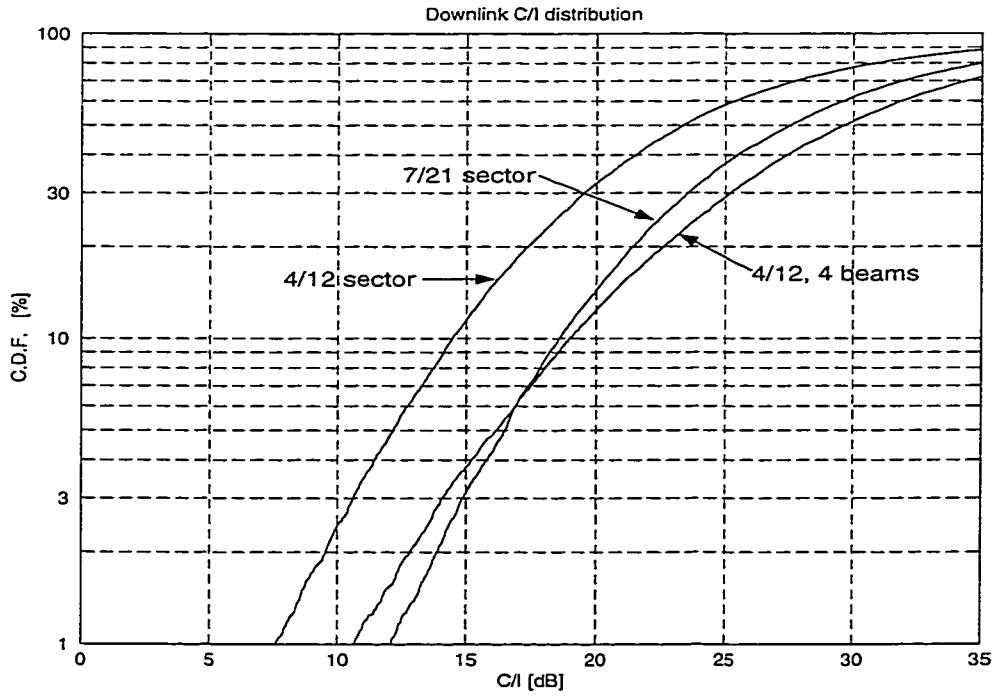

FIGURE 4.22. Cumulative Distribution Functions of downlink C/I for a 7/21, 4/12 systems with a conventional sector antenna, and a 4/12 system with four orthogonal downlink beams.

Some parameters characterizing the three C/I distributions of Figure 4.22 are summarized in Table 4.3. The mean, median and standard deviation (σ) of the C/I distribution (Figure 4.22) are calculated from the histograms, not presented here.

TABLE 4.3. Parameters characterizing the C/I distributions in Figure 4.22

Reuse	# Beams	10% CDF Level (dB)	Mean (dB)	Median (dB)	σ (dB)
4/12	1, sector	14.45	24.57	23.30	9.18
7/21	1, sector	18.57	28.77	27.55	9.28
4/12	4	18.93	30.47	29.63	9.86

From Figure 4.22, it is evident that the C/I distribution adopts a different shape when transmission in narrow beams is introduced in the system. Comparing 4/12 and 7/21 reuse systems with sectored antenna patterns, the 7/21 reuse system has substantially higher mean and median values. The 4/12 system with beamforming exhibits higher mean and median values compared to 7/21 sectored system and substantially higher mean and median values compared to 4/12 sector system. The higher mean and median values of C/I distribution means, interference experienced by the links in the system is less and hence improved quality on the links.

To estimate the increase in system capacity, the downlink C/I at the 10% CDF level is investigated as a function of served traffic. In Figure 4.23, simulation results are shown for the reference 7/21 sectored system together with results for the 4/12 reuse system under downlink narrowbeam transmission. In both the reuse systems the blocking probability is approximately same. As can be seen, an increase in traffic load entails a decrease in the downlink C/I at 10% CDF. At 100% traffic load the C/I value at 10% CDF for 7/21, 3 sectored and 4/12 with 4 narrowbeams is above the required quality (C/I) level of 17 dB or above for IS-136 systems. Hence the 4/12 reuse with narrowbeam transmission can be used in place of 7/21, 3 sectored system at a maintained quality as that of 7/21 reuse with 3 sectored system. This corresponds to an increase in served traffic by 1.75 times (21/12 = 1.75).

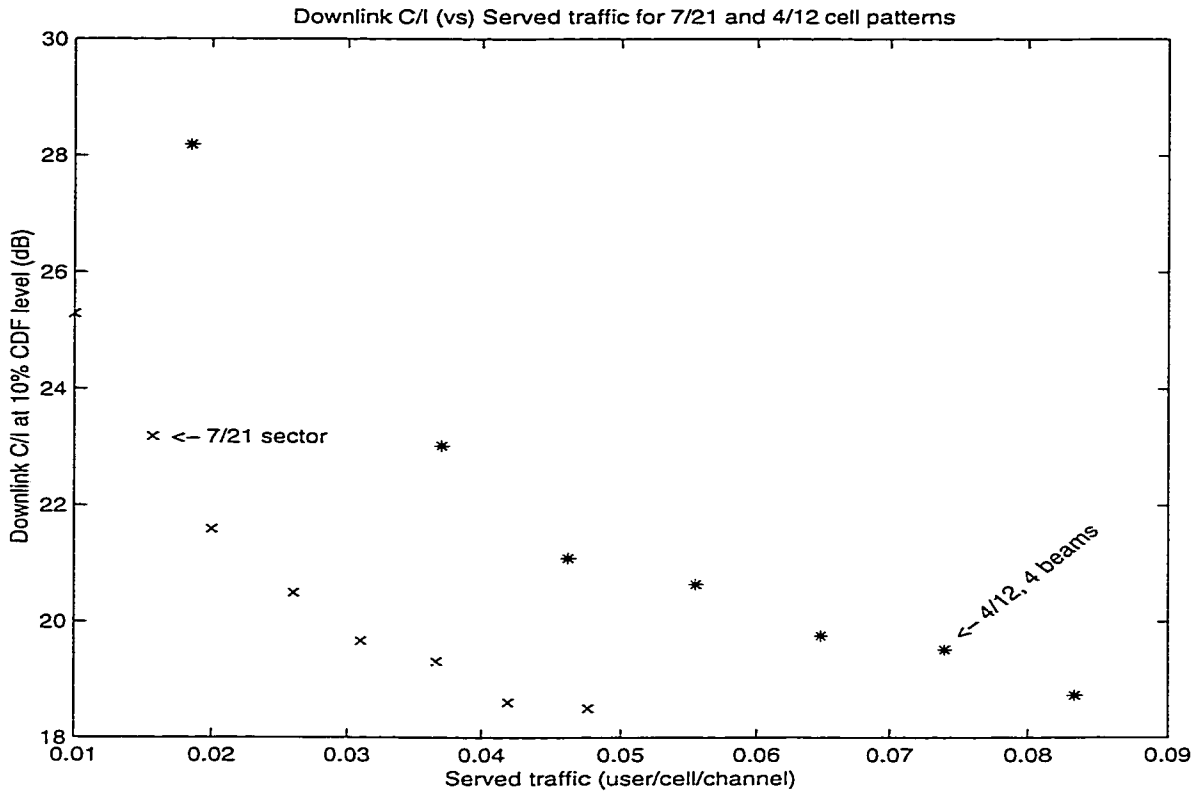

FIGURE 4.23. Downlink C/I at 10% CDF level as a function of served traffic for a 7/21 reuse system with a conventional sector antenna(*) and4/12 reuse system with four downlink beams (x).

4.8 Conclusions

In this chapter the basic concept of smart antennas was briefly explained. The constituent blocks of the smart antenna system the antenna array and beamforming techniques were discussed. Then the capacity and performance potential of switch-beam antenna solutions were investigated through simulations. The switch-beam antenna approach having 4 beams/sector improves the C/I by more than 4 dB, which allows the use of 4/12 frequency reuse plan at full load with improved communication quality. As a result system capacity can be enhanced by 1.75 times within existing IS-136 systems.

CHAPTER 5

POWER CONTROL IN CELLULAR SYSTEMS

5.1 Introduction

Efficient channel reuse is of great importance in the design of high capacity cellular radio systems. Cochannel interference caused by frequency reuse is the most restraining factor on the system capacity. Systems may be designed either to tolerate low signal to interference ratios by employing efficient modulation and coding schemes or to reduce the interference with efficient cell planning. Also, dynamic channel allocation may be used to reduce the cochannel interference.

In addition to the above schemes the use of transmitter power control has been proposed to control cochannel interference. The main idea is to adjust the power of each transmitter for a given channel allocation, such that the C/I at the receiver locations is optimum. The measure of quality usually employed in cellular system design is the carrier-to-interference (C/I) ratio. Maintaining adequate transmission quality on the actual communication link is the obvious constraint on the power control mechanism.

Some of the early work on power control schemes has been focused on algorithms that aim at keeping the desired signal at some constant level. Analytical investigations, however show that constant-received power control has only limited ability to reduce the cochannel interference [28-31].

In [29], the chosen form of power control is that the power should be reduced as the path gain (the negative path loss) is increased such that the received signal strength is kept constant at the receiver. In this case, the change in path gain is fully compensated. A variation of this scheme is also based on received signal strength, but the change in path gain is only

partly compensated. This scheme is demonstrated in [30], and has shown that there is some increase in capacity.

In other type of algorithms, the focus is on quality (Carrier-to-Interference ratio) instead of carrier strength alone. In [31], a global power control algorithm is described. This algorithm assumes knowledge of the attenuation in all transmission and interference paths and optimally minimizes the interference probability for a given threshold of C/I. This algorithm is, however, found to be somewhat impractical since the computational complexity exponentially increases with the size of the cochannel set. The numerical results presented for this algorithm indicate that there are potentially large gains to be achieved by using C/I control and gains in excess of 10 dB in interference reduction may be achieved. In [32], a centralized power control scheme is described for cellular mobile radio systems and is based on signal strength measurements. With this scheme the power is adjusted such that all the mobiles using the same channel will attain a common carrier-to-interference ratio.

The scheme adopted in [31] is not very practical in nature due to its computational complexity. For a practical implementation, we would have to rely upon power control schemes that would require far less measurements and distributed operation. In [33], the distributed power control algorithms that use only C/I ratios are investigated. This distributed algorithm was shown to be able to achieve C/I balancing with probability of one and thus when combined with cell removal algorithm, can obtain a minimum outage probability. It is also shown that a limited-information algorithm using only measurements of the signal-to-interference ratio in the wanted links can achieve results that are comparable to the centralized algorithm. Although some performance is lost compared to the "full information" algorithm, capacity gains in the order of 3-4 times can still be reached.

In [31] and [33], an iterative distributed power control scheme is presented that operates under the assumption that the transmitter power is sufficiently high to allow receiver noise to be neglected. The power of the signals for all the cochannel users is set to achieve the greatest signal to interference ratio that they are jointly capable of achieving (the same ratio for all cochannel users). In [34], the distributed power control algorithm is similar to the one in

[31] and [32] but the receiver noise is also included along with interference to set the power levels on the links. The algorithm in [33] is strictly local in that only power and interference measurements of each base-mobile link is used to set power levels on that link.

Some other distributed power control algorithms exist which can achieve much faster C/I balancing than the algorithm proposed in [33]. The algorithm proposed in [35], is such an example. Although only local information is used to adjust the transmitting power for all the distributed power control algorithms investigated in [34] and [35], a normalisation procedure is required in each iteration. That is, all base stations have to communicate with a central station to obtain a normalisation factor to determine transmitting powers in the next iteration. Without the normalisation procedure, transmitting powers may fall out of the desired range. In [36], a fully distributed power control algorithm that does not need a normalisation procedure is proposed.

One of the elements missing in most of the above literature related to power control is mobility i.e. in all the cases the distance between the mobile and base station is assumed to be constant. In [37], the study of power control combining the mobility model, where mobiles are moving with a relative speed, is carried out in a more dynamic environment.

From the implementation point of view it is believed that distributed power control algorithms are easily implementable. In [38], a fully decentralized algorithm is proposed in which only knowledge of transmitted power and received carrier to interference ratio in the current link is used to adjust power levels.

This chapter is devoted to the evaluation of power control in conjunction with switch beam antennas. The system model and algorithm used in this thesis are described in section 5.2. Simulation results and analysis of the power control for a 3 sectored antenna system are given in section 5.3. In section 5.4, simulation results of joint power control and switch beam antenna are given. In section 5.5, capacity gain is estimated and then discussion on the power control is presented in section 5.6. Lastly, conclusions are drawn in section 5.7.

5.2 System Model and Power Control Algorithm

For the purpose of investigating power control in conjunction with switched-beam antennas, it is felt that using an algorithm already available in the literature would simplify validation and benchmarking of the results when implemented with the switch beam antenna simulator model. Therefore the power control algorithm defined in [38] is chosen for the simulations. The only variation from this reference is that the power control algorithm is used for the downlink rather than the uplink. Since the algorithm requires only the knowledge of the C/I ratio and transmitted power in the current link, it can be used for both uplink and downlink.

5.2.1 Power Control Algorithm [38]

Consider a simple system with only two mobiles, ms_1 and ms_2 and two base stations, bs_1 and bs_2 as indicated in Figure 5.1. The same channel is used by both connections and a decentralized mobile power control algorithm is applied. In this algorithm, the inputs to the algorithm are the quality (C/I), and the power used in the connection. If the power is regulated towards a fixed C/I value in the downlink, say 25 dB the system may not be stable since all the links will be fighting for the same C/I value.

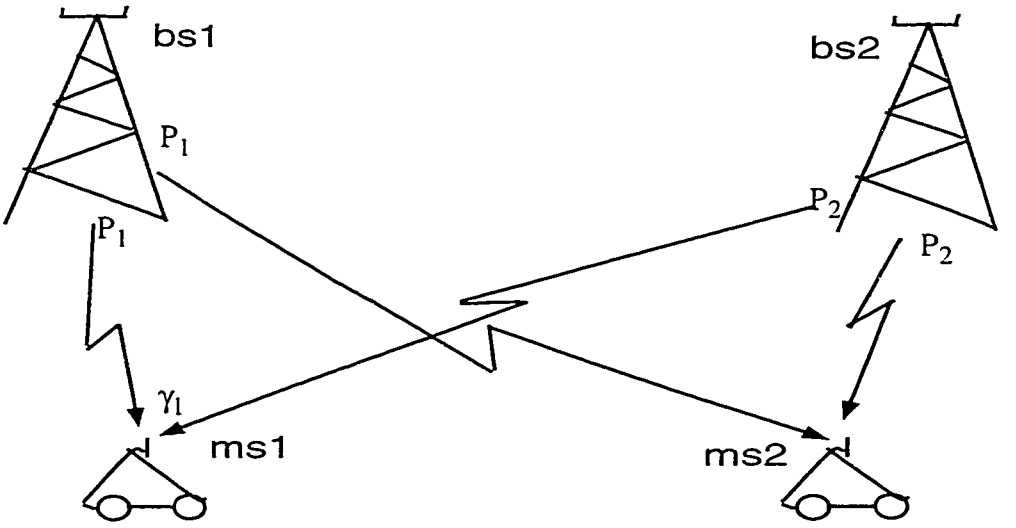

FIGURE 5.1. Two mobiles and two base stations [38]

In the following discussion, ms_i represents mobile station i, bs_i represents base station i, P_i represents the transmitted power from bs_i, and γ_i represents the C/I at ms_i, all for time instant *n*.

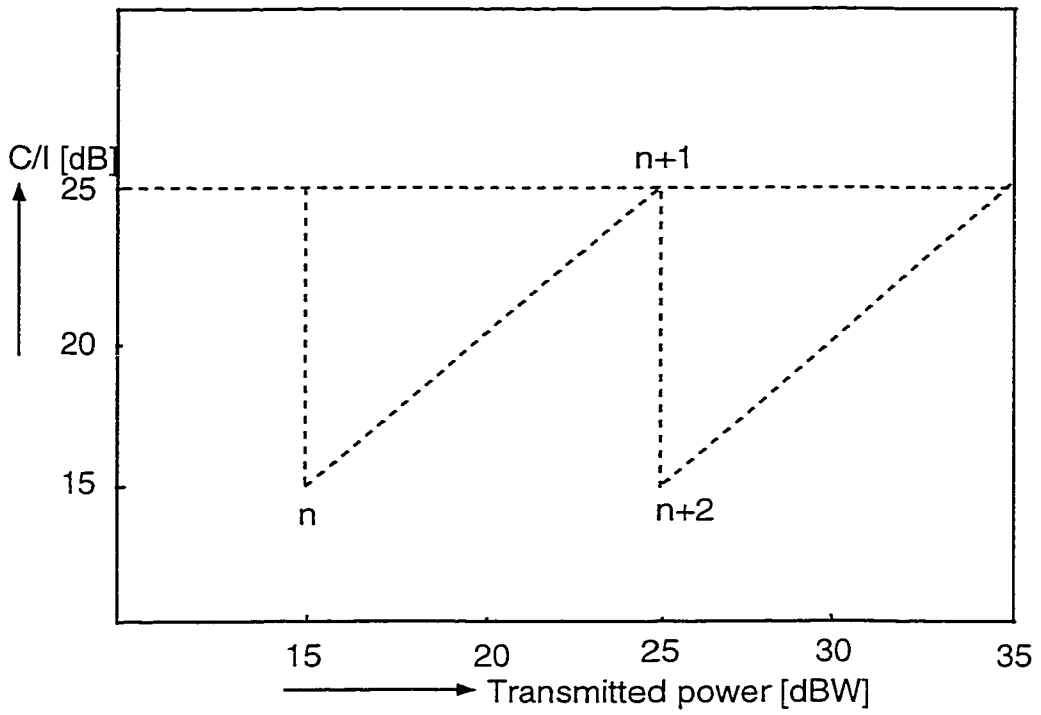

FIGURE 5.2. γ_1 at ms_1 and transmitted power at bs_1 [38]

Referring to Figure 5.2, if γ_1 for some reason decreases in ms_1 by 10 dB at time 'n', the power in bs_1 will be raised by 10 dB at time n+1. The interference will then become 10 dB higher in ms_2 and the power will be raised in bs_2 by 10 dB at time n+2. Both base stations will soon end up at their maximum power. This is sometimes described as the 'party effect' and it is obviously not a desired feature.

Instead consider another strategy. The more power that is used, the lower the quality that has to be accepted. This is illustrated in Figure 5.3. where a slope, k in the regulation target line is assumed and 'm' is an offset.

$$\gamma_1 = k \cdot P_1 + m \qquad (1)$$

The party effect will be avoided if $k < 0$. If ms_1 encounters a lower $\gamma_1^{(n)}$ at time n by 10 dB, bs_1 will raise its power at time n+1 but not as much as would be needed to fully compensate the decrease in γ_1. Then bs_2 will react on the increased interference in ms_2 by raising its power somewhat at time n+2.

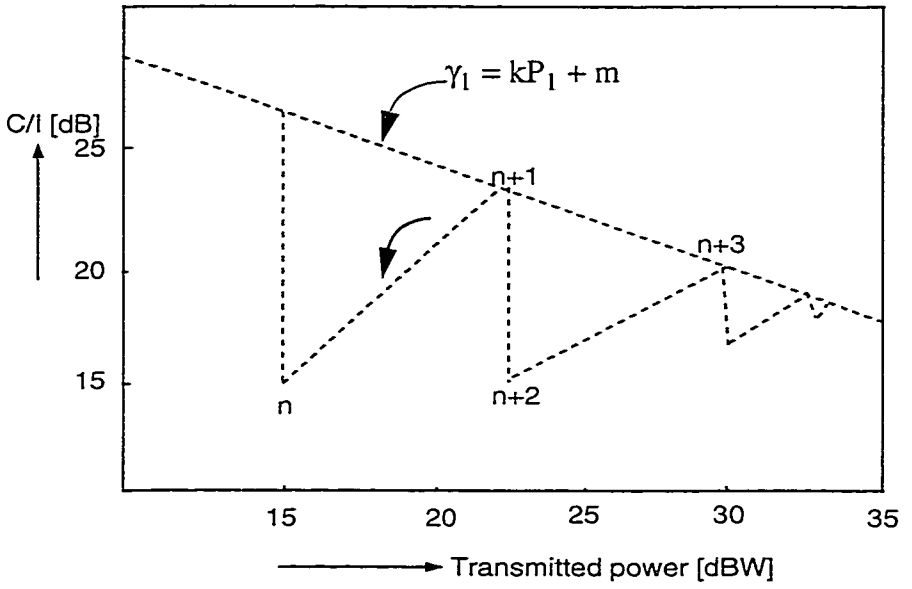

FIGURE 5.3. Desired control behaviour γ_1 in ms_2 and P_1 in bs_1

The power step will decrease in each iteration and both connections will reach the final state on the regulation target line in Eq.(1), as shown in Figure 5.3.

The control strategy is illustrated in Figure 5.4. Here, ms_1 has the C/I ratio $\gamma_1^{(n)}$ while the transmitted power in bs_1 is $P_1^{(n)}$ at discrete time n. If the power P_1 is increased, γ_1 will change according to equation (2) in ms_1 as

$$\gamma_1 = \gamma_1^{(n)} - P_1^{(n)} + P_1 \qquad (2)$$

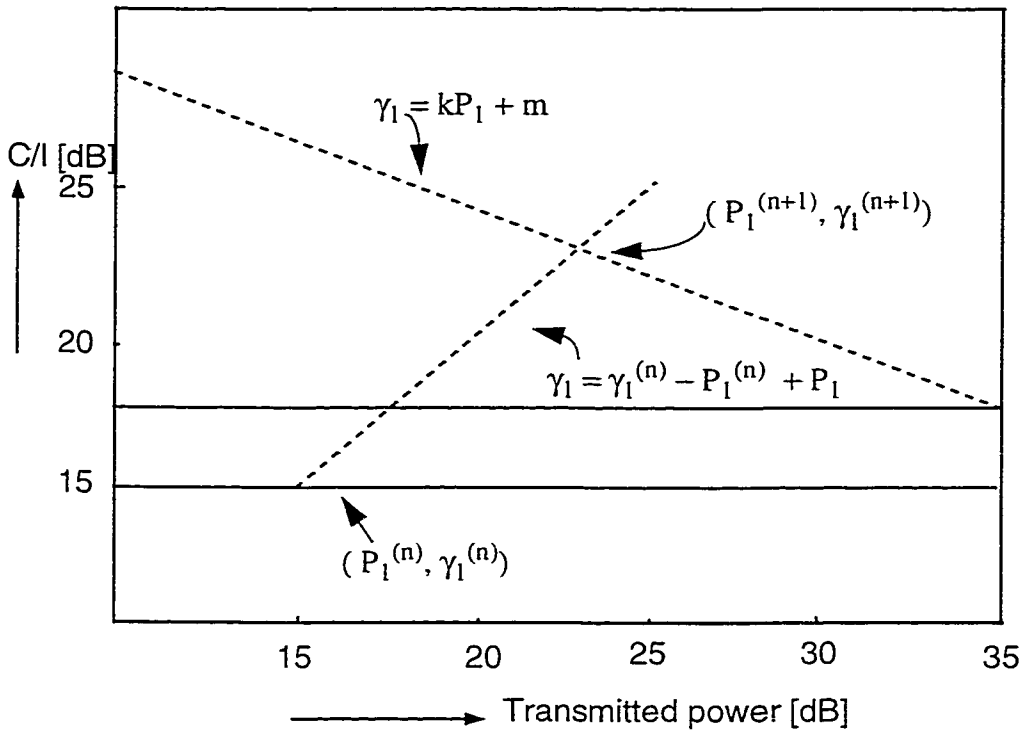

FIGURE 5.4. The control strategy

The power in the next iteration step, n+1 will be given by intersection point

$$(P_1^{(n+1)}, \gamma_1^{(n+1)}) \qquad (3)$$

Eq. (3) inserted in Eq. (1) and Eq. (2) yields,

$$k \cdot P_1^{(n+1)} + m \quad = \quad \gamma_1^{(n)} - P_1^{(n)} + P_1^{(n+1)} \qquad (4)$$

This can be written as

$$P_1^{(n+1)} = \frac{m + P_1^{(n)} - \gamma_1^{(n)}}{1 - k} \qquad (5)$$

or

$$P_1^{(n+1)} = \alpha - \beta(\gamma_1^{(n)} - P_1^{(n)}) \qquad (6)$$

where

$$\alpha = \frac{m}{1-k}, \qquad \beta = \frac{1}{1-k} \qquad (7)$$

The reasoning above is for the downlink from bs_1 to ms_1 but can be generalised for any connection ϑ according to

$$P_\vartheta^{(n+1)} = \alpha - \beta(\gamma_\vartheta^{(n)} - P_\vartheta^{(n)}) \qquad (8)$$

The iteration formula used in Eq.(8) is the control strategy used for each communication link between base station and the mobile. The power to use in the next iteration is only based on the current transmitted power and the current C/I. The parameter α controls the mean value of the transmitted power distribution and β controls the systems spread in transmitted power and C/I. Higher β will lead to lower spread in the C/I distribution and higher spread in the power distribution. When $\beta = 0$, or $k = -\infty$ in Eq.(1), all connections will transmit with the power α. i.e. no power control. When $\beta = 1$, which corresponds to $k = 0$ in Eq.(1), all connections will strive towards the same C/I and the system may be unstable.

5.2.2 Simulation Environment

The system model for simulations is described in chapter 3 and chapter 4. Initially all connections transmitted with the same power on the down link. For each parameter setting 100 trials were simulated to improve accuracy. During the trial all the connections were stationary and C/I statistics were collected after 30 iterations of Equation (8).

Certain assumptions were made in order to simplify the simulations. For part of the simulations, the available transmitted power is assumed to be infinite and the power control to be

perfect, i.e. no control delays or errors; in the latter part of simulations, the maximum available power is restricted to 30 watts.

5.3 Simulation Results and Analysis with Power Control

From simulations, the power control algorithm is demonstrated in Figure 5.5. for a value of $\beta = 0.7$. The target line is drawn and the variation of C/I in a particular link is shown with the variation of power in the downlink.

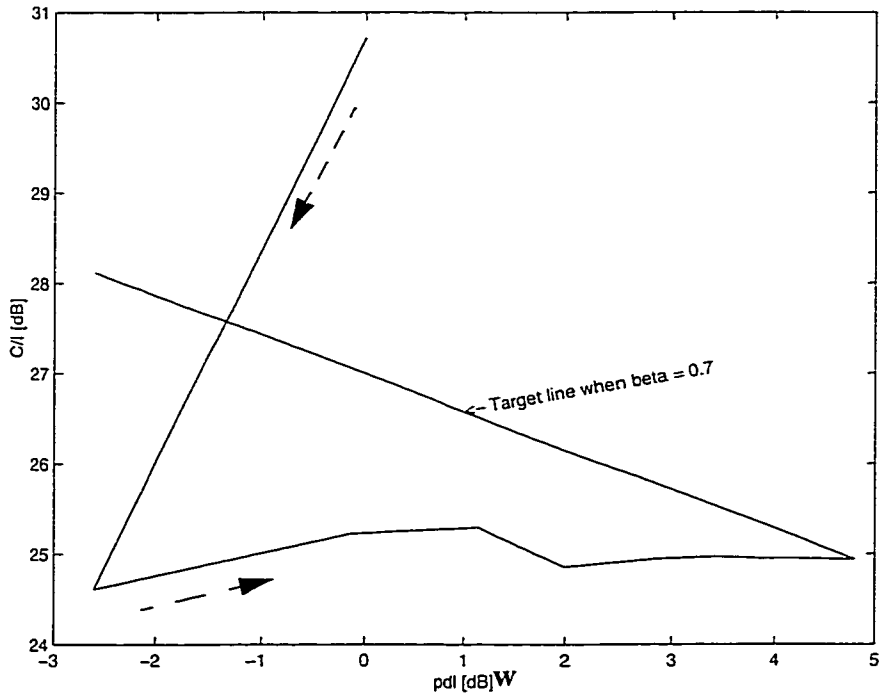

FIGURE 5.5. Power control Mechanism in Downlink from Simulations

It can be observed from Figure 5.5 that in the first iteration, when the downlink power is same for all the links, the link under consideration has a C/I of approximately 30 dB which is far more than the required 17 dB. This shows that the power transmitted on this particular link is more than required and hence can be reduced. In the next iteration when we change

the power on this link, this link is supposed to follow the target line as per the control logic of the algorithm. In this case the power is decreased from 0 dB to -2.8 dB to achieve the target C/I. But in reality this does not happen since when we reduce the power in this particular link, the power is also changed in the corresponding co-channel set. The interference from the co-channels causes the reduction in C/I in the link under consideration which is why it does not meet the target line in the first iteration with power control. The convergence occurs after 30 iterations. With the above power control algorithm, a number of simulations was performed for different values of β ranging from 0 to 0.9.

5.3.1 Simulation Results with No Power Control for Reference

As a reference for subsequent simulations, Figure 5.6 plots the downlink C/I distribution when there is no power control scheme added to the system and a conventional 4/12 sector antenna is employed with 4/12 reuse. The C/I at 10% is 14.45 dB and at 3% it is 10.58 dB, as was obtained in Chapter 4.

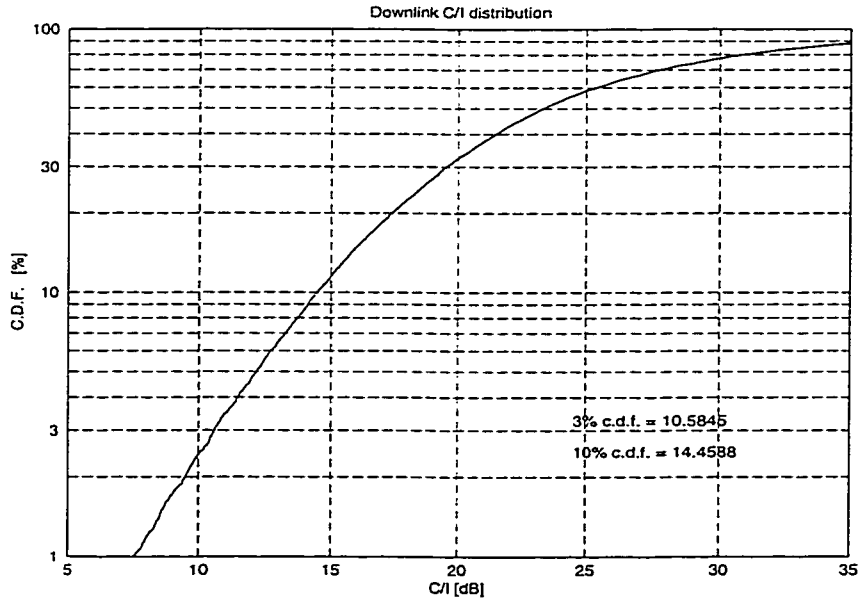

FIGURE 5.6. Downlink C/I distribution when there is no power control scheme added ($\beta = 0$)

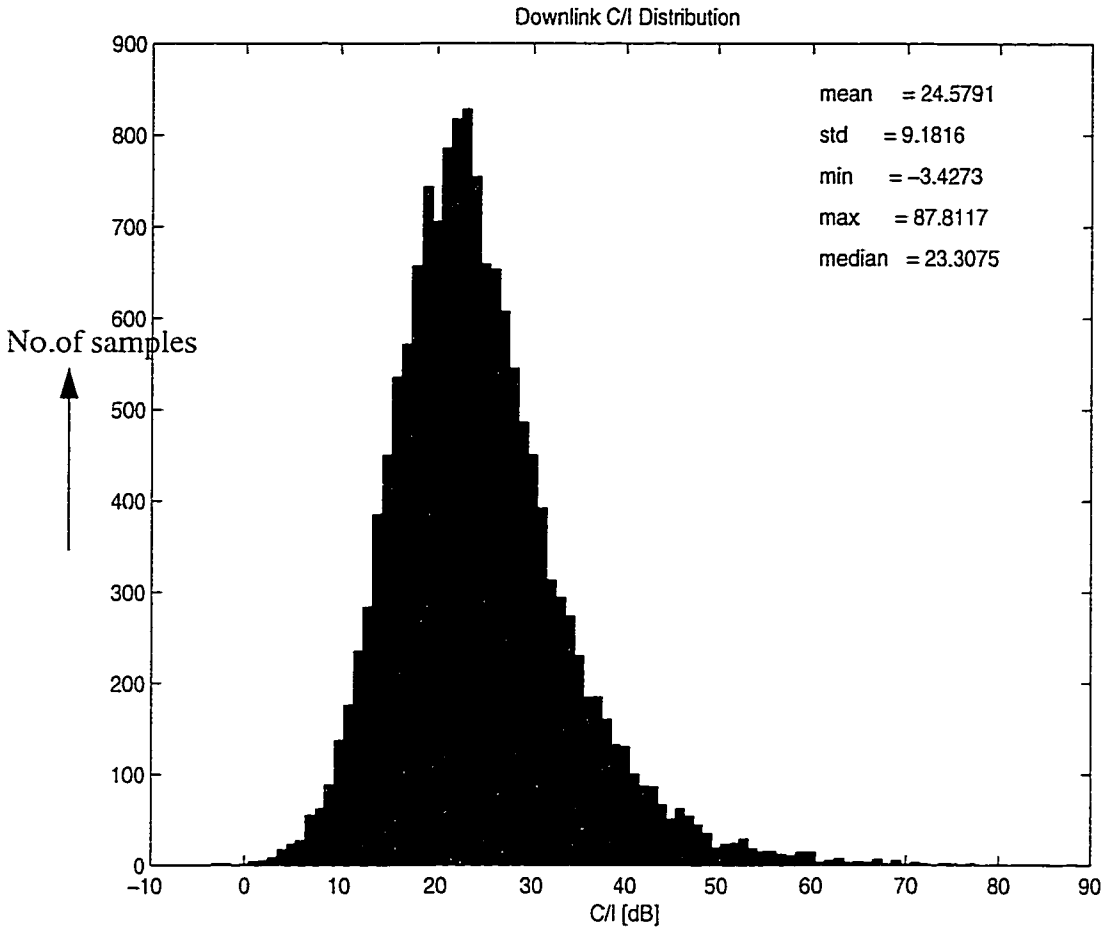

FIGURE 5.7. The histogram of downlink C/I distribution when $\beta = 0$

In Figure 5.7, the histogram of downlink C/I distribution with no power control applied is presented. The mean of the distribution is 24.57 dB and the median is 23.3 dB, as was obtained in Chapter 4. The minimum and maximum values of the distribution are -3.4 dB and 87.81 dB respectively

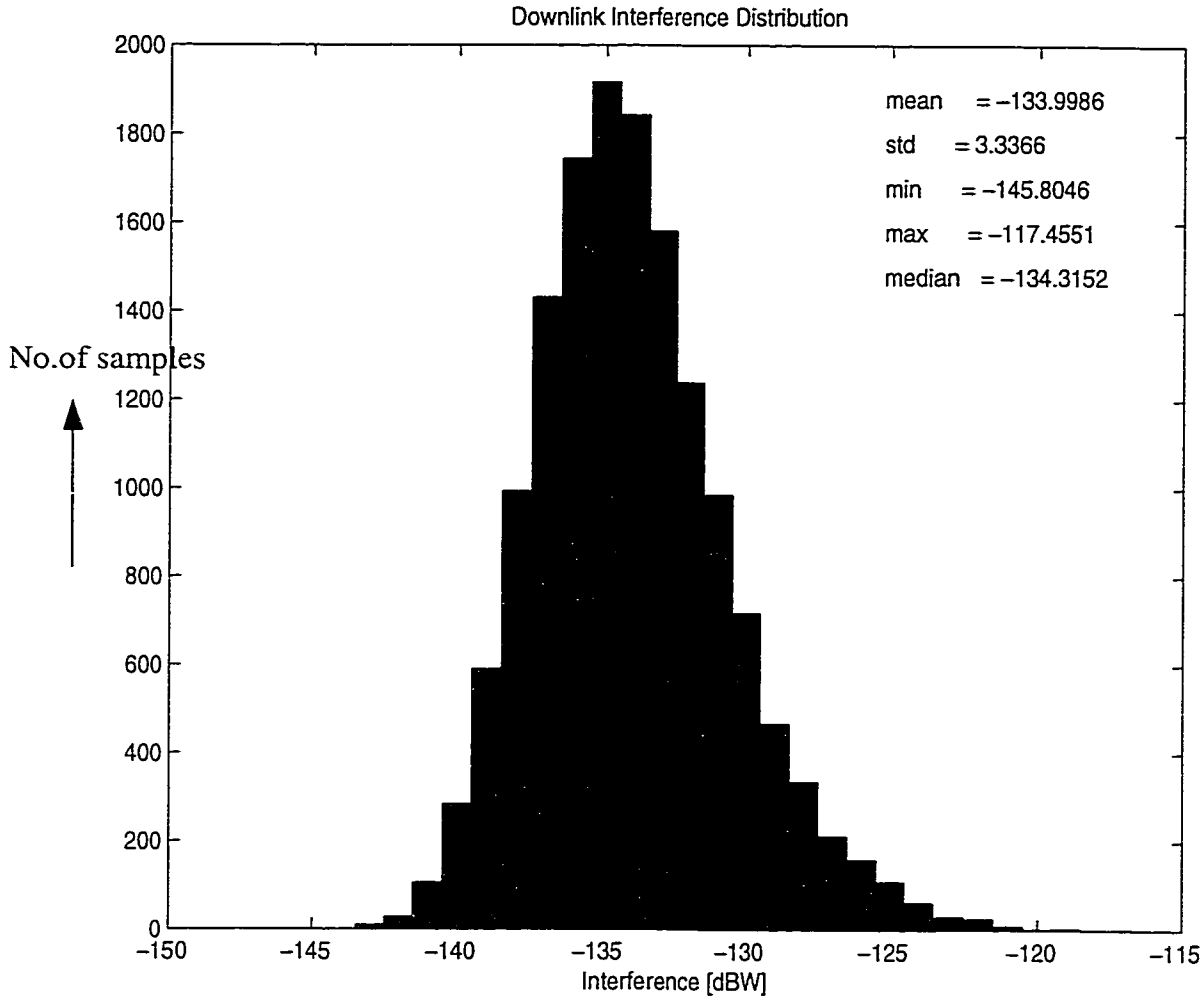

FIGURE 5.8. The histogram of downlink interference distribution when $\beta = 0$

In Figure 5.8, the histogram of downlink interference distribution with no power control applied is presented. The mean of the distribution is -133.99 dBW and the median is -134.31dBW, as was obtained in Chapter 4. The minimum and maximum values of the distribution are -145.8 dBW and -117.45 dBW respectively.

5.3.2 Simulation Results with Downlink Power Control and no limit on Maximum Power

Figure 5.10 to Figure 5.12 are the simulation results when the downlink power control is included in the system with a value of $\beta = 0.7$, and Figure 5.13 corresponds to β varying

from 0 to 0.9 in steps of 0.1. The main effect of power control is seen by comparing the C/I curves in Figure 5.6 and Figure 5.9. The C/I at 10% CDF is improved by 3.96 dB compared to the reference system. Compared to Figure 5.7 where no power control is applied, Figure 5.9 shows that as β increases the C/I distribution spread decreases from 9.18 dB to 3.07 dB. However, when β increases above 0.7 the spread starts increasing again. So an optimum value is reached at $\beta = 0.7$. In Table 5.1 the C/I values at 10% CDF and at 3% CDF are presented for different values of β. The remainder of this section presents results for the value of $\beta = 0.7$.

The downlink interference distribution and power distributions are presented in Figure 5.11 and Figure 5.12. It is noticed that, as β increases the spread in transmitted power is increased as explained in control strategy of the power regulation. In Figure 5.13 the C/I distribution curves for different values of β are presented. It can be seen that $\beta = 0.7$ is the optimum value for maximum C/I gain.

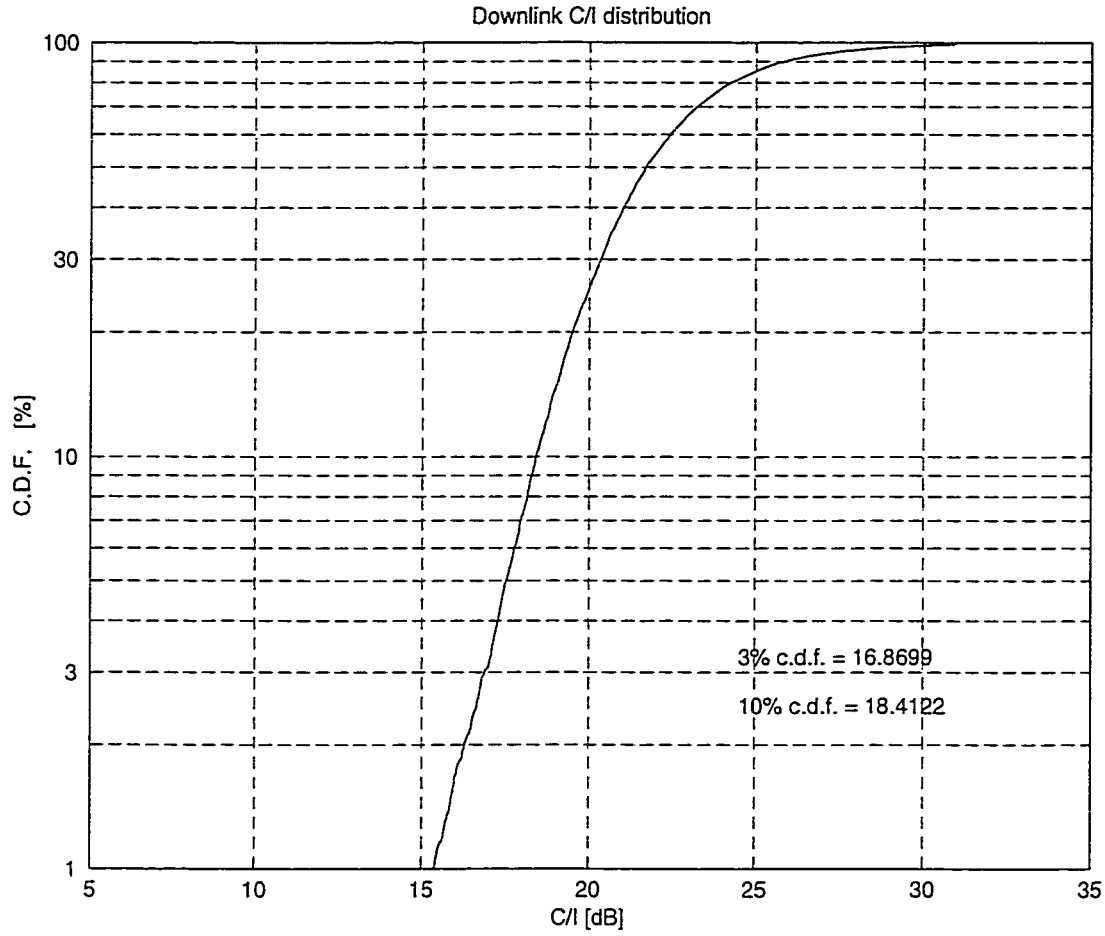

FIGURE 5.9. Downlink C/I distribution for $\beta = 0.7$

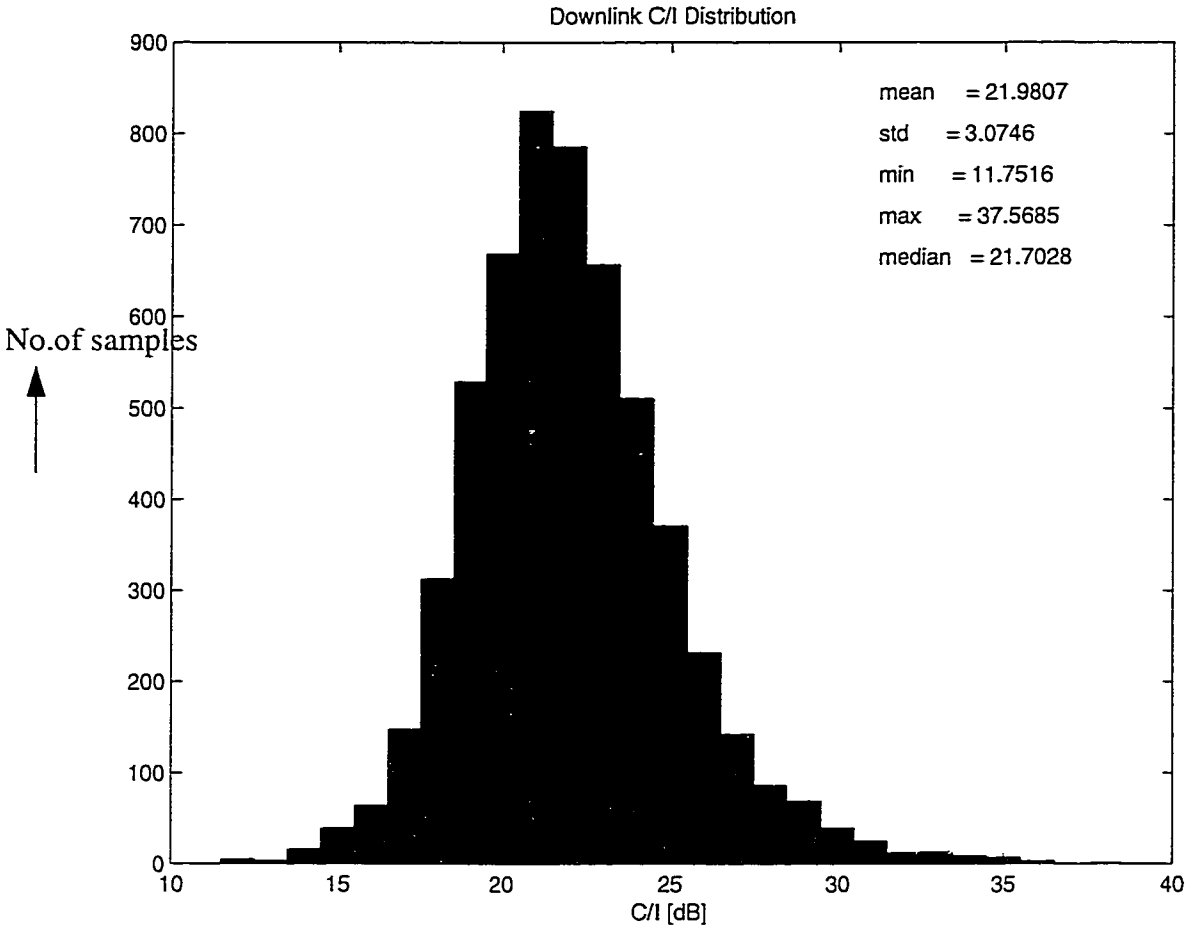

FIGURE 5.10. Histogram of the downlink C/I distribution when $\beta = 0.7$

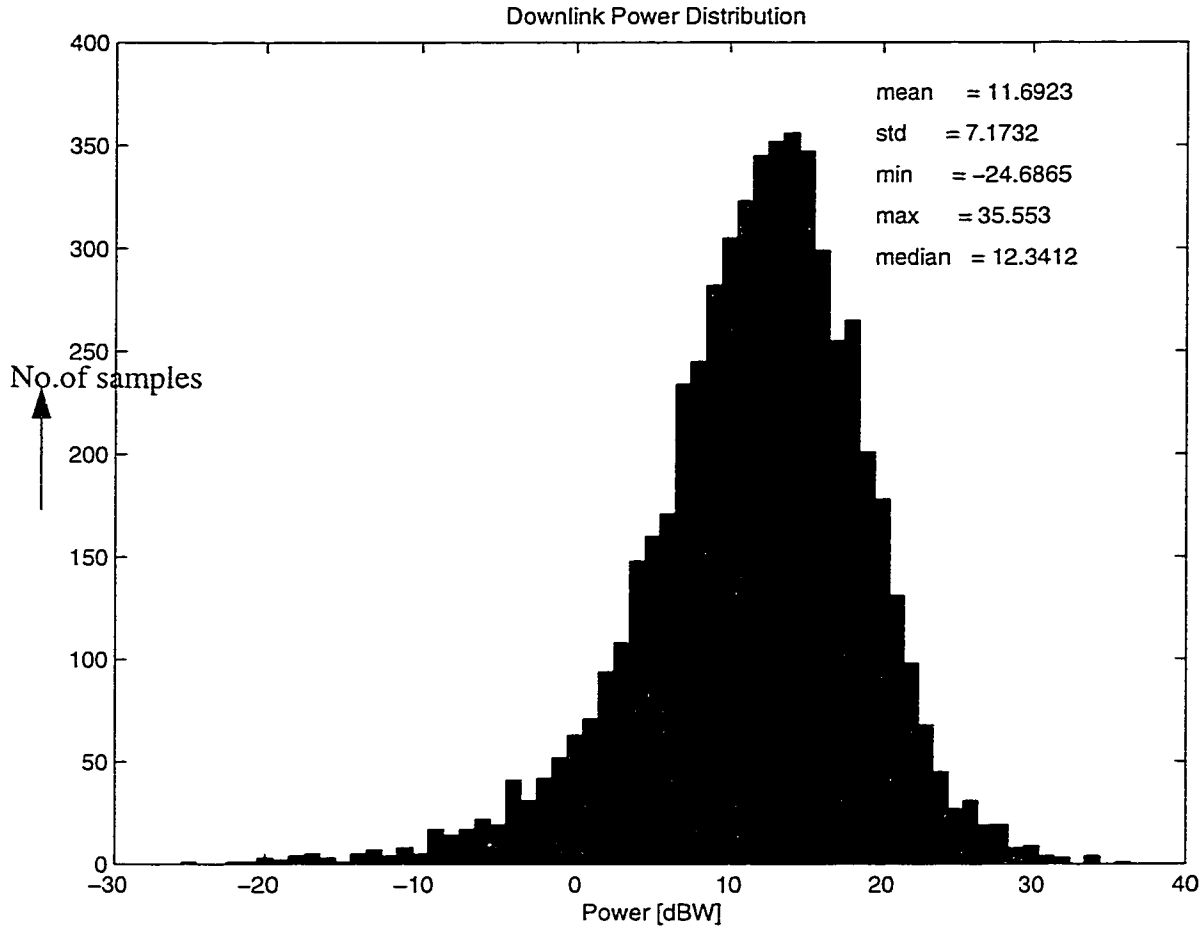

FIGURE 5.11. Downlink power distribution for $\beta = 0.7$

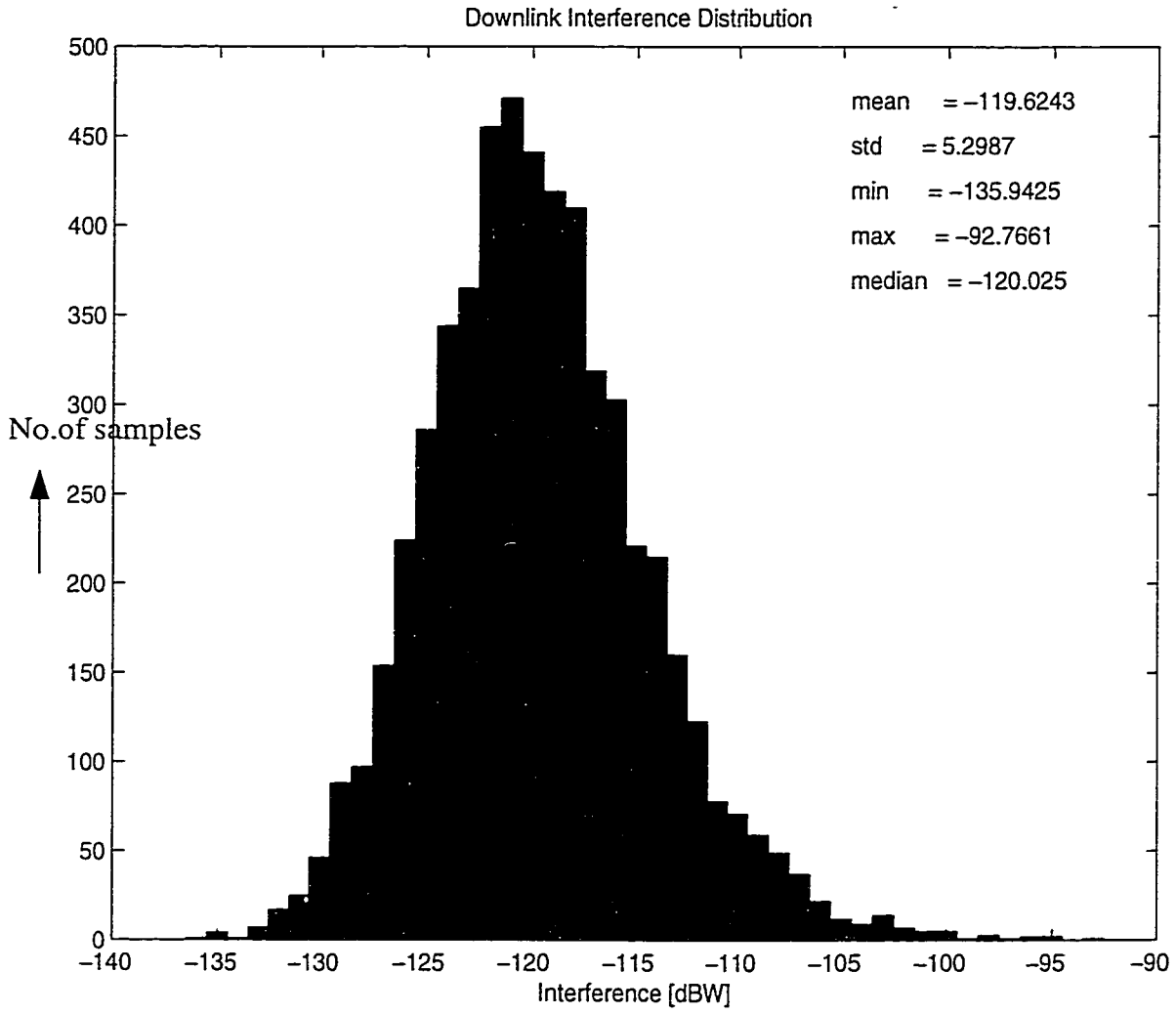

FIGURE 5.12. Downlink interference distribution when $\beta = 0.7$

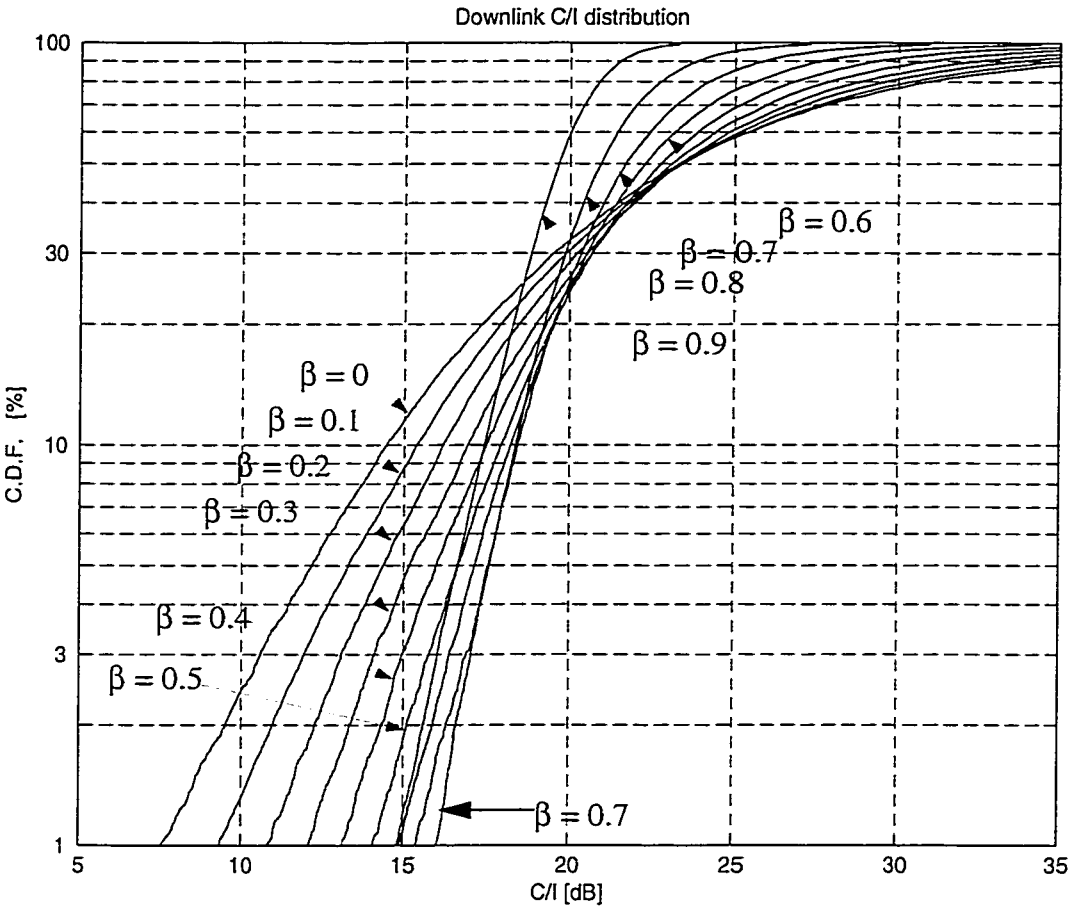

FIGURE 5.13. The C/I distribution for different values of β ranging from 0 to 0.9.

TABLE 5.1. C/I distribution at 10% CDF and at 3% CDF for β ranging from 0 to 0.9

β	C/I at 10% CDF [dB]	C/I at 3% CDF [dB]
0 (No power control)	*14.45*	*10.584*
0.1	15.3733	11.9146
0.2	16.1717	13.0799
0.3	16.9108	14.1024
0.4	17.4771	14.95
0.5	17.9289	15.7398
0.6	18.2185	16.37
0.7	*18.4122*	*16.8699*
0.8	18.3596	17.0273
0.9	17.4145	16.0109

5.3.3 Simulation Results with Downlink Power Control and a Limit of 30 watts on Maximum Power Transmitted on the Downlink

In the previous section, simulation results are based on the assumption that unlimited power is available at the base stations to transmit. Of course in practice the power available for transmission at the antenna is limited. A typical transmitter used in the cellular environment gives a 50 Watt (17 dBW) output. In a cellular environment, since many channels are used at one base station, it is necessary to use antenna combiners, which combine the transmitter outputs into the antenna port. The use of combiners results in about 2.5 dB overall loss. In some cases antenna duplexers are used to connect transmitter and receiver ports to the antenna, and this results in another 1.5 to 2 dB loss. Additional power loss usually encountered before the power reaches the antenna from the transmitter is feeder cable loss. The connection cables (7/8 inch) have a loss of about 4 dB/100 meters and other power loss encountered is due to connectors used to connect the cables to antenna ports. If the connectors are not properly connected then we encounter some loss there also (~0.5 to 1 dB). So subtracting all the above mentioned losses from the transmitter output of 17 dBW, the optimistic value of the power available at the antenna port for transmission is assumed to be at 14.7 dBW (30 watts).

In Figure 5.14 the C/I distribution when $\beta = 0.7$ for different maximum power limits is presented. The C/I values at 10% CDF for maximum power limits of 20, 30, and 40 watts are 17.82, 18.14 and 18.81 dB respectively. C/I values at 3% CDF for the same values of power limits are 13.55, 14.03 and 14.48 dB respectively. When a constraint is placed on maximum power to be transmitted, the curve is not smooth and a kink can be noticed. The kink is due to the fact that the links in the system require more than the available maximum power to meet the C/I target line given in Figure 5.5. It is also noticed that as the power limit increases from 20 watts to 40 watts the C/I distribution improved and the curve with 40 watts is in fact close to the one with infinite power limit. To be close to the practical environment the rest of the simulations are carried out with a maximum power limit of 30 watts.

Simulation results of downlink C/I, interference, power distribution can be found in Figure 5.15 to Figure 5.18. The C/I gain over the reference system with a power limit of 30 watts is 3.69 dB (Figure 5.15) as compared to 3.96 dB (Figure 5.9). The interference distribution also improved considerably compared to the unconstrained system decreasing from a mean value of -119.6 dBW (Figure 5.12) to -123.7 dBW (Figure 5.18). This is due to the fact that the links now have a limited transmit power.

Comparing the power distributions with and without power limit (Figure 5.17 and Figure 5.11), it is noticed that with power limiting the power spread is reduced and the links are forced to transmit at lower power levels, reducing the mean value of the interference in the system. However at the same time the number of links having maximum interference is also increased, explaining the overall C/I gain reduction by 0.27 dB obtained earlier. In Figure 5.16, an histogram of C/I for $\beta = 0.7$ and a maximum power limit of 30 watts is presented. The mean and median values are 22.69 and 22.83 dB. The minimum and maximum values of the distribution are -2.79 and 47.54 dB, respectively. Figure 5.16 is given primarily to compare with the reference C/I distribution (Figure 5.7).

In Figure 5.19, the C/I distributions with and without power limits for different values of β are presented for comparison. When β is 0.2 the power spread is low and falls within the range of available power. So, even when we impose a power limit, there is no change in the

C/I distribution. On the other hand, when β is 0.7 and above the power spread goes beyond the maximum power limit causing a kink in the C/I distribution plot. In Figure 5.20, downlink C/I vs power used by all the links is presented. In one case the target line is presented without imposing a power limit, where the quality reduces as the power transmitted by the links increases, as defined in the algorithm. In the same graph the downlink C/I vs power used by all the links when the power is limited to 30 Watts is superimposed. As we can see the links follow the target line until they reach the maximum power available in the system. When the links attempt to transmit at a power level of more than 30 watts to maintain quality, they are forced to transmit at this limit, hence a sudden drop in C/I at 14.7 dBW.

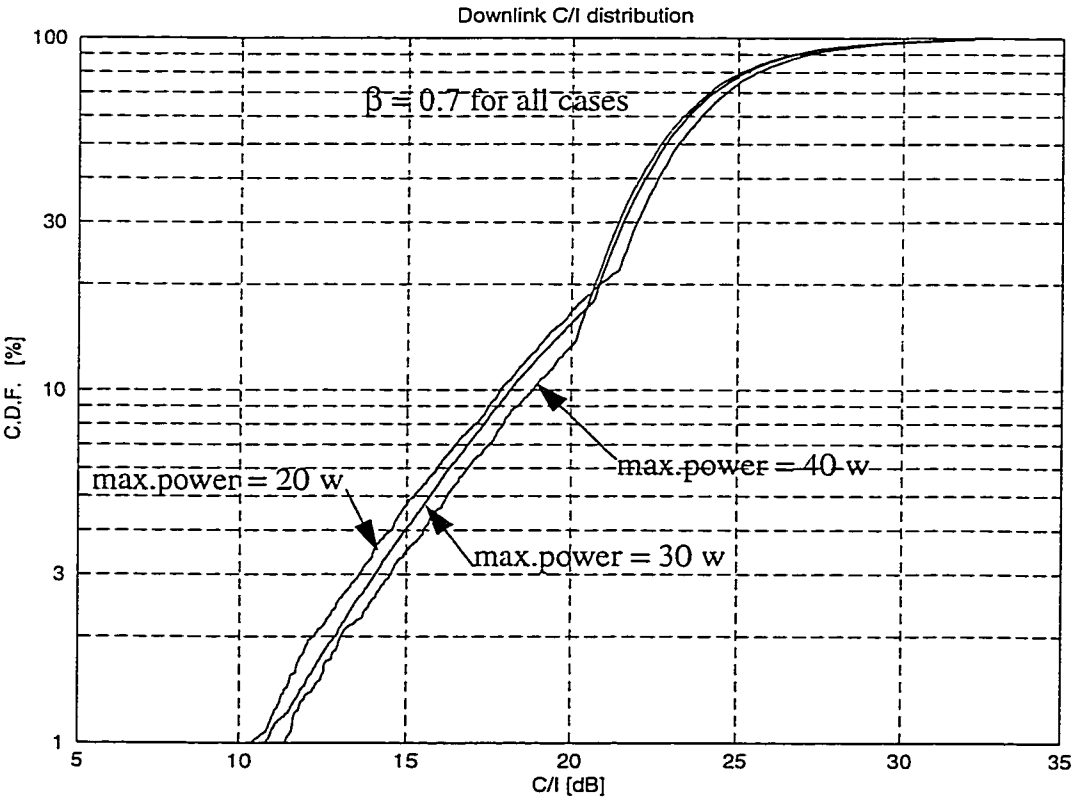

FIGURE 5.14. The C/I distribution when β = 0.7 for different maximum power limits.

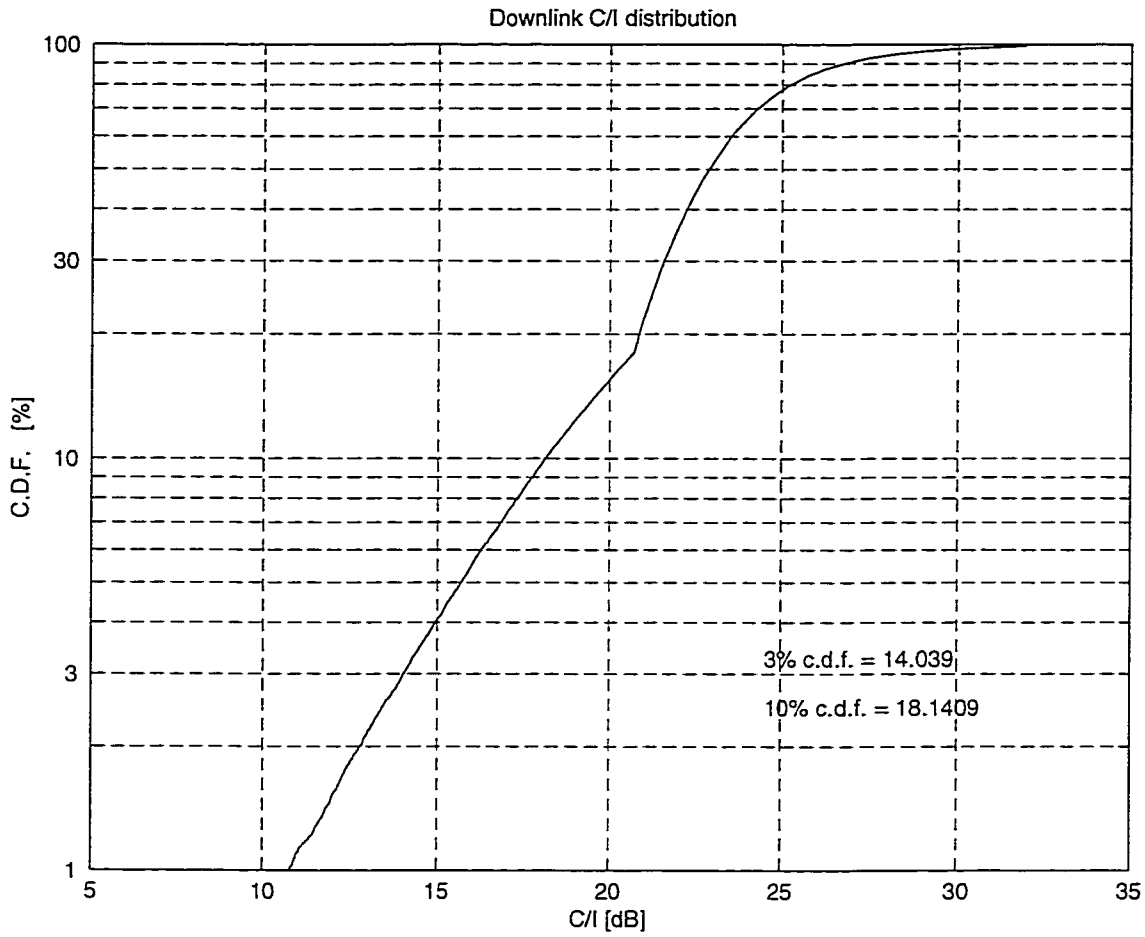

FIGURE 5.15. Downlink C/I distribution when $\beta = 0.7$ with a maximum power limit of 30 watts.

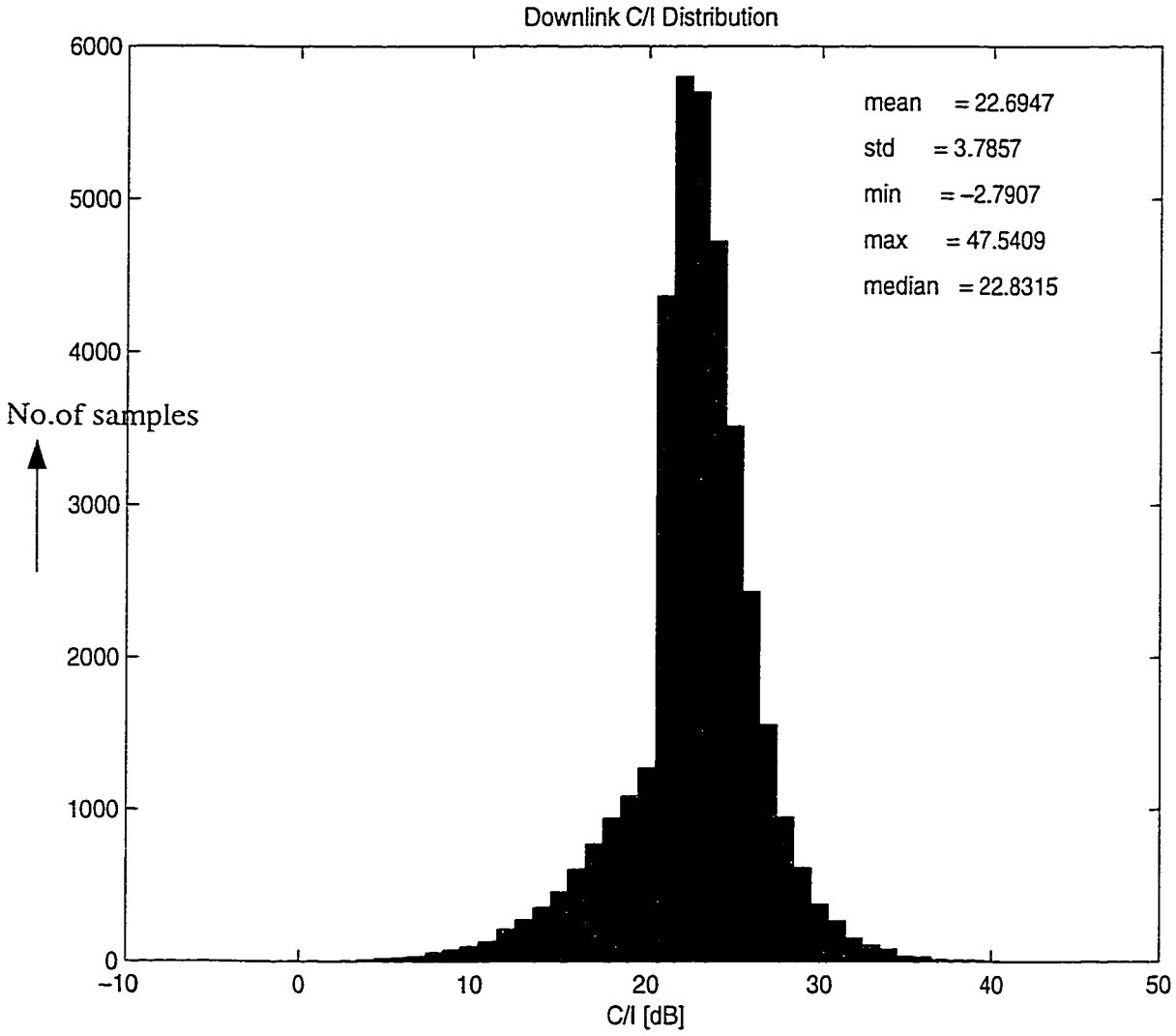

FIGURE 5.16. An histogram of C/I when $\beta = 0.7$ and a maximum power limit of 30 watts

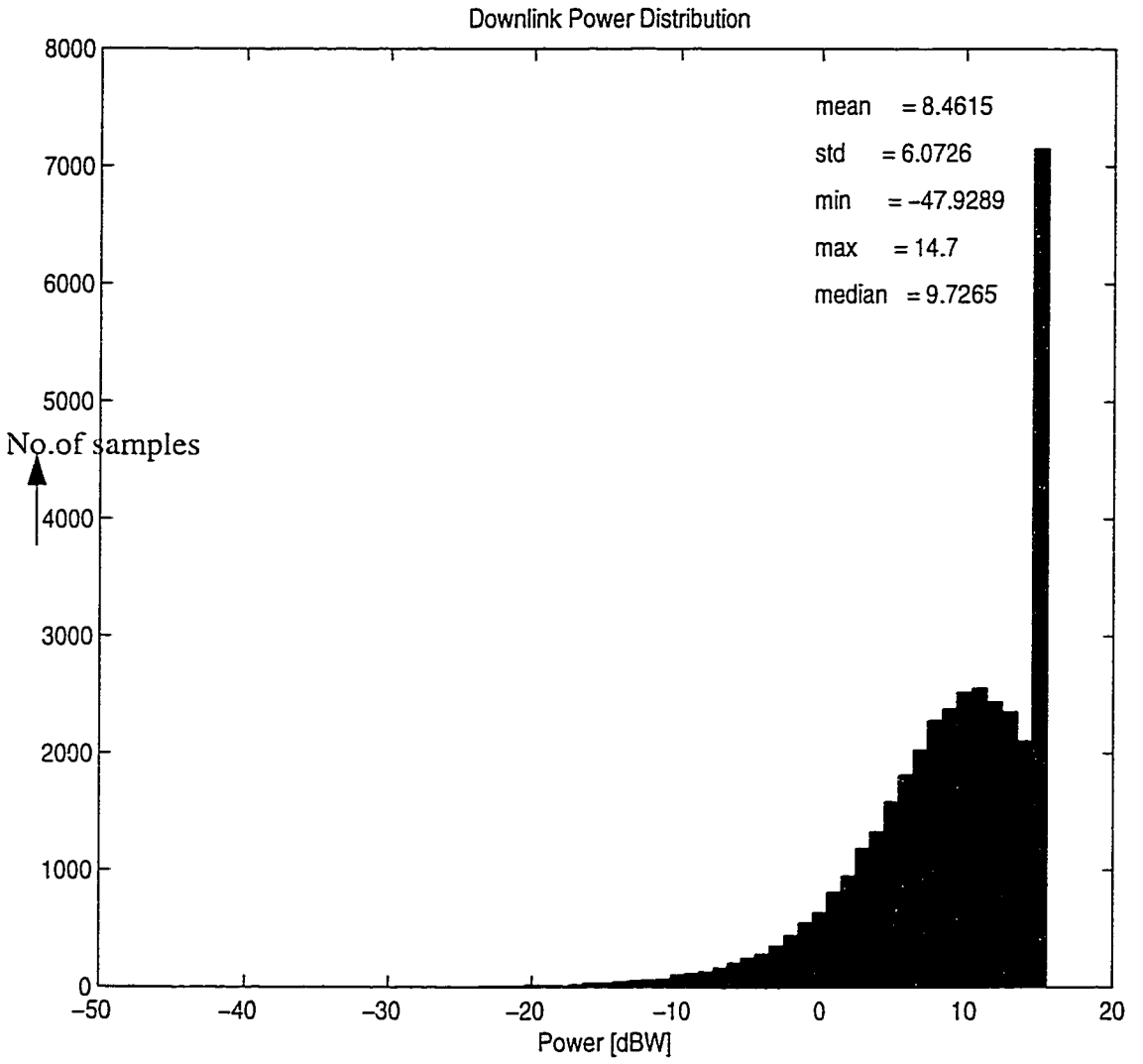

FIGURE 5.17. Downlink power distribution when $\beta = 0.7$ and a maximum power limit of 30 watts is applied

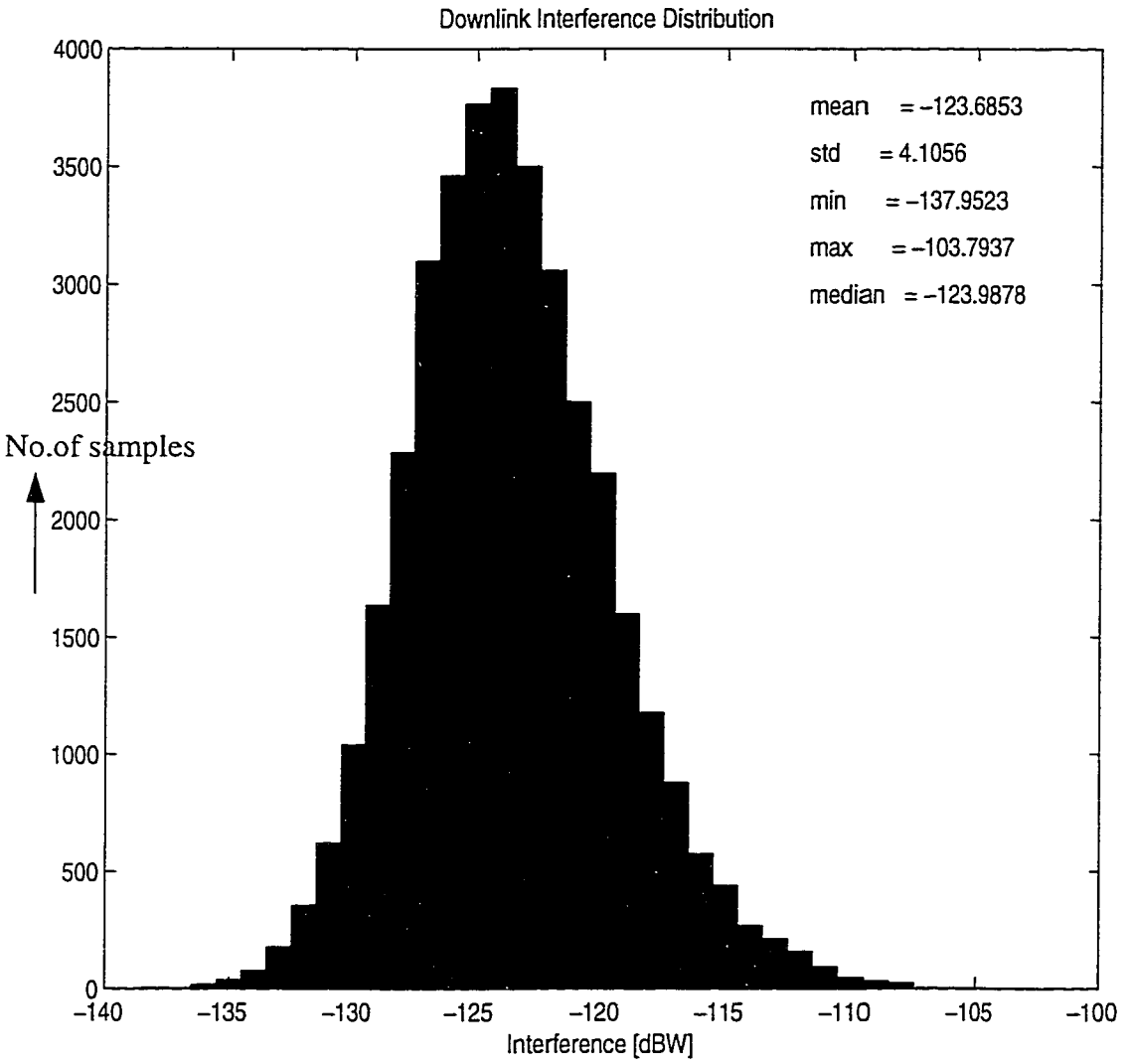

FIGURE 5.18. Downlink interference distribution when $\beta = 0.7$ with maximum power limited to 30 watts.

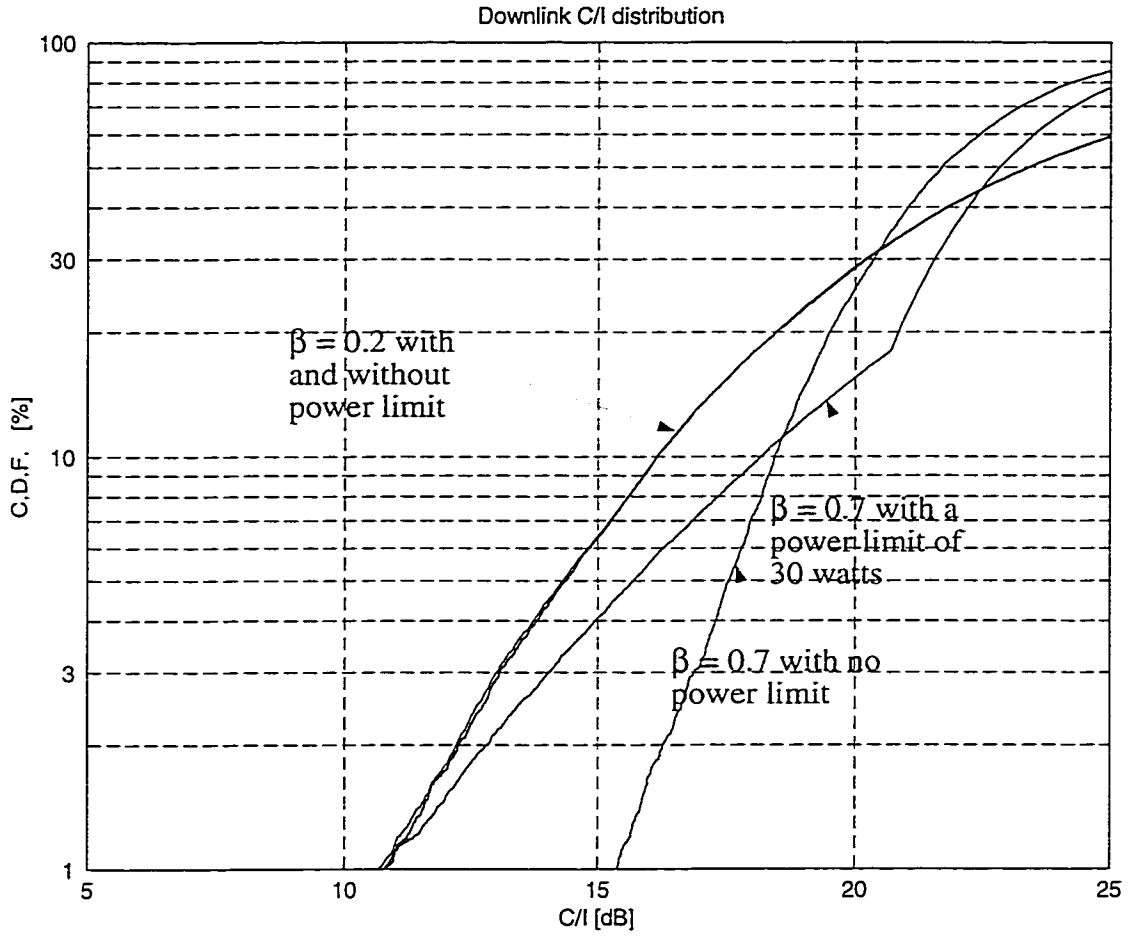

FIGURE 5.19. C/I distribution comparison with and without power limits for different values of β

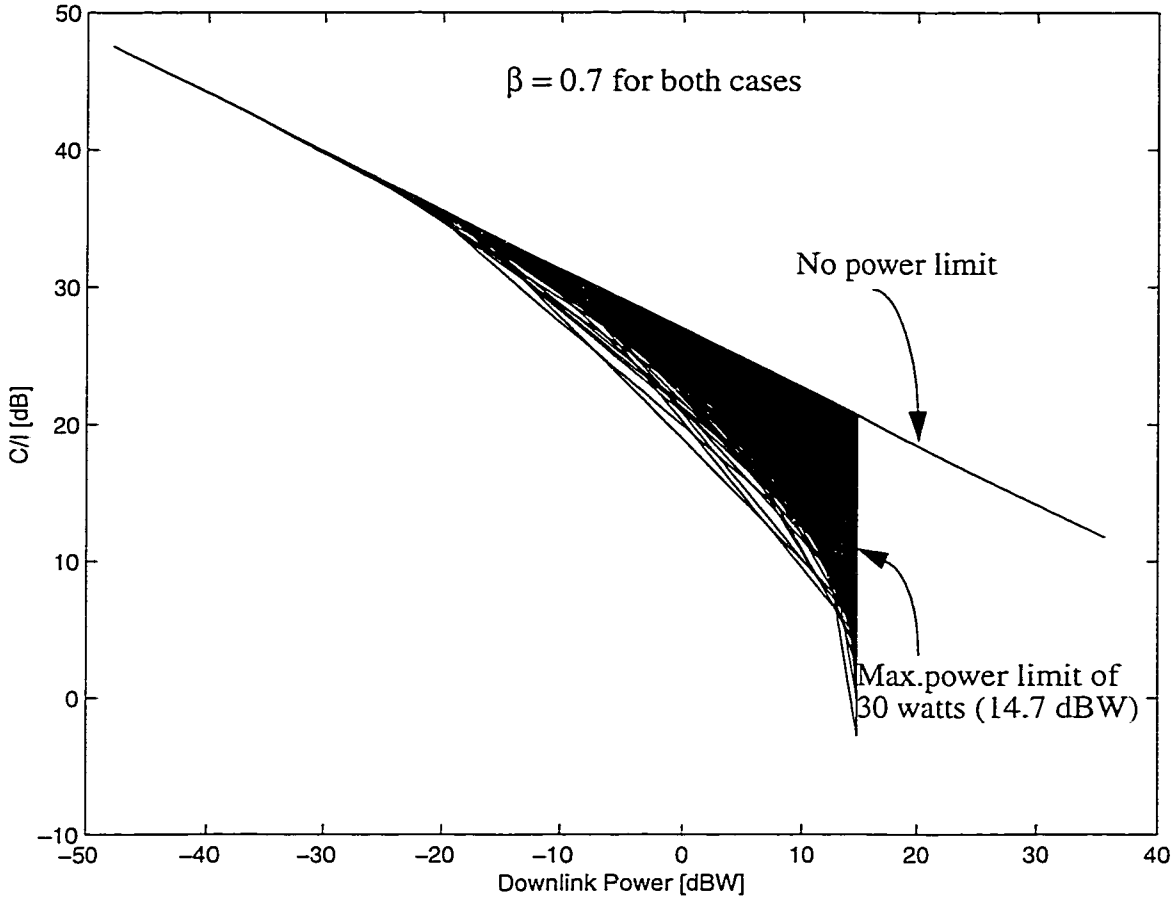

FIGURE 5.20. Downlink C/I vs Power of the links in the downlink when β = 0.7

5.4 Joint Power Control and Switch-Beam Antennas

In this section the simulation results of joint power control and narrow beam transmission are presented. In chapter 4, simulation results of a 4/12 reuse system with narrowbeam transmission were presented and it was found that by introducing 4 narrow beams in place of a sectored antenna, the C/I improves by more than 4 dB. In this section, simulation results are presented when the downlink power control scheme is included along with narrow beam transmission for 4/12 reuse. The power control algorithm described in section 5.2 is used in the simulations. As was done in section 5.3, simulation results are first presented without power limiting and then with power limiting.

5.4.1 Simulation Results with No Power Limit

When four narrow beams are used for transmission in the downlink the C/I at 10% CDF is 18.93 dB and at 3% CDF it is 14.03 dB. The beam selected for the transmission is based on the direction of the mobile from the base station. Since the energy is focused in that direction via a narrowbeam, the interference in the direction of a cochannel link is less and hence the interference in the system is less. This is the basic reason why interference reduces with the introduction of narrowbeam transmission. The effective radiated power of the antenna in a particular direction towards the mobile can be written as $P_t G_t$ where P_t is the transmitted power level and G_t is the gain of the antenna. So, to change the amount of power in the direction of the mobile, the power level can be changed accordingly, since G_t is assumed to be constant.

Figure 5.21 to Figure 5.29 and Table 5.2 present the simulation results of joint power control and four narrowbeams per sector (120^o). Here, P_t is changed to achieve the required level in a given direction of the mobile. Optimizing the power levels in the direction of the mobile further reduces the interference to the cochannels in the system.

As we have seen in Section 5.3, as β increases the C/I increases up to an optimum value of β and then it starts dropping. In Figure 5.21 the C/I distribution is presented for the optimum value of $\beta = 0.65$. The optimum value of β in the previous section with only a sectored antenna was 0.7. Actually the difference of C/I gain achieved with β being 0.65 or 0.7 is very small and so $\beta = 0.65$ is considered as optimum value for the simulations in joint power control and narrowbeam transmission. The C/I distribution spread (Figure 5.22) decreases when the power control is applied to the downlinks compared to the case with no power control. The C/I improvement with power control in this case is 3.9 dB over the case where only narrowbeam transmission is simulated (Figure 5.21 and Figure 4.18). In Figure 5.23, the downlink interference distribution for $\beta = 0.65$ is presented. The mean and median values are -139.74 and -140.29 dBW. The minimum and maximum values of the interference distribution are -157.98 and -140.29 dBW, respectively. This is presented basically to compare the interference distribution with narrow beam transmission alone (Figure 4.19), and it is

observed that there is not much variation in mean and median values but the standard deviation is increased from 5 dB to 8.4 dB.

The downlink power distribution of power controlled narrowbeam transmission is shown in Figure 5.24. The mean transmitted power is -2.25 dBW as opposed to 11.69 dBW when power control is applied in a sectored antenna system (Figure 5.11). This demonstrates that the power levels required to achieve a target C/I when power control is included with a narrowbeam transmission are substantially decreased. When low power levels are transmitted on the links, obviously the interference in the system is reduced which in turn helps to improve the C/I.

Figure 5.25 to Figure 5.28 present the C/I distribution, interference and power distributions when $\beta = 0.9$. As explained earlier, as β increases the power spread increases and the mean of the interference distribution increases compared to the $\beta = 0.65$ case (Figure 5.23 and Figure 5.24). The C/I at 10% CDF is also reduced and is equal to 22.19 dB, and 19.89 dB at 3% CDF.

In Figure 5.29 simulation results of C/I distribution for different values of β ranging from 0 to 0.99 are presented. In Table 5.2 the C/I values at 10% CDF and at 3% CDF are presented. The largest value of β used is 0.99 because if $\beta = 1$, all links will try to achieve the same C/I and in effect the system may become unstable.

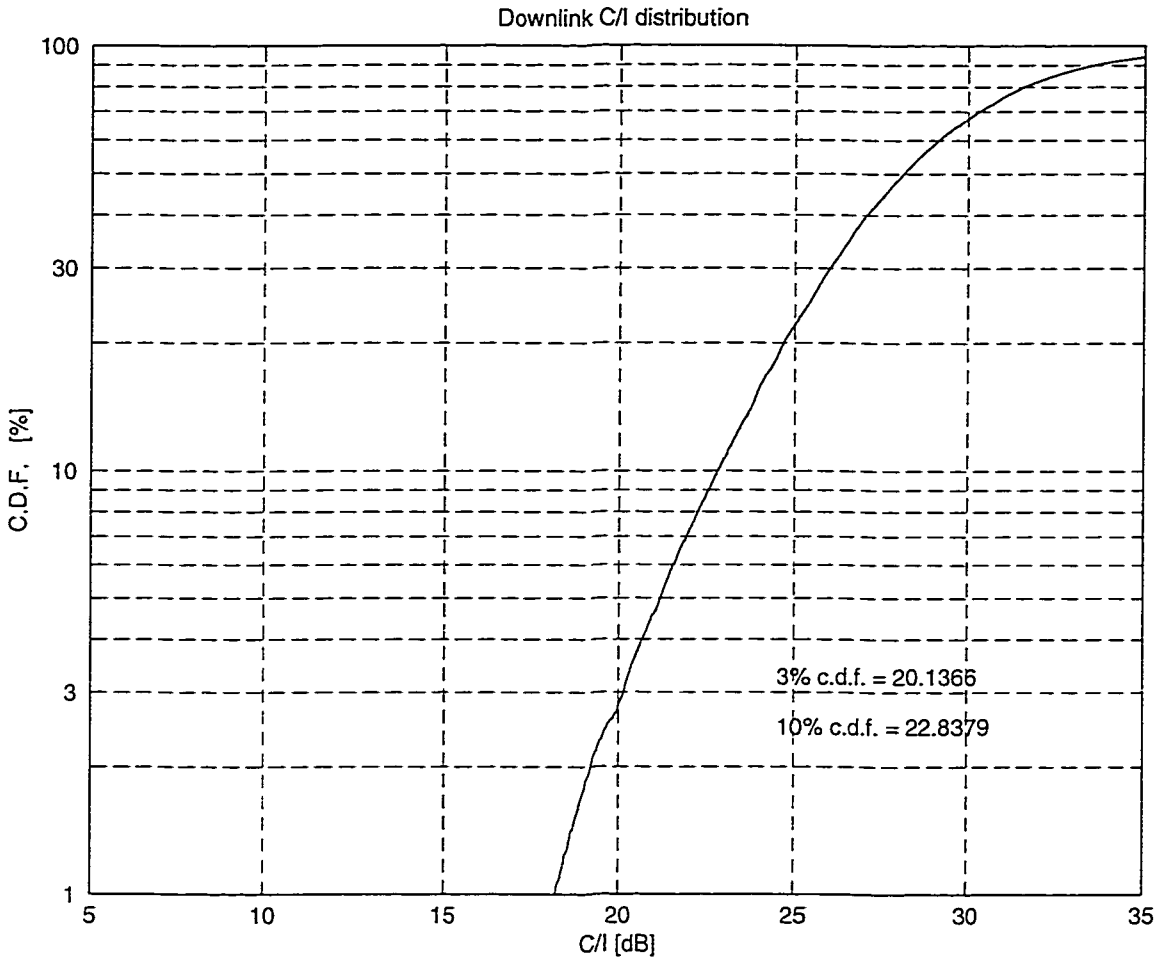

FIGURE 5.21. Downlink C/I distribution when $\beta = 0.65$

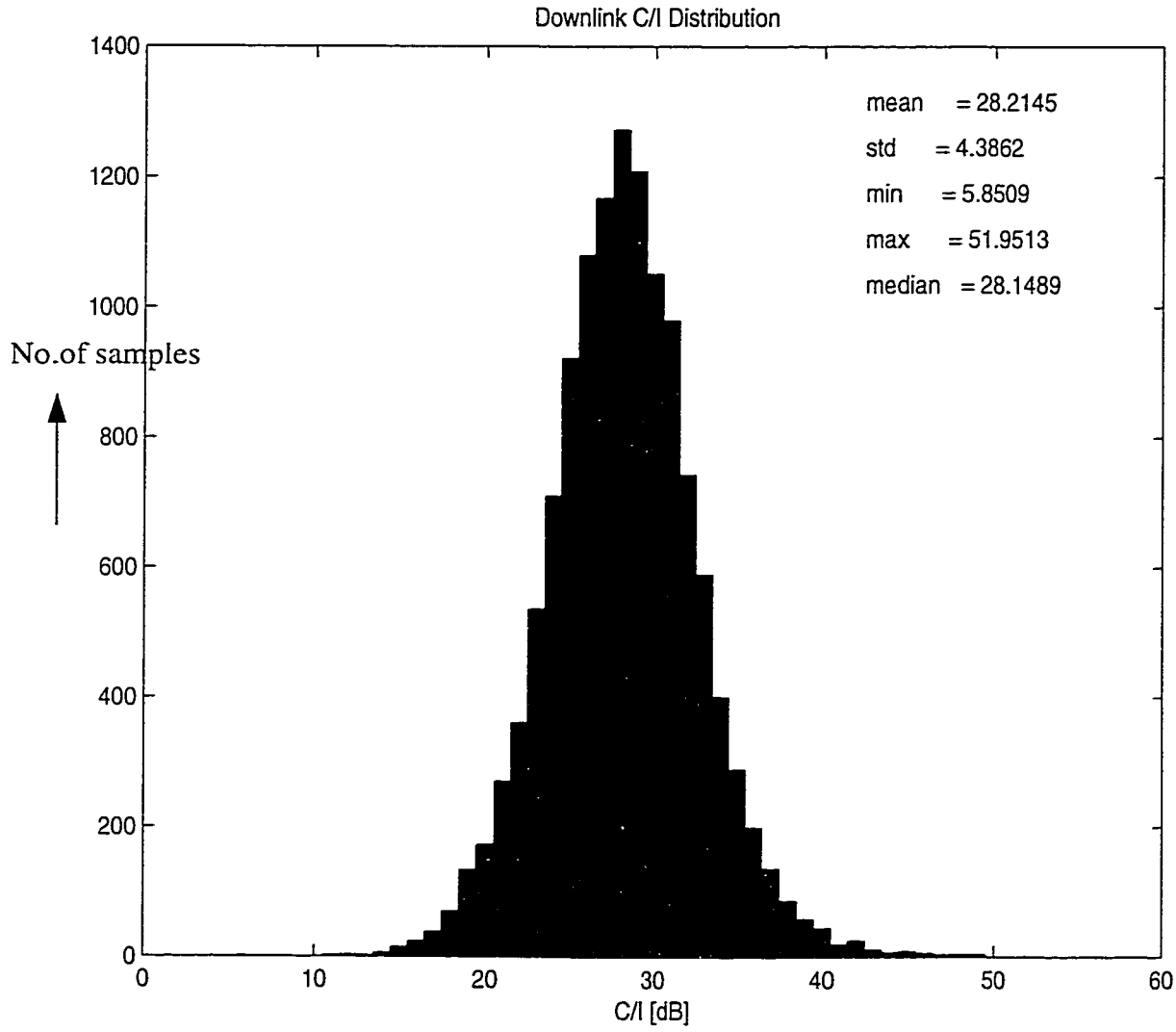

FIGURE 5.22. Histogram of downlink C/I distribution when $\beta = 0.65$

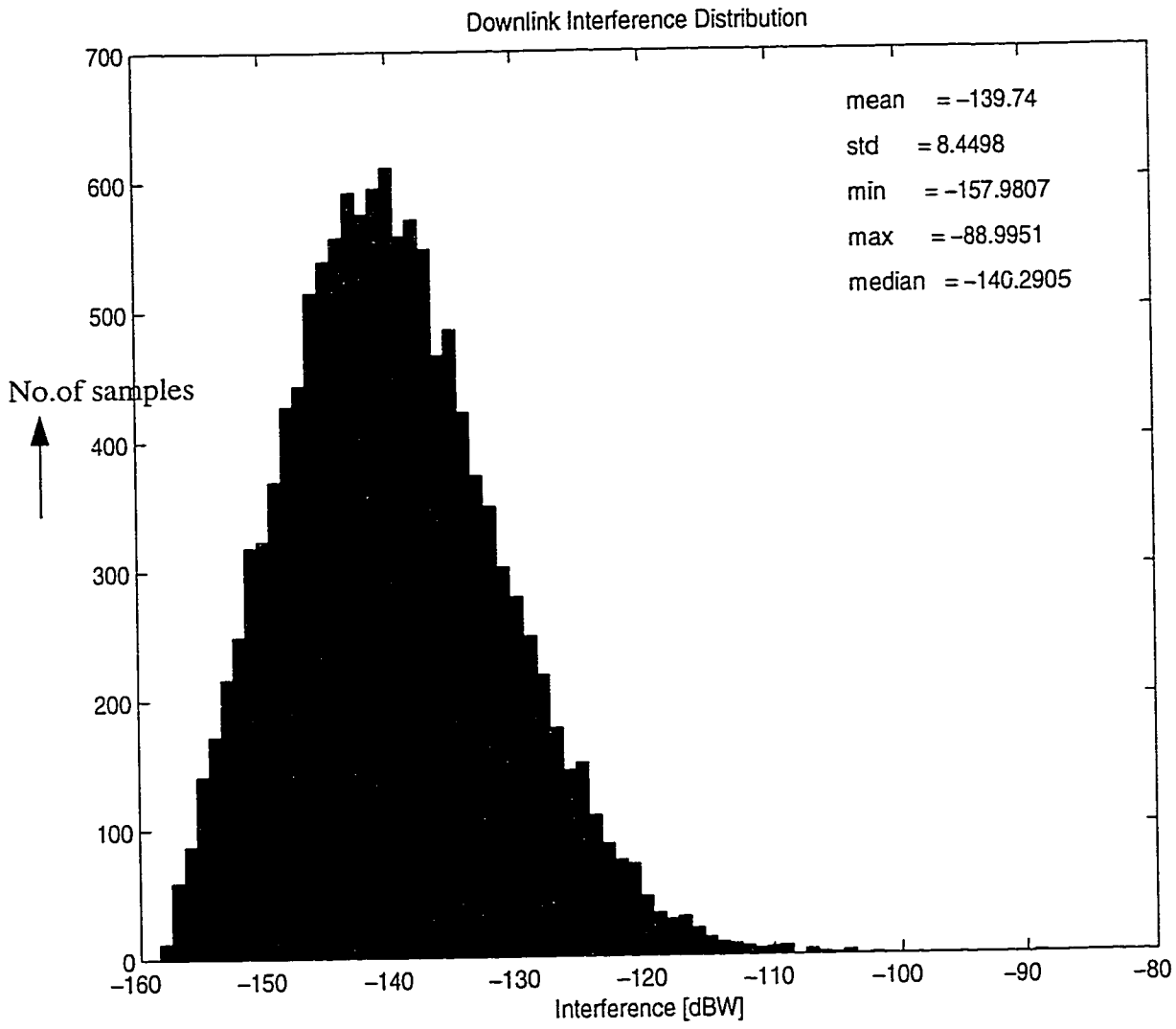

FIGURE 5.23. Downlink interference distribution when $\beta = 0.65$

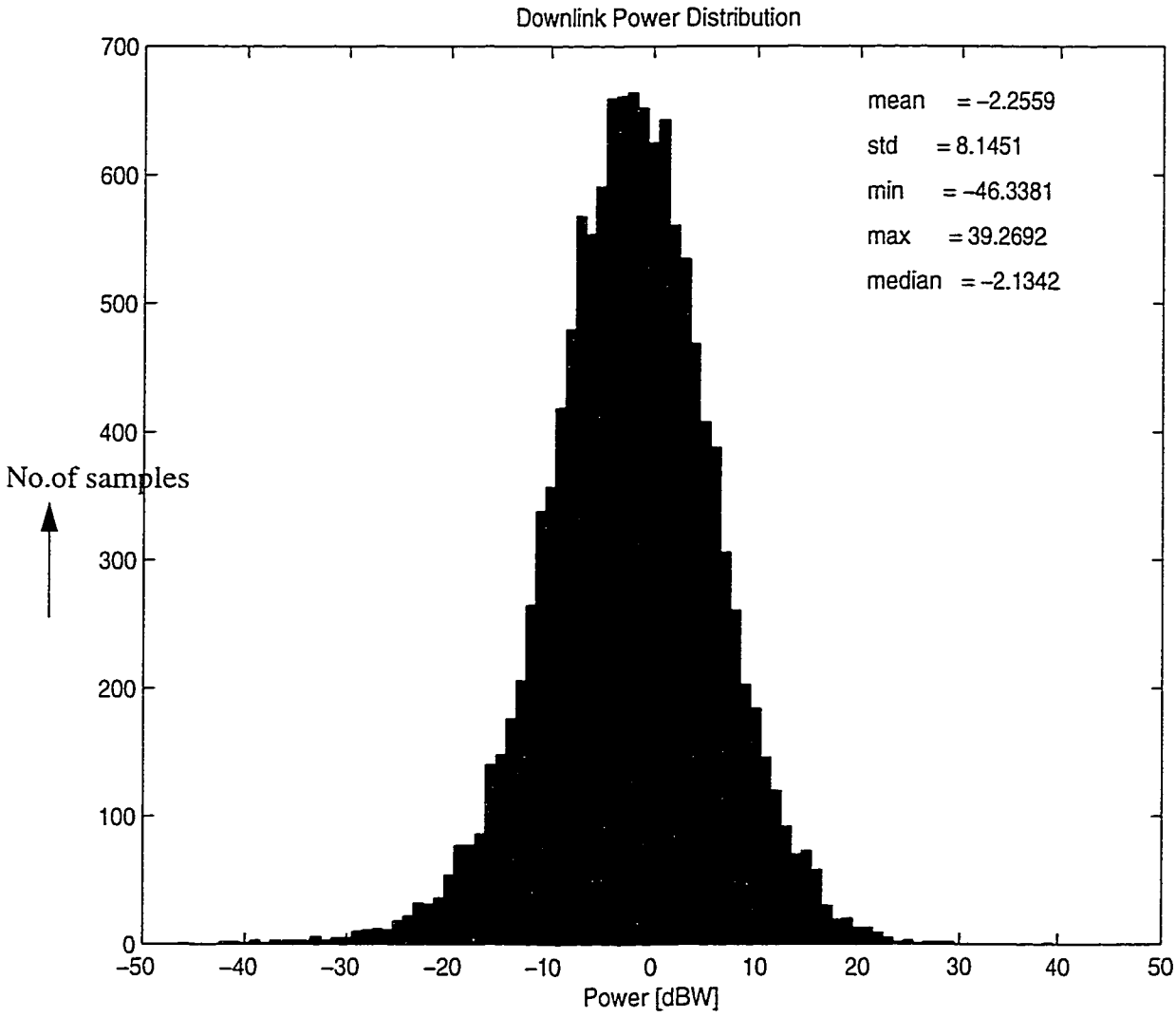

FIGURE 5.24. Downlink power distribution when $\beta = 0.65$

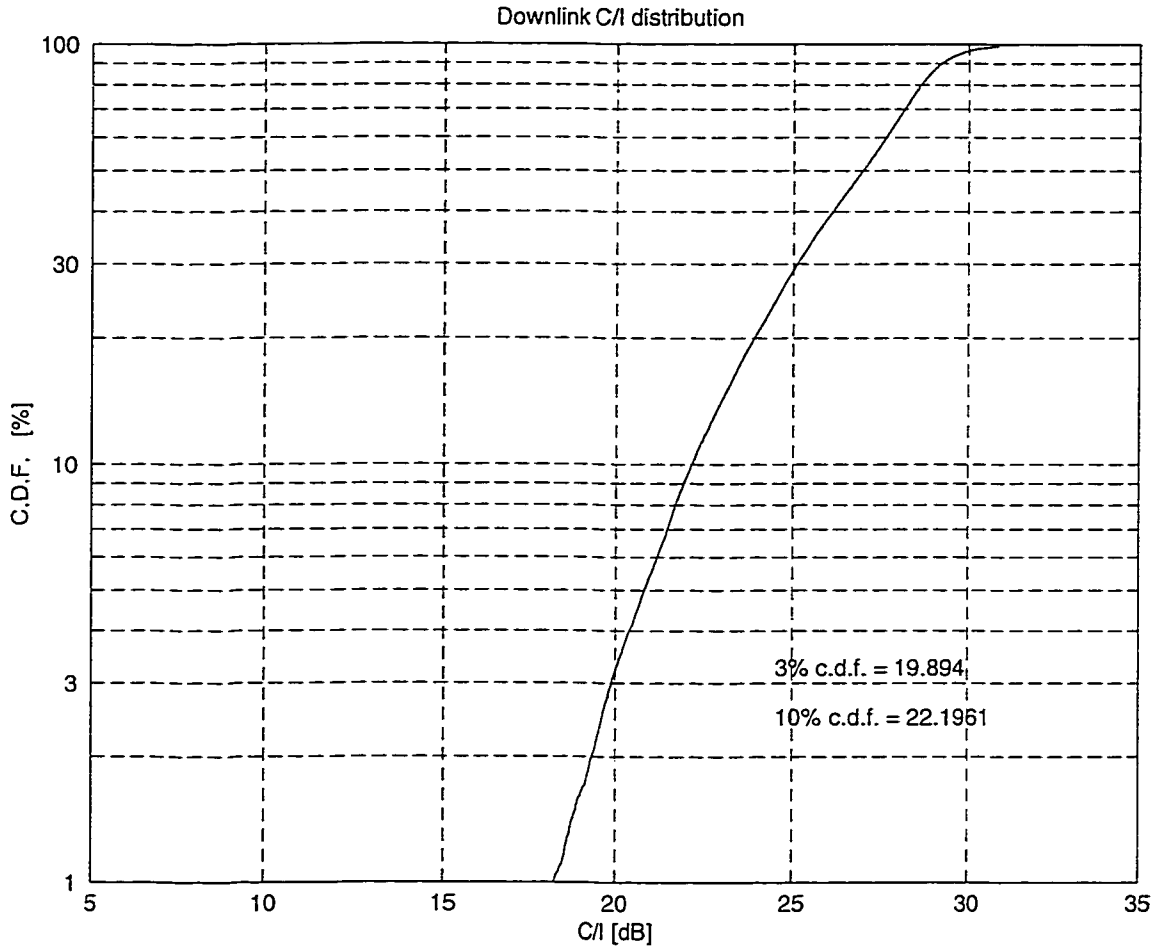

FIGURE 5.25. Downlink C/I distribution when $\beta = 0.9$

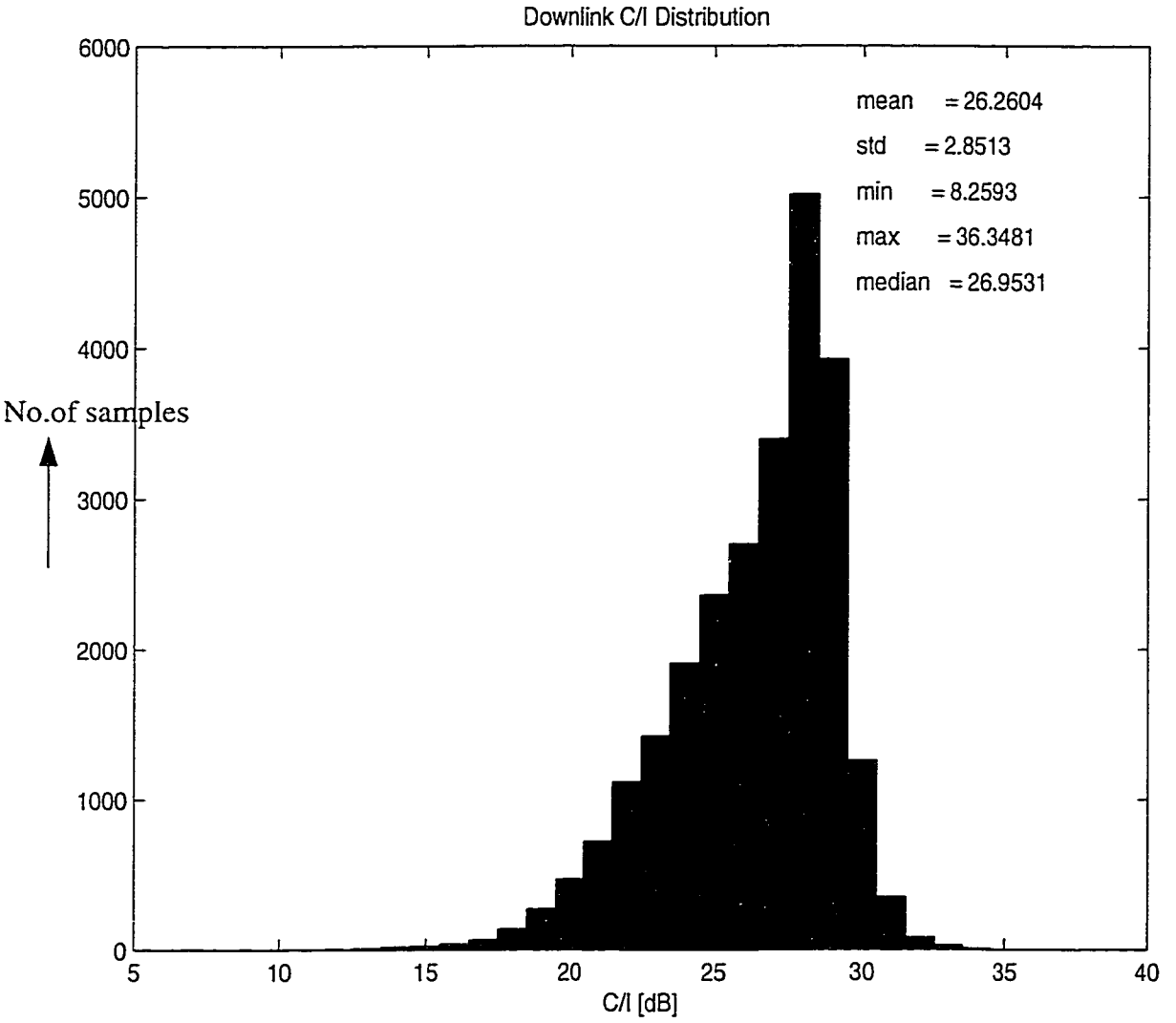

FIGURE 5.26. Histogram of the downlink C/I distribution when $\beta = 0.9$

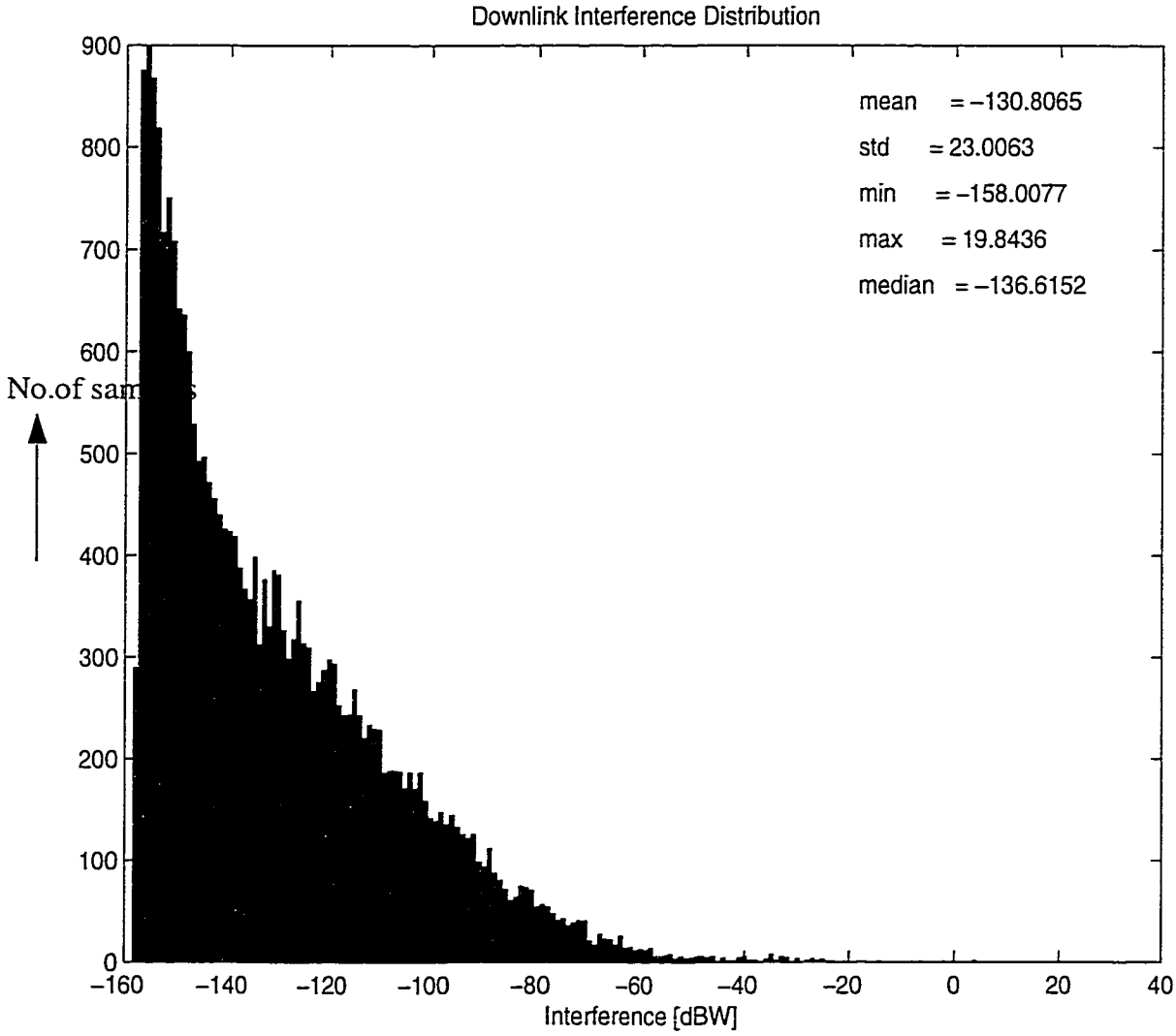

FIGURE 5.27. Downlink Interference distribution when $\beta = 0.9$

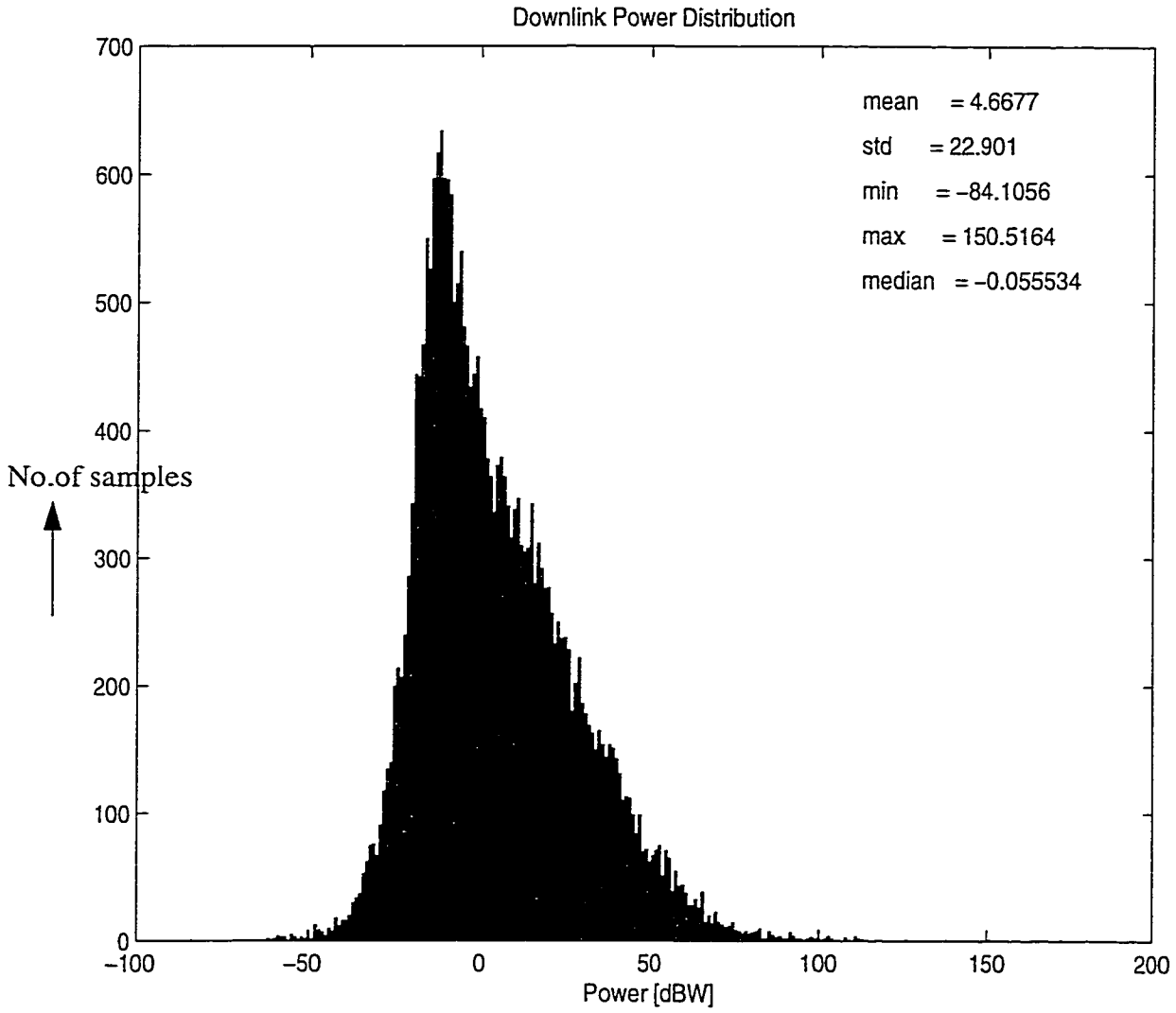

FIGURE 5.28. Downlink power distribution when $\beta = 0.9$

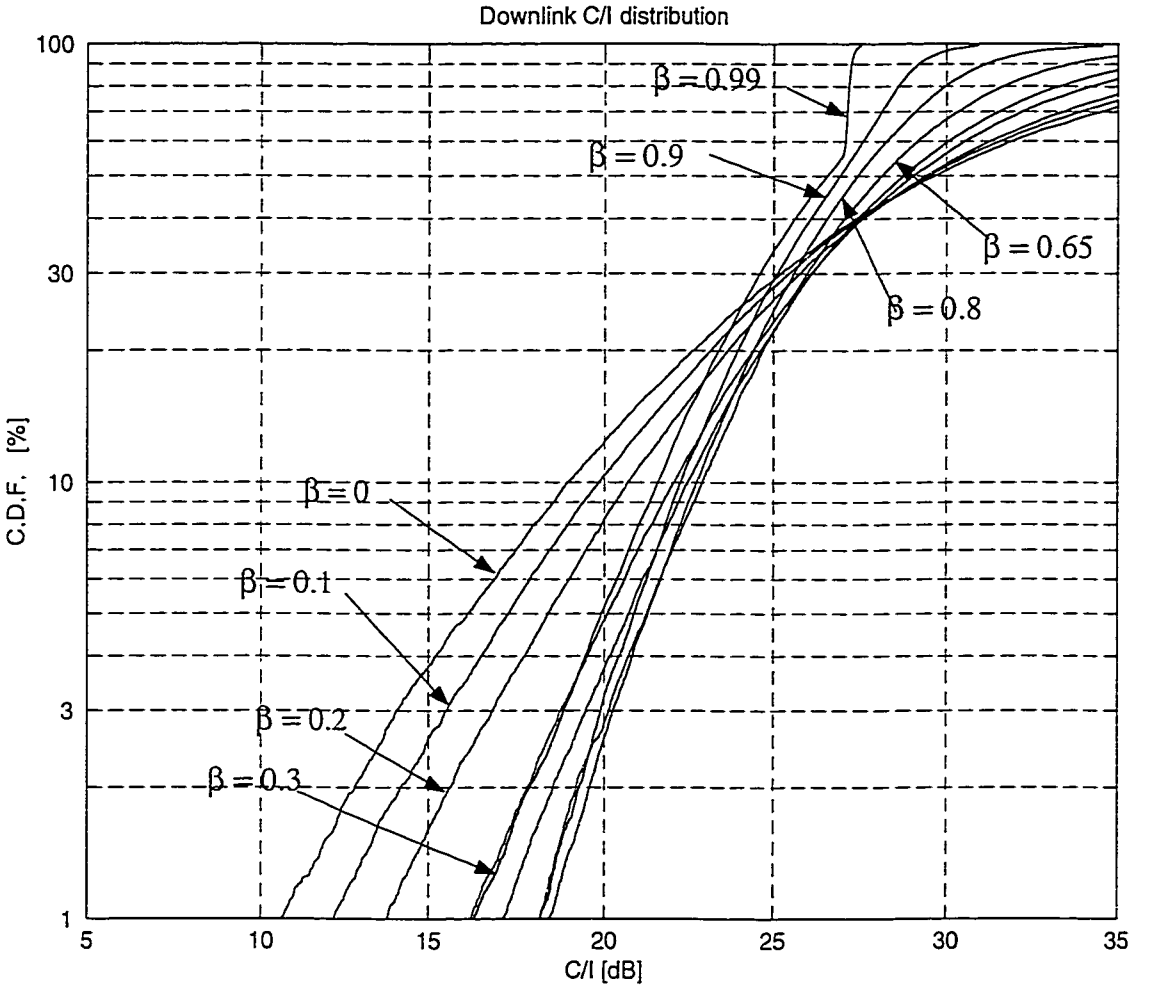

FIGURE 5.29. Downlink C/I distribution for different values of β ranging from 0 to 0.99

TABLE 5.2. C/I values at different values of β

β	C/I at 10% CDF [dB]	C/I at 3% CDF [dB]
0 (No power control)	*18.9311*	*14.0382*
0.1	19.8278	15.5148
0.2	20.6528	16.8254
0.3	21.9982	18.7554
0.5	22.4113	19.4632
0.65	*22.8379*	*20.1366*
0.8	22.6706	20.2476
0.9	22.1961	19.894
0.99	21.5249	18.8392

5.4.2 Simulation Results with a Power Limit of 30 watts

For the reasons explained in section 5.3.3 there is a need for a limit on the maximum power transmitted. In the simulator the maximum power available to the links is assumed to be 30 Watts. Figure 5.30 to Figure 5.38 and Table 5.3 present the simulation results with this maximum power limit.

Figure 5.30 to Figure 5.33 present the C/I distribution, C/I spread, interference and power distribution when $\beta = 0.65$. We can notice that the results obtained with a power limit are very similar to the ones without a power limit for $\beta = 0.65$. This is due to the fact that, with no power limit there is less power spread and most links transmit at power levels well within the maximum power level of 30 watts; however, some links transmit at a higher power level but they are very few in number. Thus, when the power is restricted to 30 watts, not many links are forced to transmit at the maximum power level. This is the reason why there is no kink in the downlink C/I distribution curve presented in Figure 5.30 as compared to the C/I curves in Section 5.3.

The above reasoning is not true for the case when $\beta = 0.9$. From Figure 5.28, the power spread is very high and the mean of the transmitted power is 4.66 dBW compared to -2.25 dBW for $\beta = 0.65$ with no power limit. Therefore, when we apply a restriction on the maxi-

mum power for the case where $\beta = 0.9$, most of the connections transmitting above 30 Watts are now restricted to this maximum available power. As a result, a kink in the C/I curve appears (Figure 5.34) and C/I of the links which are restricted to a maximum power of 30 Watts starts to deteriorate. This can be clearly viewed in Figure 5.36 where the valley-shaped interference distribution of all the downlinks is presented. Here, we see that the links transmitting lower than 30 Watts have low interference levels. For the links which are trying to achieve the required C/I by increasing their power levels to 30 Watts, their C/I starts deteriorating due to interference from other cochannels. This is the reason why most of the links either have a high level of interference or a low level and very few in the middle. The C/I at 10% CDF is 24.46 dB which is 5.53 dB over the case where only narrowbeam transmission is used and 1.5 dB greater than with no power limit. The downlink C/I distribution and power distribution are presented in Figure 5.35 and Figure 5.37 respectively for the β value of 0.9. In Figure 5.38 the downlink C/I distribution for different values of β between 0 and 0.99 are presented. In Table 5.3 the C/I at 10% CDF and at 3% CDF are presented for these values of β, indicating that optimum C/I performance is achieved with β =0.9.

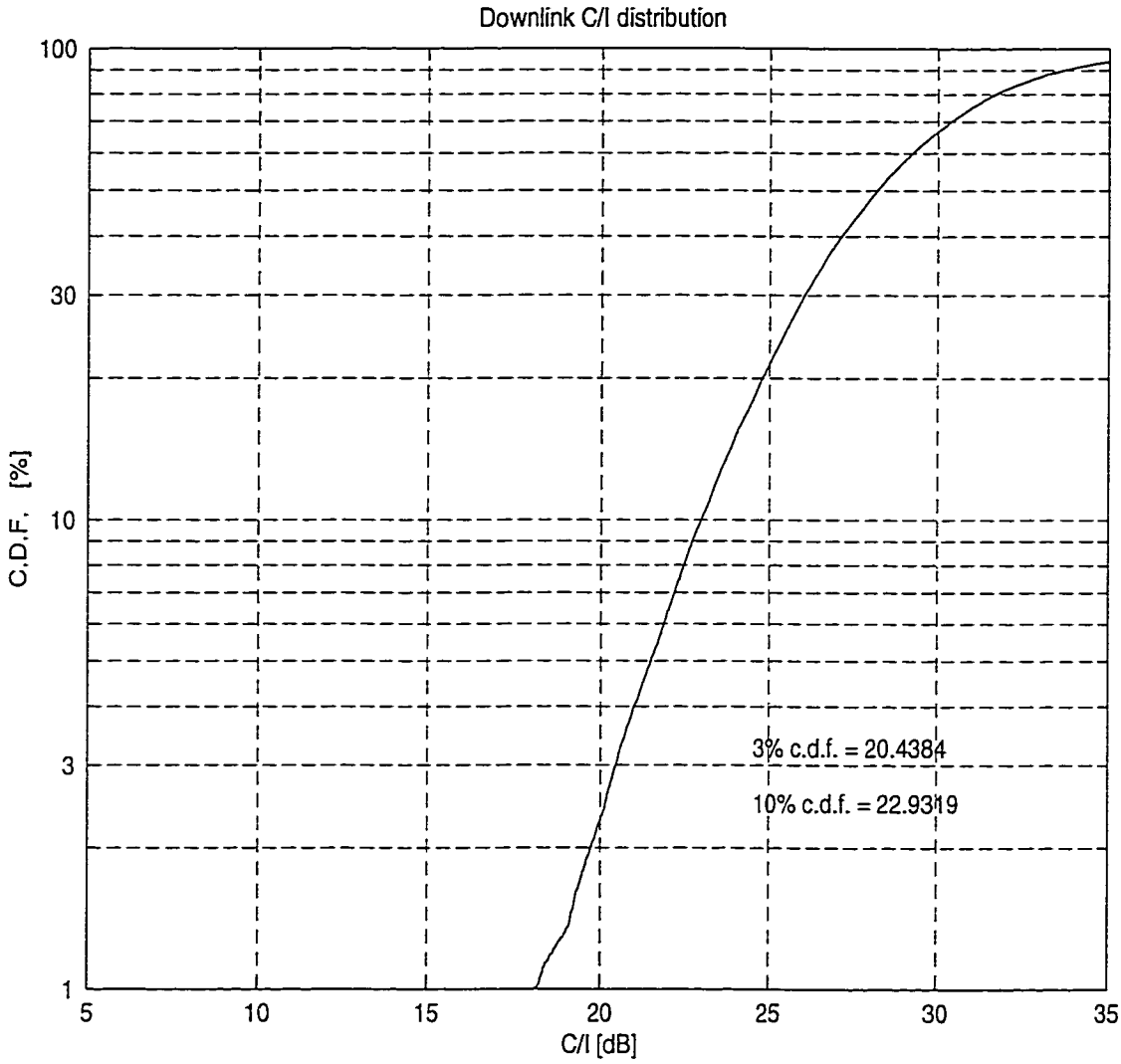

FIGURE 5.30. Downlink C/I distribution when $\beta = 0.65$

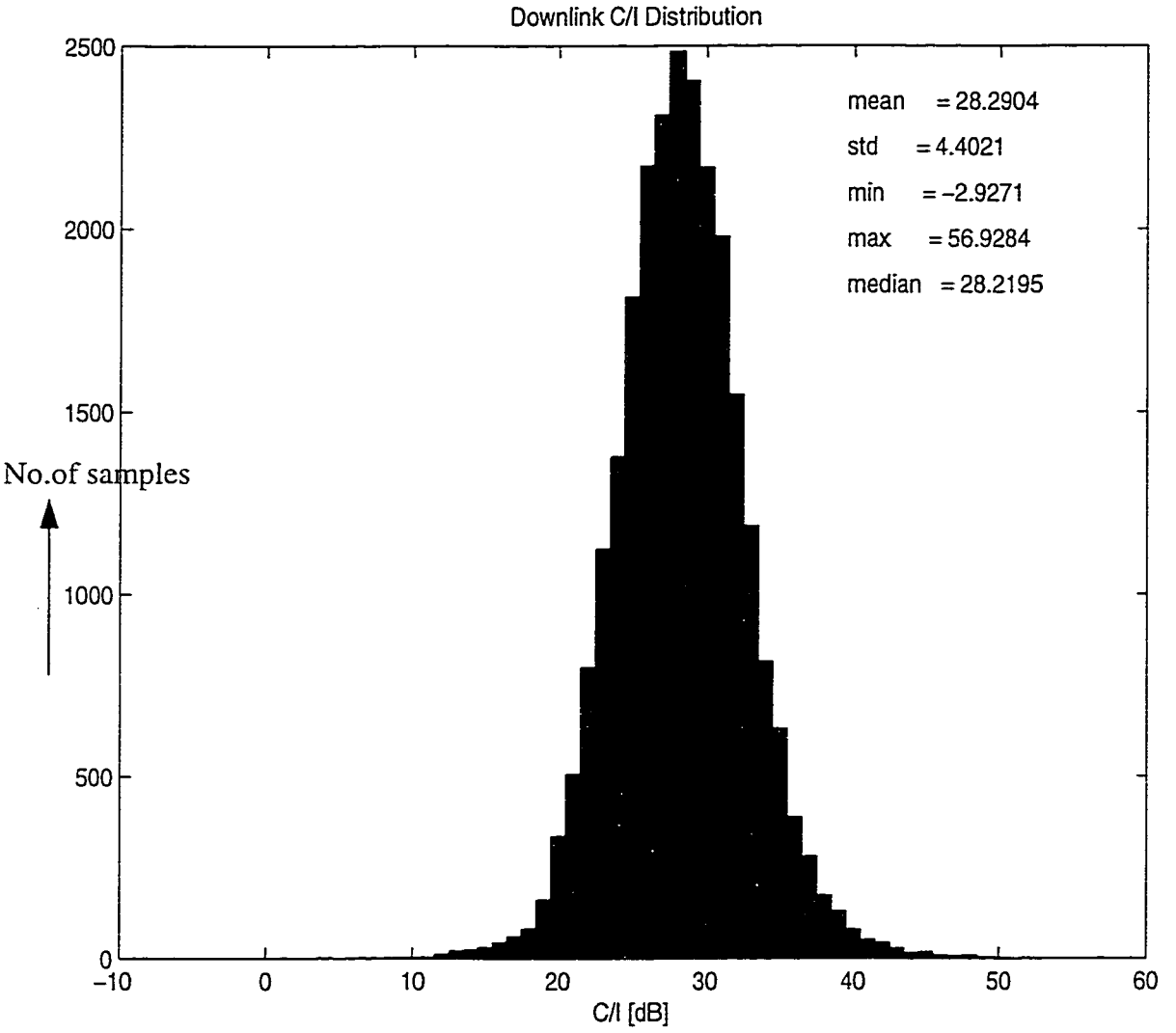

FIGURE 5.31. Histogram of the downlink C/I distribution when $\beta = 0.65$

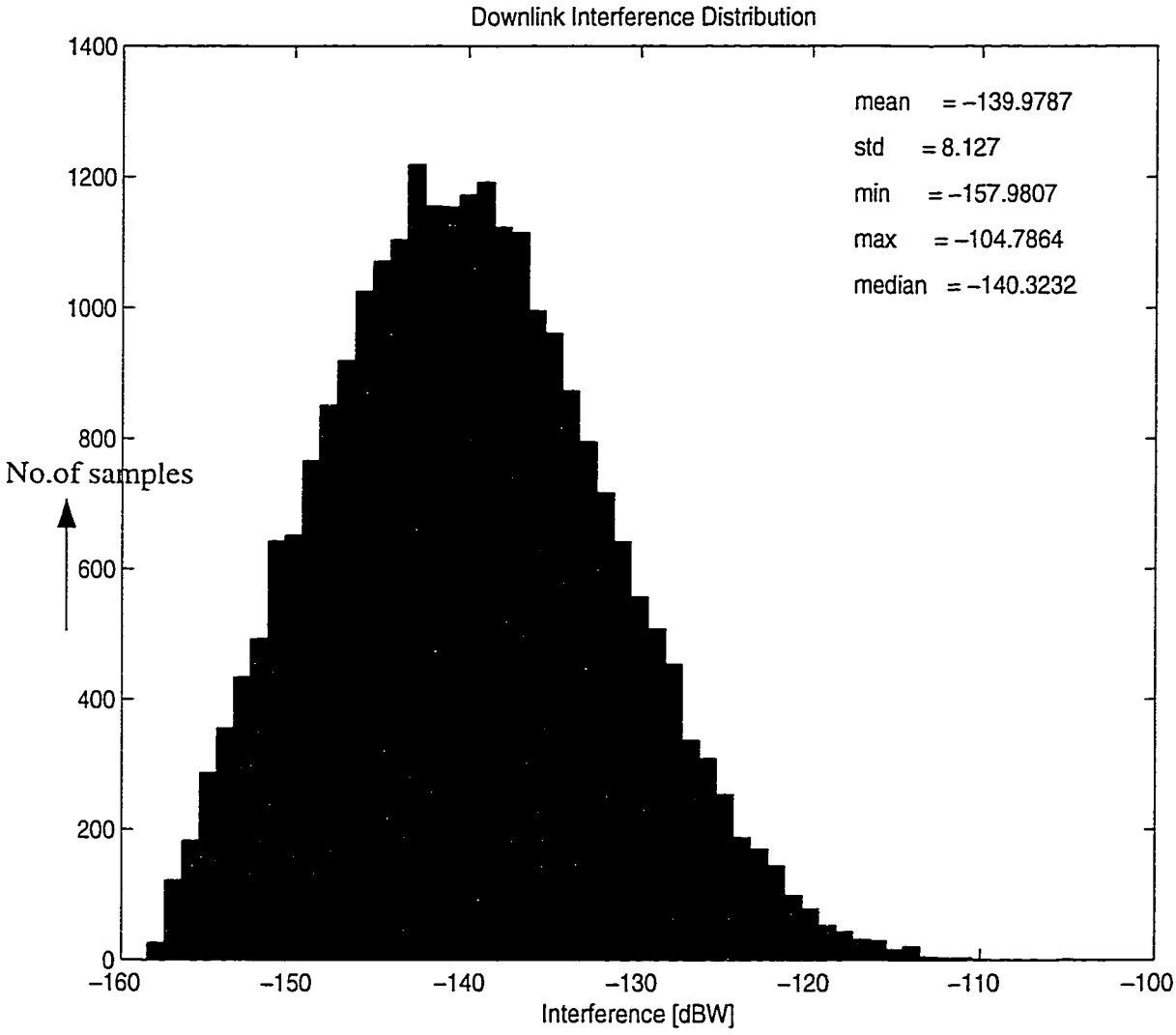

FIGURE 5.32. Downlink interference distribution when $\beta = 0.65$

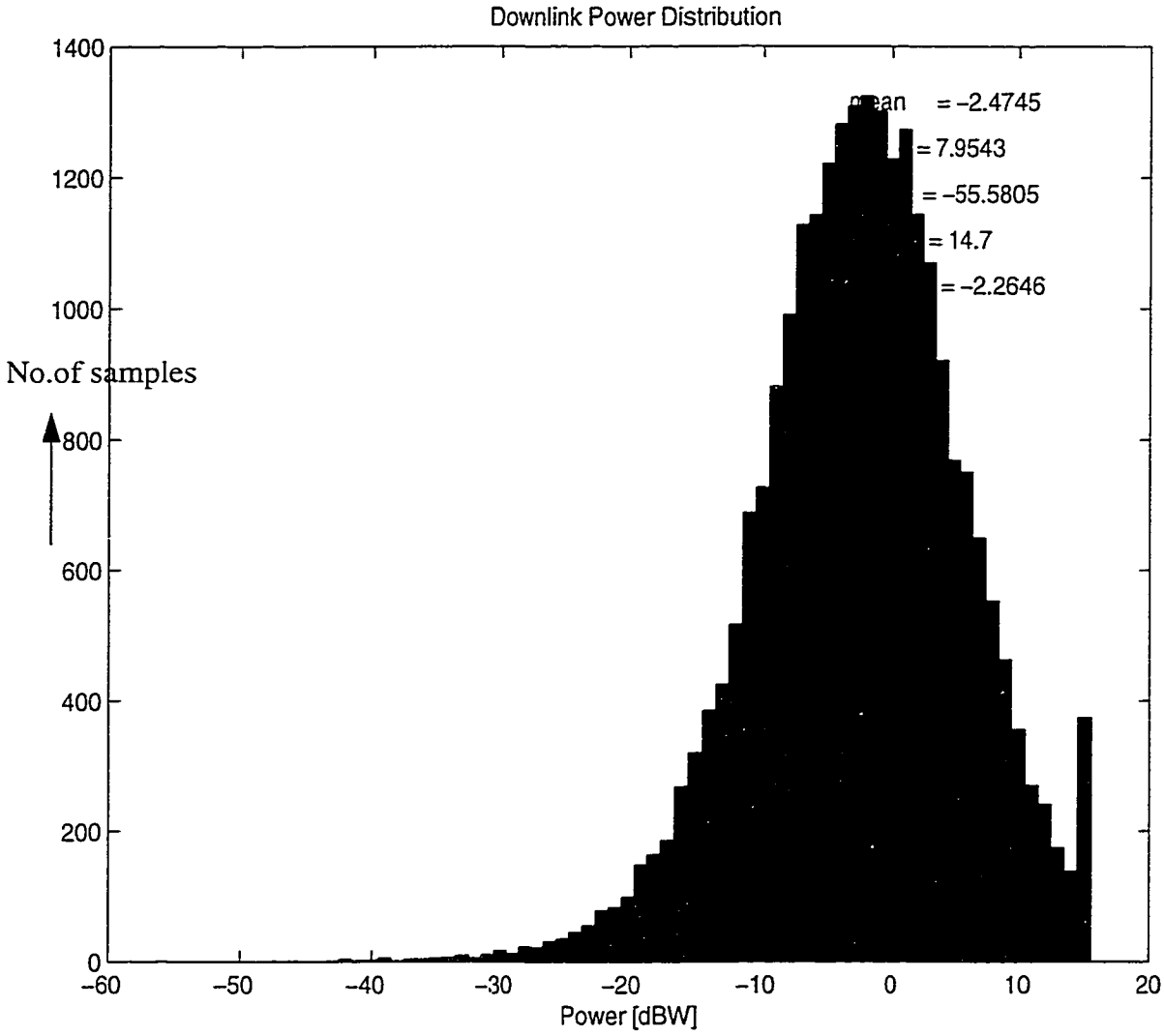

FIGURE 5.33. Downlink power distribution when $\beta = 0.65$

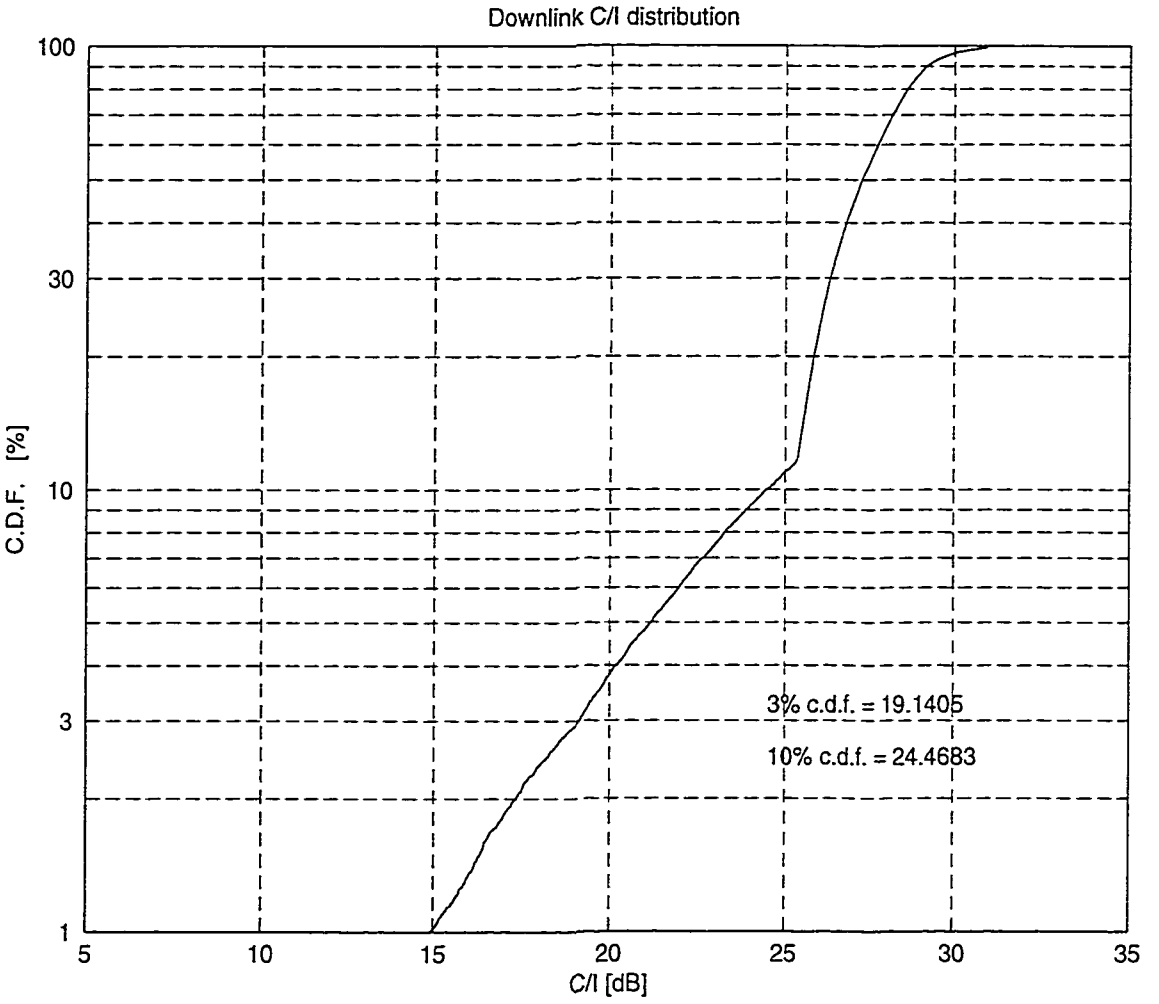

FIGURE 5.34. Downlink C/I distribution when $\beta = 0.9$

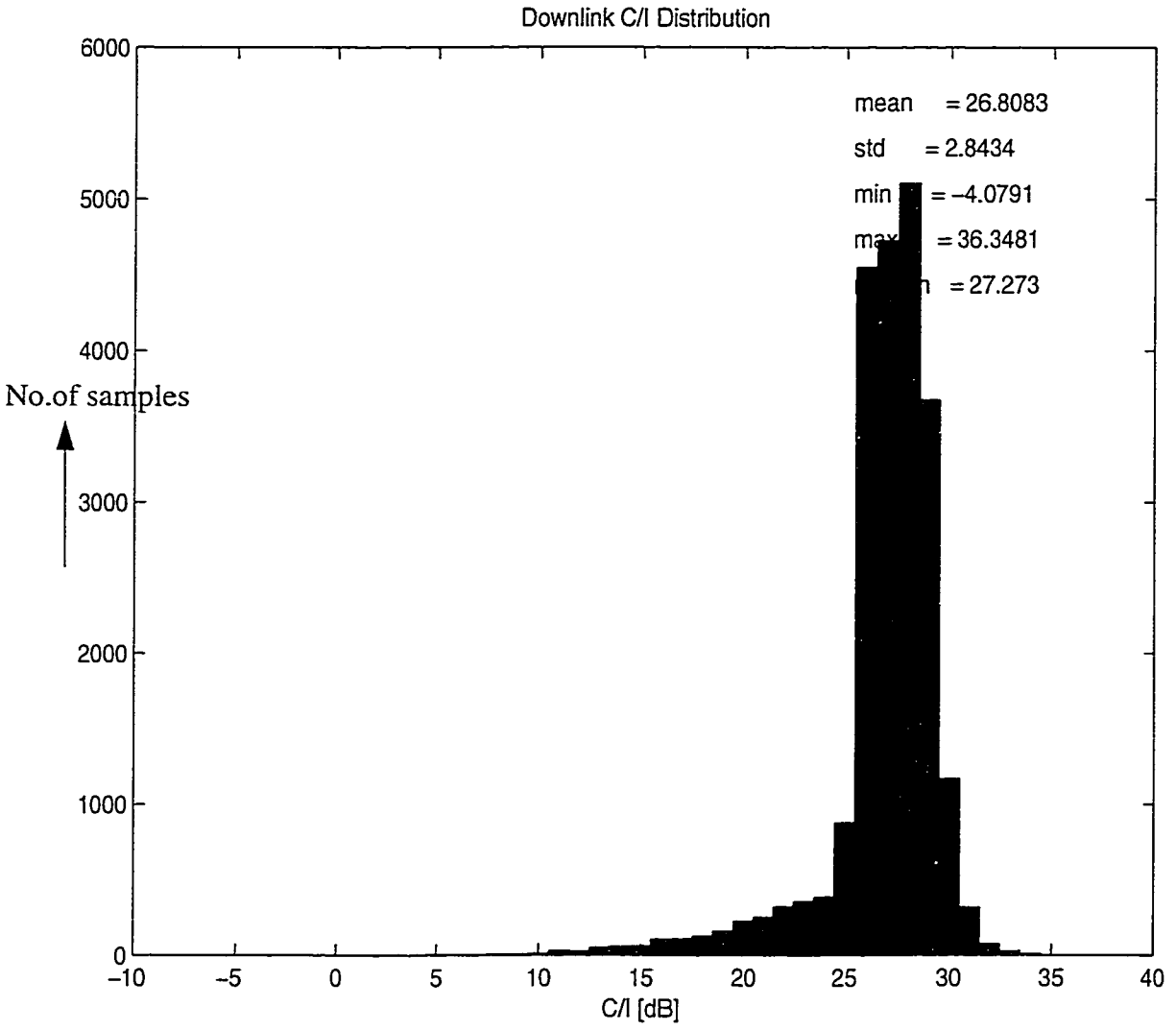

FIGURE 5.35. Histogram of the Downlink C/I distribution when $\beta = 0.9$

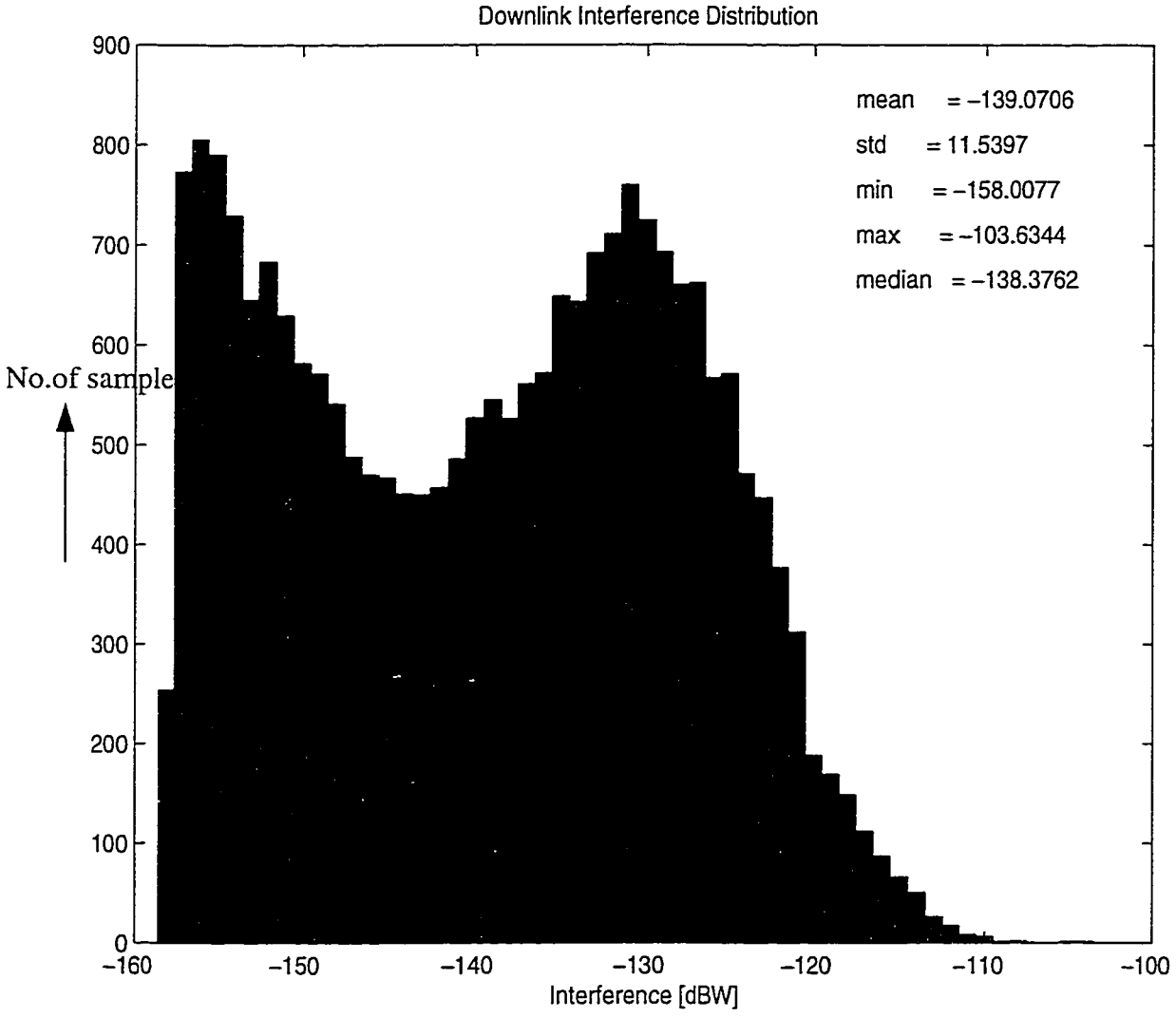

FIGURE 5.36. Downlink Interference distribution when $\beta = 0.9$

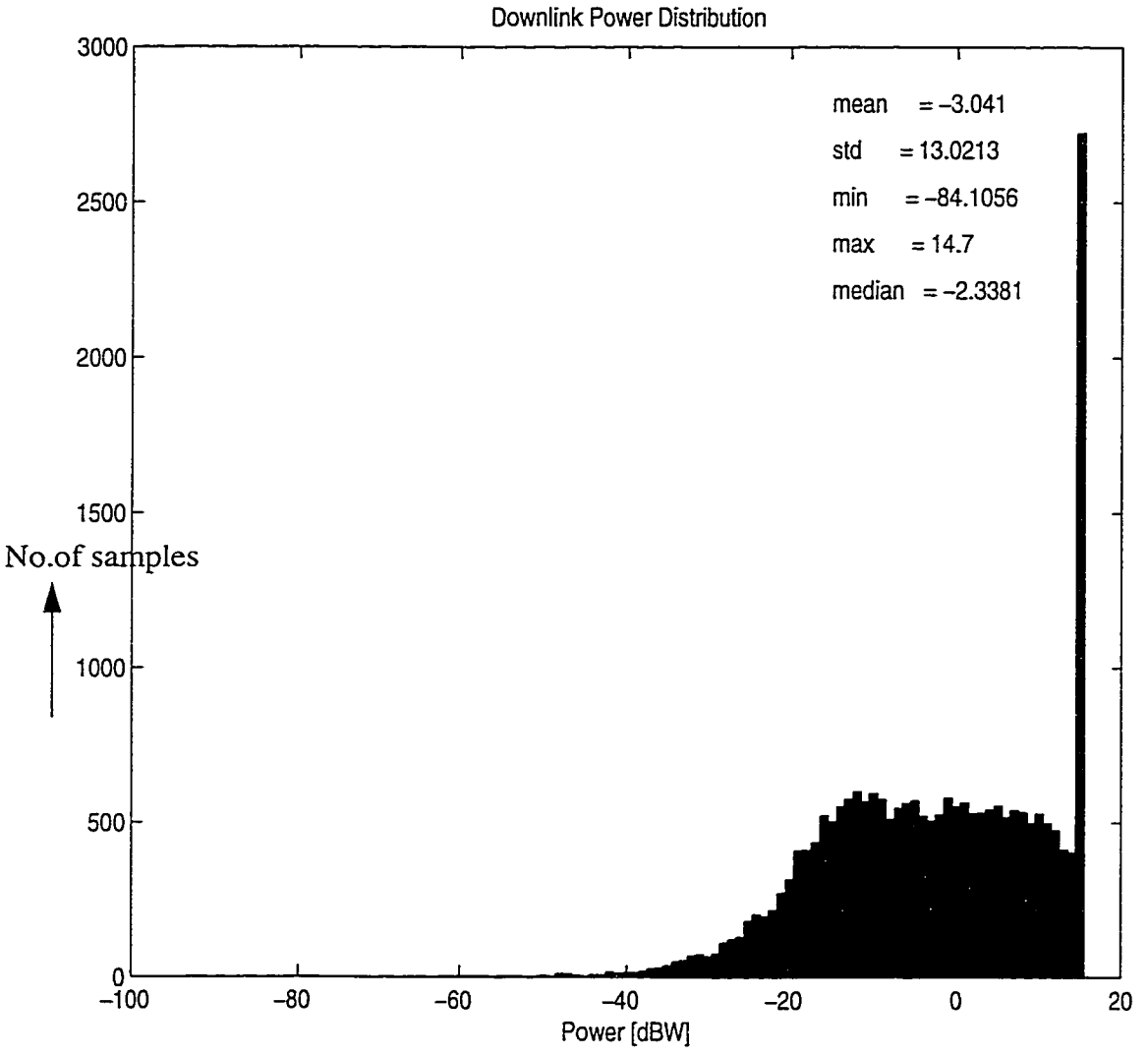

FIGURE 5.37. Downlink power distribution when $\beta = 0.9$

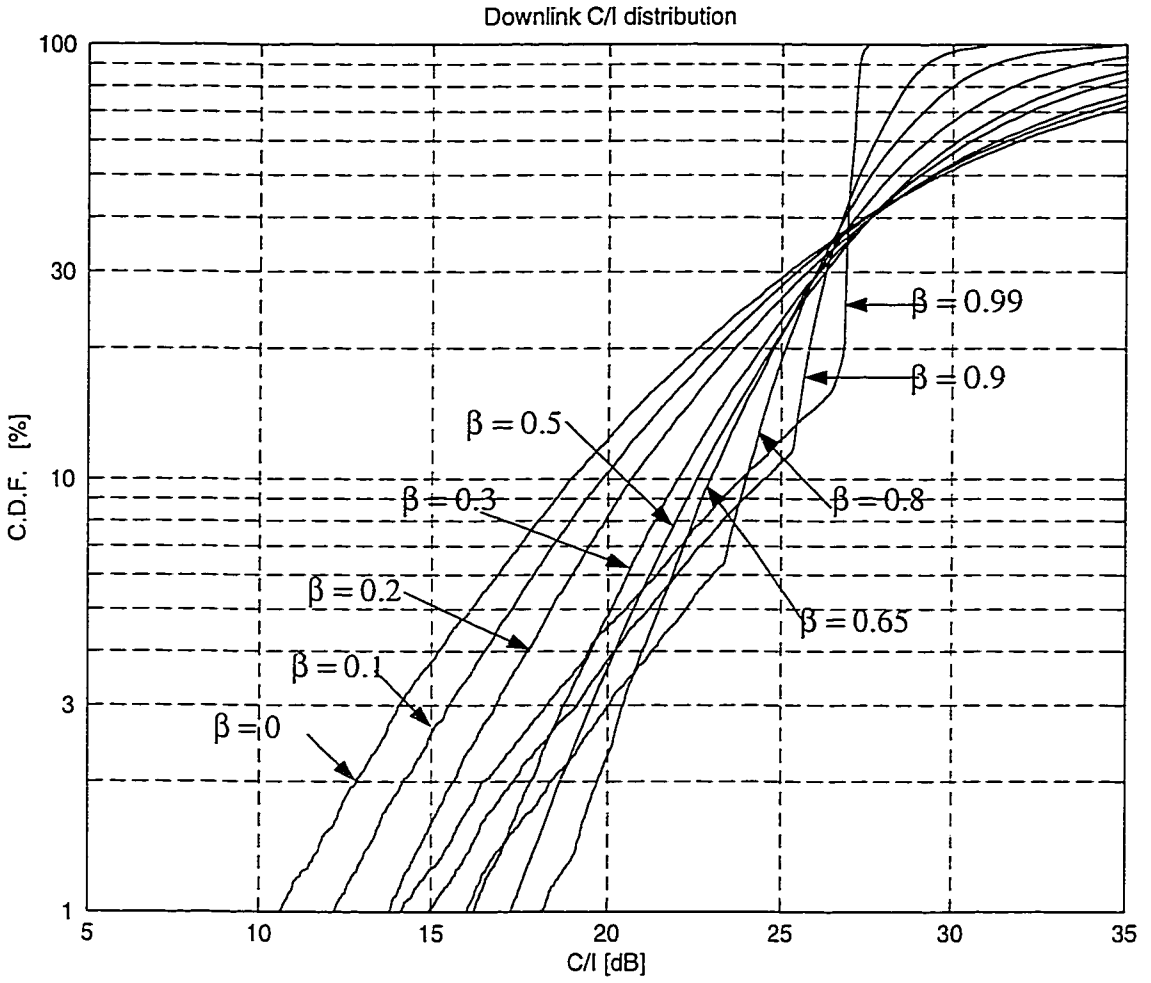

FIGURE 5.38. Downlink C/I distribution plots for different values of β ranging from 0 to 0.99

TABLE 5.3. C/I values for different values of β

β	C/I at 10% CDF [dB]	C/I at 3% CDF [dB]
0 (No power control)	*18.9311*	*14.0382*
0.1	19.8278	15.5148
0.2	20.6528	16.8254
0.3	21.9982	18.7554
0.5	22.5425	19.5391
0.65	22.9319	20.4384
0.8	23.9509	20.0146
0.9	*24.4683*	*19.1405*
0.99	23.8133	18.2588

5.5 Capacity Estimation

In Figure 5.39, cumulative distribution functions of downlink C/I are shown for the 4/12 reuse reference system with a conventional 3 sector antenna, 4/12 reuse systems with power control, 4/12 reuse systems with beamforming and beamforming with power control. From these curves it is evident that the C/I distribution adopts a different shape when power control and transmission in narrow beams is introduced.

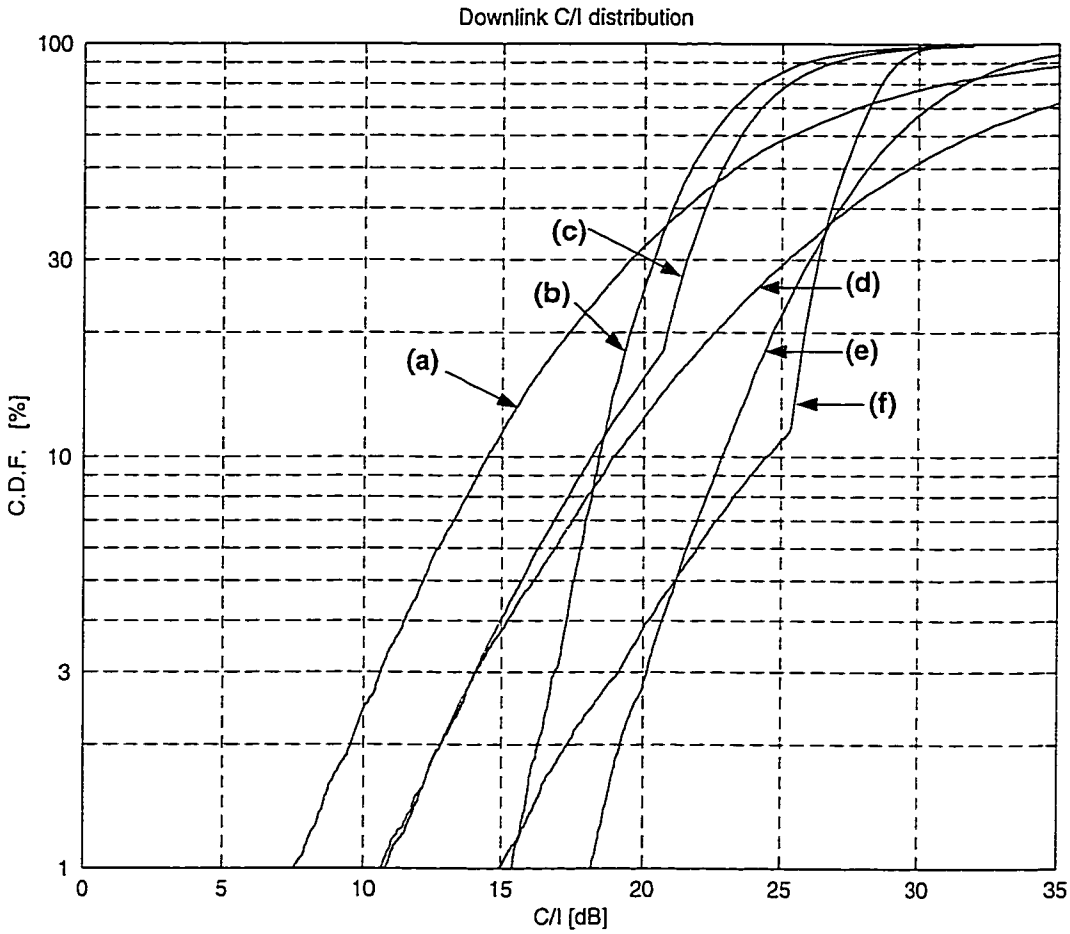

FIGURE 5.39. Cumulative distribution functions of downlink C/I for (a) a 4/12 reuse system with a conventional 3 sector antenna system, (b) 4/12 reuse system and 3 sector with downlink power control ($\beta = 0.7$), (c) 4/12 reuse, 3 sector, downlink power control ($\beta = 0.7$) and a restriction on the maximum power transmitted in the downlink (30 watts), (d) 4/12 reuse, 3 sector, 4 beams/sector, switch-beam antenna system, (e) 4/12 reuse, 3 sector, 4 beams/sector and downlink power control is applied($\beta = 0.65$), (f) 4/12 reuse, 3 sector, 4 beams/sector, switch-beam antenna system, downlink power control ($\beta = 0.9$), and a restriction on the maximum power transmitted in the downlink (30 watts).

Some parameters characterizing the C/I distributions of Figure 5.39 are summarized in Table 5.4.

TABLE 5.4. Summary of C/I values at 10% CDF and at 3% CDF presented in Figure 5.39.

Reuse	#Beams	Power control parameter	10% CDF level (dB)	3% CDF level (dB)
4/12	one beam / sector	$\beta = 0$ (no power control)	14.45	10.58
4/12	one beam / sector	$\beta = 0.7$	18.41	16.86
4/12	one beam / sector	$\beta = 0.7$ max.power limited to 30 watts	18.14	14.03
4/12	4 beam / sector	$\beta = 0$ (no power control)	18.93	14.03
4/12	4 beam / sector	$\beta = 0.65$	22.83	20.13
4/12	4 beam / sector	$\beta = 0.9$ max.power limited to 30 watts	24.46	19.14

The net improvement of C/I at 10% CDF compared to the reference 4/12 reuse (top line of the table), is 10.01 dB with beamforming and power control (bottom line of the table). A C/I gain improvement of 8.55 dB is noticed at 3% CDF compared to the reference 4/12, 3 sectored system.

The reference system has a C/I of 14.45 dB. When downlink power control or beamforming is implemented the C/I is improved from 14.45 dB to 18.14 and 18.93 dB respectively. By implementing either downlink power control or beamforming in a 7/21 reuse system, the improvement in C/I allows us to reduce the reuse from 7/21 to 4/12. This means an increase in served traffic by a factor of 1.75 assuming the level of downlink C/I limits the capacity in the system.

Implementing power control in conjunction with narrow beam transmission further improves the quality in the system. This quality gain may be sufficient for the use of 3/9 frequency reuse plan at full load with maintained or improved quality. This could mean a capacity gain of 2.3 times compared to 7/21 reuse.

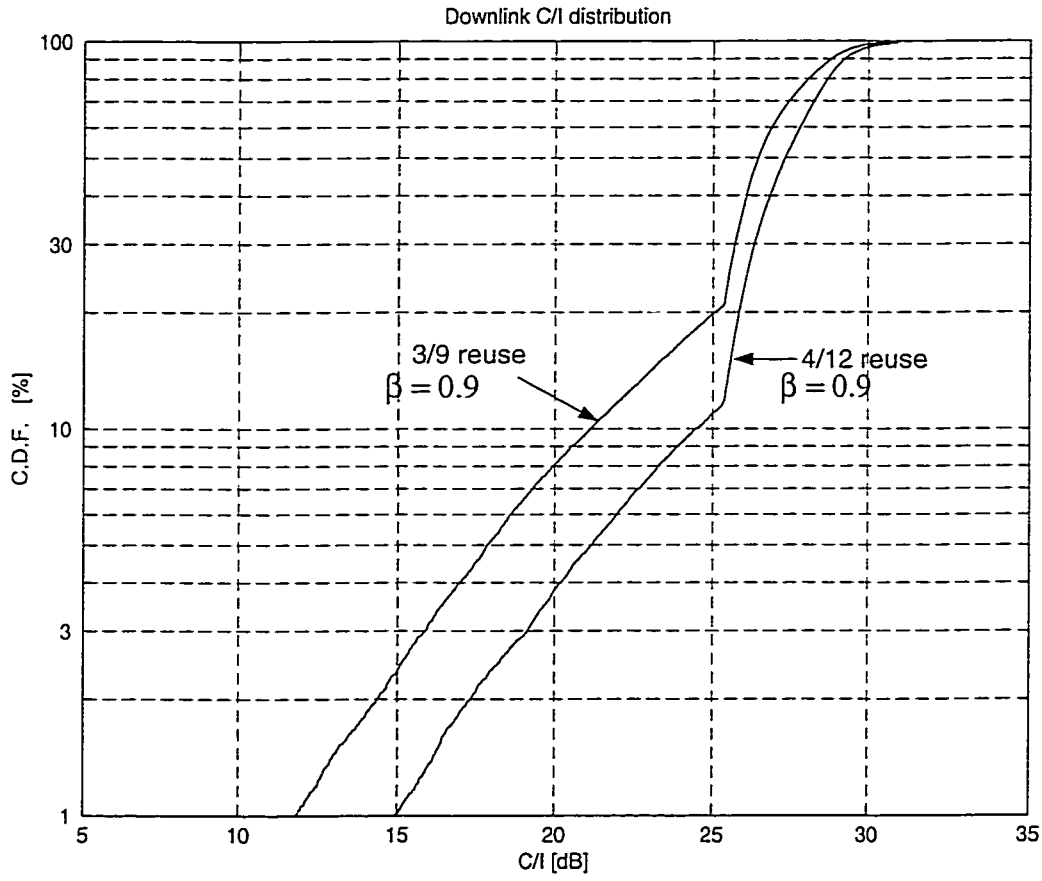

FIGURE 5.40. Cumulative Distribution Functions of downlink C/I for 4/12 reuse with switch-beam antennas and downlink power control, and 3/9 reuse with switch-beam antennas and downlink power control

Simulations were carried out using 3/9 reuse and employing both narrow beam transmission and downlink power control in the system. Figure 5.40 presents Cumulative Distribution Functions of downlink C/I for 4/12 reuse and 3/9 reuse implementing both switch-beam and downlink power control schemes. In 3/9 reuse the distribution spread is increased compared

to 4/12 reuse and C/I at 10% CDF is 21.12 dB while at 3% CDF it is equal to 15.86 dB, compared to 24.46 dB and 19.14 dB for 4/12 reuse at 10% CDF and at 3% CDF respectively. Since in DAMPS acceptable quality is usually defined by C/I at the 10% CDF level higher than 17 dB, then for 3/9 reuse, the C/I of 21.12 dB at 100% traffic load is more than the required quality level. Thus the gain achieved with narrowbeam transmission and downlink power control in 4/12 reuse system is sufficient to use a 3/9 reuse plan at full load thereby allowing a capacity gain of 1.33 times compared to 4/12 reuse system and 2.33 times compared to 7/21 reuse systems.

5.6 Discussion

From section 5.3, the C/I gain achieved by implementing power control in a 4/12 reuse, 3 sector cell system is 3.9 dB compared with no power control case. Similarly, when narrowbeam transmission is introduced in the system the C/I improvement is 4.48 dB. When power control is combined with narrowbeam transmission, the total gain achieved is approximately 10 dB. The combined individual gains of the downlink power control and narrowbeam transmission is 3.9 + 4.48 = 8.38 dB. The gain achieved when the downlink power control is clubbed with narrowbeam transmission is greater than the combined individual gains. The reason for this is the following: when narrowbeam transmission is introduced the interference in the system is drastically reduced because the radiated energy is only focused to wards the mobile, thereby eliminating undue interference in the system. Over and above narrowbeam transmission, when power control is implemented, the base stations adjust the power levels in such way that the link quality is maintained at all times. This avoids the interference due to extra power transmitted by certain links in the system. The reduction in interference due to these two schemes gives a combined gain which is greater than the sum of the individual gains implemented separately. Some of the implementation aspects of the power control algorithm used in these simulations are discussed below.

In a cellular system whose power control is based on C/I, some connections may be transmitting at vastly different power levels than others, leading to a risk of instability in the system. The system may be unstable for two reasons. The control strategy may be using β

greater than or equal to 1, or the control can be based on incorrect or old information which will cause control errors. Considering the first possibility, if β is greater than or equal to 1 then all the links will be striving for the same C/I and this will cause the party effect. It is for this reason that the simulations were carried out for values of β up to 0.99.

The second reason for instability is that incorrect or old information may be used in the control strategy. Power control strategy is based on the current C/I information of the link under consideration. If the information received from the mobile is incorrect then it will cause control errors.

Another difficulty with the C/I based power control algorithm is that it might be difficult to explicitly observe C/I, although it may be approximated in digital systems as a function of the Bit Error Rate (BER). However when there is a large time dispersion present there may be little or no correspondence between BER and C/I. Another difficulty with this approach is that BER is a statistical estimate, which means it may take some time to get good estimate. This delay in estimating BER when combined with a dynamic system causes control errors.

In most cellular systems, traffic load varies both in time and space. Radio network algorithms must adapt to the current traffic situation. For example, the power control algorithm based on current C/I information (as is used here) may handle these variations well. If the traffic load is low in a region the interference is low and the connections can use lower power, while still reaching higher power if needed. On the other hand, if the traffic load is high in a region, the connections may have to use higher power to maintain sufficient quality.

In a system with no power control, the transmitted power has to be estimated for the worst case scenario. So, all the connections transmit at a power level required for the worst case, i.e. many connections use excessive power. When power control is based on C/I, the transmitted power corresponds to the actual situation in the current link, meaning that transmitted power is often lower.

5.7 Conclusions

In this chapter, a power control algorithm was described based on the C/I of the downlinks. First, simulations were carried out for a 4/12 reuse, 3 sectored antenna system with no power limit and then with a power limit of 30 Watts on the maximum power transmitted. The results indicate that the C/I is improved by 3.96 dB with no power limit and 3.69 dB with a power limit of 30 Watts. Later, simulations were carried out for joint power control and narrow beam transmission. The results show that, C/I is improved by approximately 10 dB compared to the reference 4/12 reuse with 3 sectored and no power control. The improvement in C/I enhances the capacity of the system by using a more tighter reuse in the system, for example 3/9 in place of 7/21 reuse.

CHAPTER 6

CONCLUSIONS AND RECOMMENDATIONS

6.1 Conclusions

In this thesis, an overview of cellular systems was first given in order to provide an understanding of the basic concept of cellular systems such as frequency reuse, cochannel interference, multiple access schemes, mobile standards used in North America, etc. with particular emphasis on cell sectoring. Then the simulator used for the subsequent analysis was described, allowing the main performance parameters such as system capacity, system performance and average system utilization to be understood.

With this background, the concept of smart antennas was discussed. Different smart antenna approaches were described. The general features of antenna arrays for mobile communications were presented with an emphasis on phased arrays and main beam scanning. Also different beamforming techniques such as digital and analog beamforming were described briefly. A number of IS-136 system simulations with beamforming was then undertaken. Simulation results indicate that with a switched narrow beam focused towards the mobile, interference in the system can be reduced considerably. The 4.5 dB C/I gain thus achieved can be used to implement a tighter frequency reuse with maintained quality allowing a 1.75 times increase in system capacity (4/12 rather than 7/21 reuse).

In general, power control at both the mobile and base station improves traffic capacity by reducing the amount of emitted interference. Base station power control ensures that the required amount of power is transmitted to the mobiles. Since the radiated energy is controlled in both power and focused towards the mobile in a narrow beam, the probability of the traffic channel causing interference to the co-channel used by other mobiles is very remote.

In this thesis a downlink power control algorithm used in subsequent simulations was described. Simulation results from various scenarios with base station power control yield a C/I gain of approximately 4 to 5 dB over and above the 4 dB improvement achieved through narrow beam transmission alone. With the implementation of downlink beamforming and base station power control, the results show that an even tighter frequency reuse (3/9 instead of 4/12) can be used and hence a 2.3 times increase in system capacity could be achieved over the reference 7/21 reuse system.

6.2 Recommendations for Future Research

Narrow beam transmission on the downlink greatly reduces the cochannel interference in the system. This has been shown to be one of the major factors that can greatly improve system capacity. The basic idea is not to spill the radiated energy in any direction other than the required direction in a narrow beam. This can only be done when there is no antenna pattern distortion. To avoid any undue interference due to pattern distortion, a better understanding of array structures, mutual coupling between the elements, spacing between the elements and the effect of beam cross-over losses is necessary.

The direction of arrival (DOA) information is very vital to assign a beam to the mobile for communication between base station and the mobile. In this work it is assumed that DOA is available and accurate. In a future work, array processing algorithms for direction estimation need to be developed and evaluated.

Portable mobility is another area requiring study. In this work, mobiles are considered to be static and hence no hand-offs are initiated. But in practice the mobile moves around with a certain speed and hence hand-offs are necessary. A future undertaking would be the study of inter-cell and intra-cell hand-offs when switch-beam antennas are implemented in the system. Also an investigation of the capacity gains achieved by combining switch-beam antenna techniques with adaptive channel allocation techniques (ACA) would be required.

One problem in IS-136 systems that requires a careful study is that the mobile station utilize information in slots surrounding their assigned slot for synchronization and equalization. It may hence be necessary to transmit parts of the downlink bursts in multiple beams directed towards several mobile stations. This may require the introduction of transmitter diversity.

It is also important to study the combined effect of portable mobility and power control on system stability and traffic capacity. As a portable is moving away from its base stations, the transmitter power has to be increased from the lower power setting to the higher power setting to compensate for the increased signal propagation loss. The sudden increase in the transmitter power affects all mobiles using the same beam and may cause more interference on the corresponding co-channels. If a call cannot adjust to the increased interference, the call is dropped.

REFERENCES

1. S.C. Swales, M.A. Beach, D.J.Edwards and J.P.Mcgeehan, "The Performance Enhancement of Multi-Beam Adaptive Base-Station antennas for Cellular Land Mobile Radio Systems, IEEE Transactions on Vehicular Technology, vol.39. No.1, Feb.1990

2. Soren Anderson, Mille Millnert, Mats Viberg and Bo wahlberg, "An Adaptive Array for Mobile Communication Systems", IEEE Transactions on Vehicular Technology, Vol.40, No.1, February 1991

3. Joseph Fuhl and Andreas F. Molisch, "Capacity Enhancement and BER in a combined SDMA/TDMA System," IEEE Vehicular Technology Conference 1996, Vol. 3, pp.1481-1485

4. C.Passerini, M.Frullone, M. Missiroli and G. Riva, "Performance of Adaptive Antenna Arrays For Wideband Wireless Indoor Communications," IEEE Vehicular Technology Conference 1996, Vol.3, pp.1501-1504

5. Yingjie Li, Marty Feuerstein, Patrick Perini and Doug Reudink, "Gain improvement of a cellular base station multibeam antenna," IEEE Vehicular Technology Conference 1996, Vol. 3, pp.1680-1684

6. Fehri Benhamida, Jeam-Francois Sante and Gie Cofira, "The capacity enhancement of the DCS network by the use of switch-beam antennas", 5th IEEE International Conference on Universal Personal Communications 1996, Vol.1, pp. 463-467

7. Ming-Ju Ho, Gordon L. Stuber and Mark D. Austin, "Performance of switched-beam smart antennas for cellular radio systems," IEEE International symposium on Personal Indoor and Mobile Radio Communications, Taipei, Taiwan, October 15-18, 1996

8. David J.Y. Lee and Ce Xu, "Capacity and trunking efficiency of smart antenna, IEEE Vehicular Technology Conference 1997, Vol.2 pp. 612-616

9. Preben E. Mogensen, Klaus I. Pedersen, Plou Leth-Espensen, Bernard Fleury, Frank Frederiksen and Kim Olesen, "Preliminary measurement results from an adaptive antenna array test bed for GSM/UMTS," IEEE Vehicular Technology conference 1997, Vol. 3, pp.1592-1596

10. G.V. Tsoulos, M.A. Beach and S.C. Swales, "On the capacity enhancement of a TDMA system with adaptive multibeam antennas," IEEE Vehicular Technology conference 1997, Vol. 1, pp.165-169

11. Robert L. Cupo, Glenn D. Golden, Carol C. Martin, Karl L. Sherman, Nelson R. Sollenberger, Jack H. Winters and Peter W. Wolniansky, "A four-element adaptive antenna array for IS-136 PCS base stations" IEEE 47th Vehicular Technology conference Proceedings, 1997, Vol. 3 pp. 1577-1581

12. S.S. Jeng, H.P. Lin, G. Xu and W.J. Vogel, "Experimental Study of Spatial Signature Variation of an Antenna Array" in Proc. of 1995 IEEE Vehicular Technology Conference, Chicago, IL, July 1995

13. Sang- Youb Kim and Guanghan Xu, "Antenna Gain for Adaptive Smart Antenna Systems", IEEE 47th Vehicular Technology conference Proceedings, 1997, Vol. 2 pp. 1168-1172

14. Jack H. Winters, "Smart Antennas for Wireless Systems", IEEE Personal Communications, Feb.1998 pp. 23-27

15. Bo Hagerman and Sara Majur, "Adaptive antennas in IS-136 systems", 48th IEEE Vehicular Technology Conference, 18-21 May 1998, Ottawa, Vol. 3, pp. 2282-2286

16. R.T.Compton, Adaptive Antennas- concepts and performance, Prentice-Hall, 1988

17. Antenna Theory Analysis and Design, Constantine A Balanis, Harper & Row, Publishers, New York

18. Antenna Theory and Design, Warren L. Stutzman, Garry A. Thiele, by John Wiley & Sons, Inc., 1981

19.Butler J., and R.Lowe, "Beamforming matrix simplifies Design of Electronically scanned antennas," Elect. Design, Vol.9, 12 April 1961, pp. 170-173

20.Allen, J.L., "A theoretical limitation on the formation of lossless multiple beams in linear arrays," IRE trans., Vol. AP-9, July 1961, pp.350-352;

21.Kahn, W.H., and H. Jurss, "The uniqueness of the lossless feed network for a multibeam array," IEEE Trans., Vol. AP-10, Jan.1962, pp.100-101

22.White, W.D., "Pattern limitations in multiple beam antennas," IRE Trans., Vol. AP-10, July 1962, pp. 430-436

23.Stein, S., "Cross couplings between feed lines of multibeam antenna due to beam overlap," IEEE Trans., Vol. AP-10, Sept. 1962, pp. 548-557

24.Dufort, E.C., "Optimum low sidelobe high crossover multiple beam antennas," IEEE Trans., Vol. AP-33, No. 9, Sept. 1985, pp. 946-954

25.Neil J. Boucher, The Cellular Radio Hand Book, by Quantum Publishing Inc. 1992

26.Theodore S.Rappaport, Wireless communications, Principles and Practice, Prentice-Hall, Inc.,1996

27.Vijay K.Garg, Joseph E.Wilkes, Wireless and Personal Communication Systems, Prentice-Hall Inc., 1996

28. J.M.Aein, "Power balancing in systems employing frequency reuse" COMSAT Tech. Rev., vol.3, no.2, Fall 1973

29. W. Tschirks, "Effects of transmission power control on the cochannel interference in cellular radio networks" Electrotechnik and informationstechnik, vol.106, no.5, 1989

30. J.F.Whitehead, "Signal-Level-Based Dynamic Power Control for Co-channel Interference Management" Proc. 43rd VTC, May 1993 PP 499-502

31. Jens Zander, "Performance of Optimum Transmitter Power Control in Cellular Radio Systems", VTC, Vol.41, No.1, Feb.92

32. Sudheer A. Grandhi, Rajiv Vijayan, David J. Goodman, and Jens Zander, "Centralized Power Control in Cellular Radio Systems" IEEE Transactions on Vehicular Technology, vol. 42, No. 4, November 1993

33. Jens Zander, "Distributed Cochannel interference Conttrol in Cellular Radio systems, IEEE Transactions on Vehicular Technology, Vol. 41, No. 3, August 1992

34. Gerard J. Foschini and Zoran Miljanic, "A simple Distributed Autonomous Power Control Algorithm and its Convegence," IEEE Transactions on Vehicular Technology, Vol. 42, No. 4, November 1993

35. S.A.Grandhi, R. Vijayan, D.J. Goodman, "Distributed power control in cellular radio systems," IEEE Trans.on Comm., vol. 42, nos. 2/3/4, pp. 226-228, Feb/Mar/Apr. 1994

36. Tsern-Huei Lee and Jen-Cheng Lin, "A Fully distributed Power Control Algorithm for Cellular Mobile systems," IEEE Journal on Selected areas in Communications, Vol. 14, No. 4, May 1996

37. Chin-Tau Lea and Li-Chun Wang, "Modelling Mobility in Power Control," IEEE 1997

38.Magnus Almgren, Hakan Anderson and Kenneth Wallstedt, "Power Control in a Cellular system, VTC 94

39.Vijay K. Garg and Laura Huntigton, Application of Adaptive Array Antenna to a TDMA Cellular/PCS System, IEEE Communications Magazine, October 1997, pp.148-152

40.Digital Beamforming in Wireless Communications, John Litva and Titus Kwok-Yeung Lo, Artech House, Inc., 1996.

IMAGE EVALUATION TEST TARGET (QA-3)

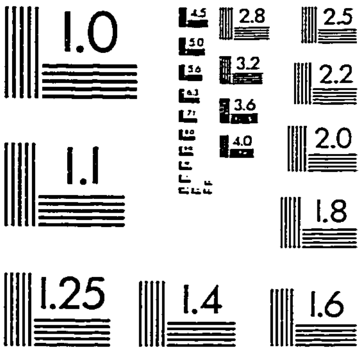

150mm

6″

APPLIED IMAGE, Inc
1653 East Main Street
Rochester, NY 14609 USA
Phone: 716/482-0300
Fax: 716/288-5989

© 1993, Applied Image, Inc., All Rights Reserved